POLITECNICO DI TORINO

Department of Applied Science and Technology

SOLIDS AND GAS HYDRODYNAMIC CHARACTERISTICS IN SQUARE-BASED SPOUTED BEDS FOR THERMAL APPLICATIONS

PhD School in Chemical Engineering

(XXVII Cycle)

Coordinator: Prof. Marco Vanni

Candidate: Massimo Curti

Advisor: Prof. Giorgio Rovero

Index

1 Introduction

Gasification is considered a favourable method to convert a biomass or other organic materials to a multipurpose gas; the syngas produced can be addresses to the chemical industry as a synthesis reactant or considered a mere fuel. New concepts based on the valorisation of non-conventional resources have been developed in the recent years to save fossil fuels and reduce the generation of civil and industrial waste. According to these ideas, refuses can be transformed into a valuable energy source instead of being disposed. In conformity with these perspectives, updated technologies should be investigated, both to optimize gasification processes and obtain a medium heating value gas.

The quality of syngas depends on the properties of the raw material used, the operative conditions and the design of the gasifier. In case the fuel used is a by-product of a certain industrial operation, the chemical composition cannot kept constant, and only an average value can be estimated to predict the composition of the syngas generated by the thermal reaction. According to these considerations, the gasification reaction should be run in a unit adaptable to a variable source of materials.

The present work aims at improving the understanding of spouted beds, which display advantages if compared to more common fluidization techniques; a spouted bed can be operated with a better hydrodynamic control, thanks to lower pressure drop and gas flow rate, slightly exceeding the minimum spouting condition, rather than a much higher flow rate required by bubbling or turbulent fluidization. Additionally, the hydrodynamic features of a spouted bed offer optimal mixing of solid phases characterized by very different density or shape; specifically, a light particulate reacting waste, continuously added to a stationary buffer inert, is not affected by segregation.

Spouted beds appear to go through a revival, proved by a very recent and comprehensive book on the topic (Epstein and Grace, 2011). This renewed interest arises by implementing new concepts in scaling-up spouting contactors and devising potential applications to high temperature processes, noticeable examples being given by pyrolysis and gasification of biomass, kinetically controlled drying of moist seeds to guarantee the requested qualities and polymer upgrading processes.

Moving to our area of interest, a textile district produces waste fibres and fibre fragments at a noticeable mass rate. As a case study, a survey within the Biella district has revealed a daily generation close to 5000 kg. This by-product represent a cost for

the sector because they have to be compacted, stored and disposed, while a small-scale thermal process can be a prompted reasonable solution of valorisation.
A square-based spouted bed pilot unit was designed and constructed to investigate the gasification of various types of textile waste, fed to the reactor upon pelletization. To guarantee a reducing or low oxidizing atmosphere in the reaction zone at gas flow rate proper for spouting, steam was in-line generated by gas combustion to close the mass and enthalpy balance.

2 Fluidization

2.1 Principles of fluidization

The fluidization is a process were a solid phase is converted by an ascending fluid phase; the aim of the operation is to optimize this two-phase contact between the different phases, improving the hydro dynamic and transport phenomena.
Gas fluidization is a hydrodynamic regime in which a bed of solid particles is expanded, suspended, or even transported by an upward fluid flow. This regime is established when the fluid velocity exceeds a value corresponding to the minimum fluidization.
At low velocity rate, a gas simply percolates between the granules, thus generate a pressure drop through the bed. By increasing the velocity, the aerodynamic drag forces will begin to counteract the gravitational force, causing the bed to expand in volume as the particles move away from each other. When the pressure drop reaches a critical value corresponding to the weight of the particles, the fluid phase is able to sustain the bed and this is called fluidized regime.
A standard fluidized bed reactor is composed by a vessel with a perforated plate at the bottom through which the gas enters the fluidization unit and it is uniformly distributed through the particles up to reaching the free surface. The basic design of a fluidized unit is carried out by considering a vessel having a cross section of any geometry (circular, squared or rectangular) with a perforated distributor, which separates the volume holding the solids from the underneath gas plenum.
Fluidization, besides being influenced by the solid characteristics, depends on the physical properties of the fluid and its superficial velocity. This phenomenon can be easily depict considering the relationship between air flow rate and pressure drop across a section of the bed, as schematically shown fluidization diagram of in Figure 2.1.

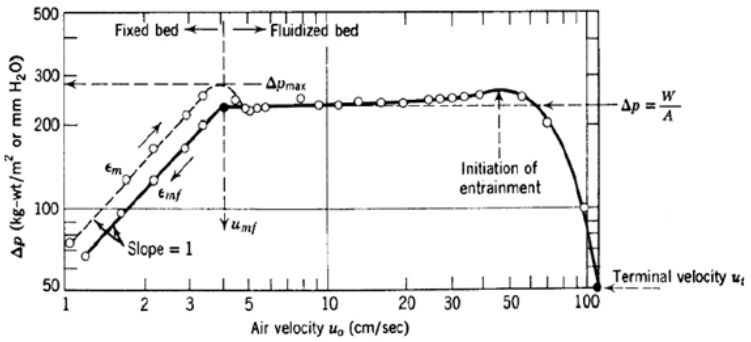

Figure 2.1 – The effect of gas velocity on the pressure drop. Source: Kunii, D., Levenspiel, O. "Fluidization Engineering".

When the superficial air velocity is very low, the fluid merely percolates through the particles and no movement is induced, this condition being defined as "static bed". By rising the flow rate, frictional forces between particles and fluid increase: when the upward component of force counterbalances the particle weight, the minimum condition to expand the bed is reached. All the particles being suspended by the fluid, the bed can be considered in a state of "incipient fluidization" and the pressure drop through any bed section equalizes the weight of the fluid and solids in that section.
By further increasing the velocity, some phenomena of instability such as "bubbling" or "turbulent fluidization" may occur, depending on the system geometry and particle properties. In a gas-solid system operated at high fluid velocity, gas bubbles tend to coalesce and grow in volume during their upward travel; if the bed is not wide enough, a gas bubble can occupy all the vessel cross section, then the solid particles are lifted as a piston, giving origin to the so-called "flat slugging". This undesired occurrence easily happens with coarse particles, because of high gas velocity as well with cohesive powders, as a consequence of fine particle interaction.
Finally, when a critical value is reached, the velocity of the gas is high enough to transport individually or in clusters the bed particles in a "pneumatic conveying" fashion. These hydraulic regimes are schematically shown in Figure 2.2.

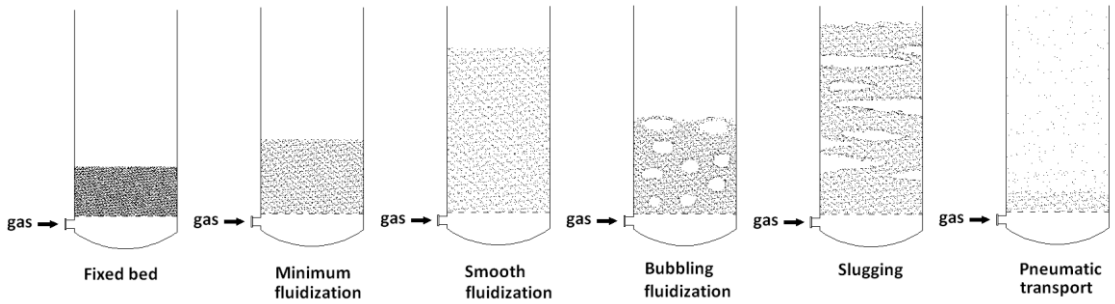

Figure 2.2 - Schematic representation of various fluidization regimes.

When a fluidized regime is reached, the reactor shows a number of features, which are summarized below, see *Kunii and Levenspiel, 1991*:

- forces are in balance and there is no net force acting in the system;
- the solid particle bulk exhibits a liquid-like behavior: the surface of the solids remains horizontal by tilting the vessel;
- if two or more vessels operating in a fluidization regime are connected, the solids reach an identical hydrostatic level;
- in the presence of a side opening under the bed surface, particles gush as a liquid flow;
- heterogeneous bodies with a lower density than the bed density will float on its surface (float son phase), while objects with a higher density sink to the bottom of the bed (jet son phase).

Beside considering the properties of the fluidization medium, particle features play an essential role. A fundamental mapping was proposed (*Geldart, 1973*) to group particulate solid materials in four well-defined classes according to their hydrodynamic behavior. To follow this categorization, Figure 2.3 shows the four different regions, proper of air/solids systems at ambient fluidization conditions and particles of the same shape, excluding pneumatic transport conditions.

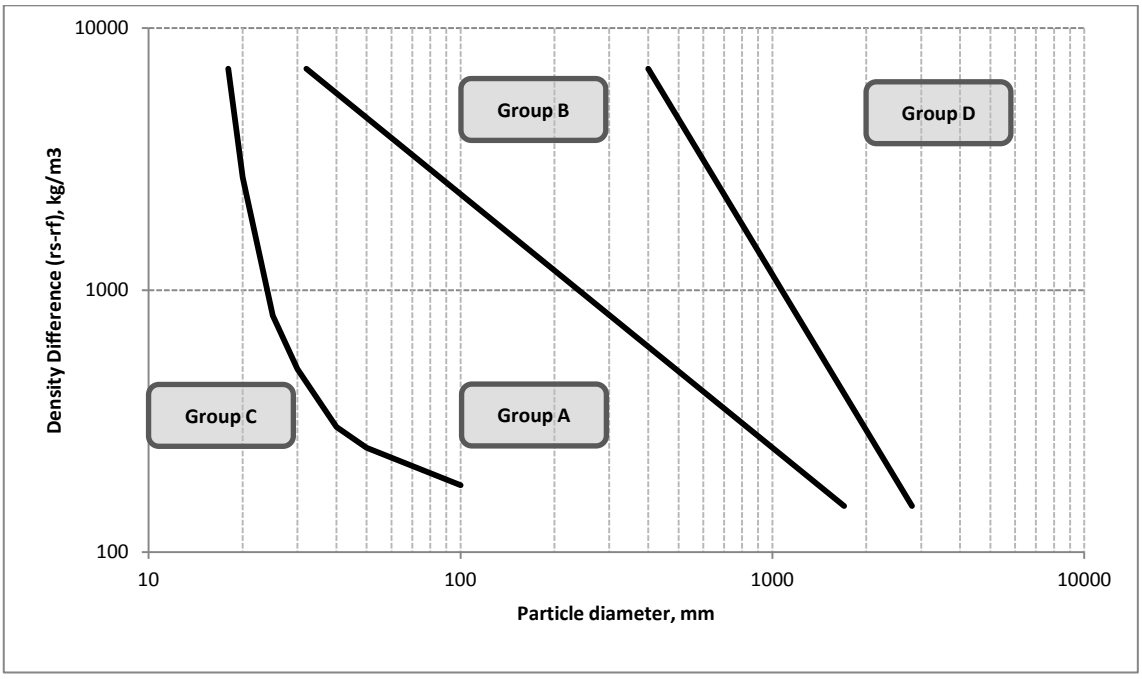

Figure 2.3 – Particle classification according to Geldart.

The particles of the regions can be described as follows:

- A type or *"aeratable"*: solids with small diameter and density lower than about 1400 kg/m^3. The minimum fluidization velocity can be reached smoothly; then fine bubble fluidization occurs at higher gas velocities.

- B type or *"sand-like"*: these particles are coarser than the previous ones, ranging from 40 to 1000 μm and densities from 1400 to 4000 kg/m^3. A vigorous fluidization with large bubbles may be established.
- C type or *"cohesive"*: very fine powders, with a mean diameter generally lower than 50 μm. Strong interparticle forces render fluidization difficult.
- D type or *"spoutable"*: coarser particles within a broad density range. These systems are characterized by a high permeability, which generates severe channeling and uneven gas distribution: the standard fluidization geometry should be modified to give origin to spouted systems, where channeling is controlled by the spouting action.

In the field of fluidization several geometrical configurations different from the standard bubbling beds have been defined, such as turbulent bed, circulating beds, etc., each of them characterized by advantages and drawbacks. Since the aim of this work is to propose and configure an equipment ready to treat thermally different types of solids, in terms of size, shape and chemical composition, a particular type of fluidization reactor, named spouted bed, was chosen.

2.2 Spouted bed reactor

The term "Spouted Bed" was coined with an early work carried out at the National Research Council of Canada by (Gishler and Mathur, 1954). A comprehensive book by (Mathur and Epstein, 1974) provided a systematic summary of the scientific work done in the years; recently (Epstein and Grace, 2011) the most advanced knowledge in the field has been updated.

Spouted beds were originally developed as an alternative method of drying moist seeds needing a prompt and effective processing. Sooner the interest in spouted beds grew and their application included coal gasification and combustion, pyrolysis of coal and oil shale, solid blending, nuclear particle coating, cooling and granulation, as well as polymer crystallization and solid-state polymerization processes. Fundamental studies were carried out to establish design correlations, the performance of spouted beds as chemical reactors, motion patterns and segregation of solids, gas distribution within the complex hydrodynamics.

Most studies were carried out in plain cylindrical geometries, either full sectional, half-sectional or even in a reduced angular section of a cylinder to explore scale-up possibilities. In any case adding a flat transparent wall was demonstrated to interfere to a moderate extent with the solids trajectory vectors in the annulus (Rovero et al., 1985), while does not affect the measurement of the fundamental parameters of spouted beds (U_{ms}, H_m, D_s). A limited number of examples consider multiple spouting, either in parallel or in series, squared and rectangular cross sections (Mathur and Epstein, 1974).

A typical spouted bed scheme is given in Figure 2.4. This representation depicts the gas inlet and outlet, the upward movement of solids in the spout, their trajectories in the

fountain and the subsequent descent in the annulus to reach the spout again at depths which depend on the path-lines originated by the landing positions on the bed surface. The particles holdup can be loaded batchwise or, alternatively, in a continuous mode. The latter option depends on process requirements, nevertheless a continuous solids renewal in no way alters the above features. A proper solids feeding should minimize bypass towards the discharge port; in this view a direct feeding over the bed surface at a given side appears to offer the best option and guarantee at least one circulation loop in the annulus to all the particles. A direct distributed feed over the fountain is required only in case of particles with high tendency to stick.

The solids discharge from continuous operations is generally carried out with an overflow port, unless a special process control is required. This case may be given by coating processes, where the total bed surface area should be controlled. In this case a submerged port preferentially discharges coarse material, due to local segregation mechanisms (Piccinini, 1980), while the entire spouted bed retains good mixing capacity, which can be regulated by the fountain action.

The gas flow distribution between spout and annulus is completely independent whether the solids are batch or continuously fed: part of the gas progressively percolates from the spout into the annulus by moving toward higher elevations. In case of a bed of sufficient height the gas in the annulus may reach a superficial velocity close to the minimum fluidization velocity of the solids. In this event, the annulus may collapse into the spout top, thus defining the "maximum spoutable bed depth, or H_m". This parameter represents one of the fundamental criteria to design a spouted bed unit (Mathur and Epstein, 1974); H_m depends on vessel geometry, fluid and particle properties.

The second fundamental parameter is given by the minimum rate of gas required to maintain the system stable, the so-called "minimum spouting velocity, or U_{ms}". This operating factor can be either determined by an experimental procedure (as described in Figure 2.5) or can be calculated by the existing correlations.

A spouted bed, thanks to its flexibility, can be operated with a wide range of solids load to fill part or all the cone ("conical spouted beds"), or otherwise to engage also the upper portion of the vessel ("cylindrical spouted beds"). In both cases the conical included angle is in the range of 60 to 90°; by further diminishing the angle instability in solid circulation might occur, while increasing excessively the angle decreases solids circulation at the base and generate dead zones. A gross criterion that distinguishes conical and cylindrical spouted beds can be given considering the type of reaction to carry out: when the solid phase undergoes a fast surface transformation, the optimum residence time of the gaseous phase is very short. This condition is satisfied by shallow beds as in the case of catalytic polymerization or coal gasification and pyrolysis. When the reaction is controlled by heat or mass transfer, the gas-solid contact must be adjusted with a deeper bed configuration as in drying, coating, solid phase polymerization, etc…

Thanks to this flexibility, the mean residence time of the solids in continuous operations can be regulated by optimizing the solids hold-up in a single vessel, which gives origin to a well mixed unit. Otherwise, it is possible to conceive a cascade of several units to have a system approaching a plug flow. In the latter case square based units can have a

number of advantages over a conventional cylindrical geometry. Specifically, the construction is cheaper, more compact and the heat dissipation toward the outside lower. Some scientific aspects remain open though: the design correlations that should be validated, the spouting stability of multiple units proved both during the start-up and at steady state conditions and the possibility of fully predicting the solids residence time distribution as a function of geometry and number of stages.
Some additional improvement in the gas-to-solids contacting can be provided by independently aerating the annulus, thus generating the so-called "Spout-fluid Beds" (Chatterjee, 1970). Differently, a perforated draft-tube can be placed to surround the spout, thus contributing in terms of stability and operational flexibility (Grbavčić et al., 1982).

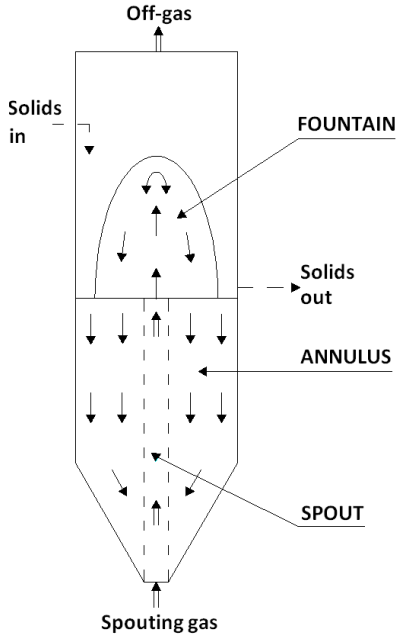

Figure 2.4 – Typical spouted bed scheme.

Stable spouting can be obtained by satisfying two hydrodynamic requirements:

- the bed depth must be lower than the H_m value;
- the gas flow rate has to exceed U_{ms}.

From an initial condition of a static bed with a nil gas flow, by increasing the gas flow a certain pressure drop is built up through the bed of particles. The graph given in Figure 2.5 describes this hydrodynamic evolution, which implies a pressure drop/flow rate hysteresis between an increasing flow and the reverse situation. The hysteresis is caused by different packing conditions of the bed particles, that expand to attain a loose state once a spouting condition is reached.
Starting from the static bed condition denoted by *A*, the pressure drop increases with the fluid velocity and reaches a maximum pressure drop (ΔP_M at *B*). With an additional increase of the gas velocity, the bed displays a moderate progressive expansion and a

corresponding decrease of pressure drop to reach *C*. Finally, an abrupt spouting leads to a sudden decrease of pressure drop that stabilizes at a nearly constant value (*D*), which is maintained in all the operating range of gas rate. This situation represents a stable spouting.

In case of fluid velocity decrease, the pressure drop remains constant down to the spout collapse (*E*), which compacts the system to some extent and the pressure drop increases again to *F*, giving origin to the afore mentioned hysteresis. The minimum spouting velocity is recorded at *E*.

The whole system hydrodynamics is given by knowing ΔP_M, U_{ms}, ΔP_s and the U/U_{ms} ratio chosen for a stable spouting. A recent paper compared data obtained in the mentioned 0.35 m side square-base unit to the existing literature correlations (Beltramo et al., 2009). The design data for the blower are ΔP_s and U, while the maximum pressure drop and the relative transitory flow rate can be easily generated by a side capacitive device, to be used at the start-up only.

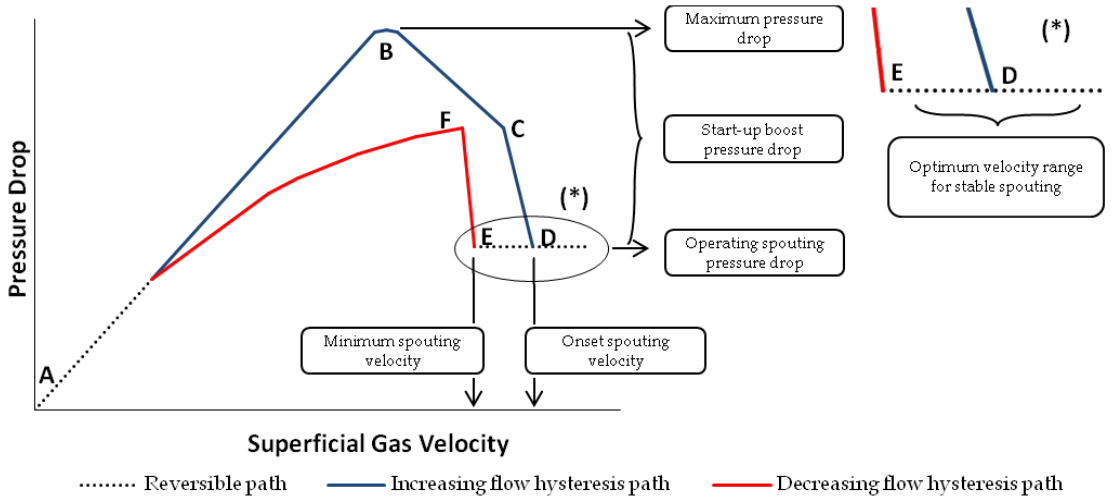

Figure 2.5 - Hydrodynamic diagram for spouting onset.

Figure 2.6 displays a sequence of pictures that show the spout onset from the initial cavity generation (*A*) to the full spouting. The third picture qualitatively corresponds to the point *B* in Figure 2.5, the fourth picture shows the rapid sequence between *C* and *D*, while the last picture may describe any point in the interval *E*-*D*, or higher flow rate.

It is important knowing that the hydrodynamic transient can be as short as a few seconds, so that the capacitive device can be designed with a characteristic time shorter than a fraction of a minute.

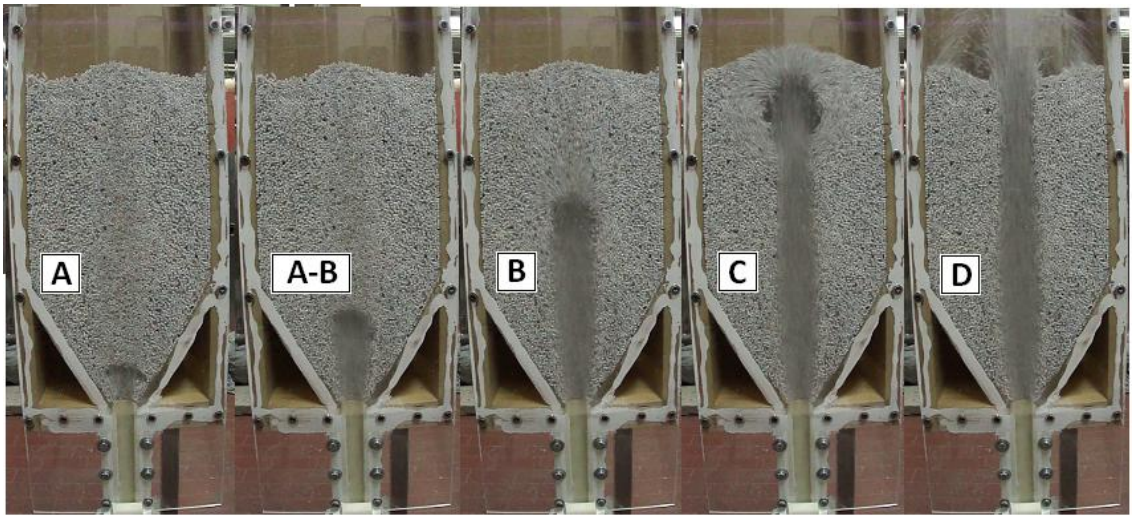

Figure 2.6 - Photographic sequence of the evolution of a spouting process performed in a squared-based half sectional 0.2 m side unit.

2.3 Comparison between fluidized bubbling bed and spouted bed

Fluidization is an operation characterized by several interesting peculiarities with desirable associated to non-optimal features. On one hand, this technique guarantees a smooth and liquid-like flow of solid particulate materials that allows continuous and easily controlled operations. The good mixing of solids provides a large thermal flywheel and secures isothermal conditions throughout the reactor. If some minor wall-effects are neglected, the solids-to-fluid relationship is independent of the vessel size, so this operation can be easily scaled up and large size operations are possible.
On the other hand, fluidization may reach conditions of instability, such as bubbling or slugging, which usually represent a situation of inefficient contact between the two phases. Moreover, in high temperature operations, as well as with sticky particles, solids sintering or agglomeration easily occur. Finally, but not less important, generation of fines, erosion of vessel, internals and piping is a serious problem caused by the random and intense movement of particles (i.e. particle carry-over exerted by the fluid).
Mass and heat transfer related to physical and chemical reactions are kinetically limited by surface area of large particle, either when the operation occurs in the fluid phase or on the solids. In these cases fluidized systems must operate with fine particulate materials; examples are given by heterogeneous catalysis or combustion/gasification of coal fines.
For reasons intrinsic to many processes (upgrading of agricultural products, agglomeration, pelletization, etc.), large particle handling is required and fluidization does not represent an optimal technology. Material comminution to reach the size required by conventional fluidization is an additional negative aspect which increases the exergetic overall process cost. A very noticeable gas velocity is required to reach fluidization of large particles, which often far exceeds the amount required for the physical or chemical operation considered. It should also be noted that fluidized systems

are operated at a gas rate double or triple with respect to the minimum fluidization velocity to confer the system adequate mixing and avoid dead zones. In conclusion, fluidization appears an interesting operation thanks to easy scale-up, though its extensive feature (need of large gas flow rate), as well as its intensive characteristics (random fluid-to-particle hydraulic interaction) counterbalance its favourable aspects to some extent.

A spouted bed can be realized by replacing the perforated plate distributor typical of a standard fluidized bed with a simple orifice, either located in the central position of a flat bottom or at the apex of a bottom cone, whose profile helps the solids circulation and avoids stagnant zones. Examples of non-axial orifices appear in the scientific literature, too. The fluidizing gas enters the system at a high velocity, generates a cavity protruding upward through the "spout", with an almost cylindrical silhouette, can be characterized by its diameter value D_s. When the gas flow rate is high enough, the spout reaches the bed surface and forms a "fountain" of particles in the freeboard. The fountain can be more or less developed depending on the gas rate and the overall system features. After falling on the bed surface, the solids continue their downward travel in the "annulus" surrounding the spout and reach different depths before being recaptured into the spout. The dual hydrodynamics, good mixing in the spout and fountain and piston flow in the peripheral annulus with alternated high and slow interphase transfer, in the spout and (in the annulus respectively), makes spouted beds unique reactors.

Consequently, spouted beds offer very peculiar features, which can be summarized as:

- very regular circulation of particles and absence of dead zones;
- reduced pressure drop and lower gas flow rate required to attain solids motion with respect to the minimum fluidization velocity, this result being possible as the gas transfers its momentum to a limited portion of solids constituting the whole bed;
- wide range of operating conditions starting from a value slightly exceeding the minimum spouting velocity;
- possibility of handling coarse particles having a wide size range and morphology.

The pressure drop across the bed is always lower by at least 20% (Nemeth J. and Pallai I., 1979) than the one required to support the weight of the bed. From this point of view a spouted bed is qualitative similar to a fluidised bed with channelling (Zenz F.A. and Othmer D.F., 1960).

In a spouted bed system, the agitation of the entire hold-up is achieved by the gas jet, which also provides an intimate contact between the particle and the gas, both in the jet and in the annulus, the latter being fed by the gas crossflow from the spout.

Consequently, the axial pressure gradient in the annulus varies with height, rising a maximum value at the top, while in standard fluidized bed the pressure gradient is constant

Another important feature that characterizes the spouting against other fluidization technologies is a mean reduced segregation within the solid phase. Segregation occurs, when two or more solid phases are not theoretically mixed by the gas flow; typically the light phase migrates to the top, thus generating the so-called "flotsam", while the heavy one sink to the bottom to give origin to the "jetsam". This event has to be avoided, especially in thermal processes, where the light reacting phase has to be surrounded by the inert and dense phase to optimize thermal transfer. In this case hot-spots are minimized. Standard fluidization reaches this condition only at very high flow rates
A simple test can be carried out to understand better segregation: a 5 cm cylinder with a performed plate at the base, was charged with rice husk (light phase, ≈ 250 kg/m^3) and silica sand (dense phase, ≈ 2500 kg/m^3); to emphasize this phenomenon, rice husk is set at the base, Figure 2.7 (A). After 5 min of fluidization at 1.5 U_{mf}, Figure 2.7 (B), the light phase has migrated totally to the surface, while the sand has sunk.

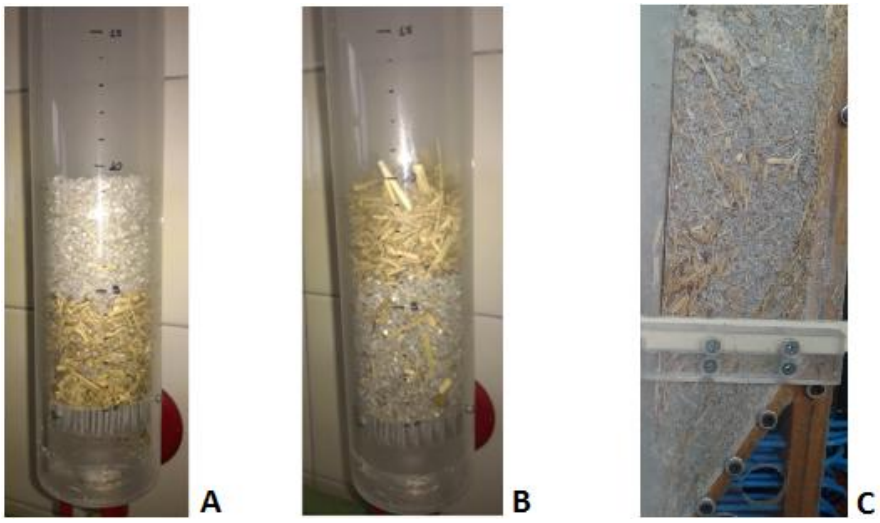

Figure 2.7 – Segregation and mixing phenomena in bubbling bed, compared to a spouted bed. A: initial set-up, B: regime condition, C: spouting effect.

The same experiment performed in a spouted bed reactors, gives a completely different result, as shown in Figure 2.7 C.
The test confirms that a spouted bed reactor appears to be an optimal choice to perform thermal valorisation of solids having very different physical properties. Our interest is focused on fibre scraps a light biomass in an inert bed of sand, by preventing segregation.

3 Scaling a spouted bed

3.1 Scale-up criteria

Due to the peculiarities of spouted beds, their application to industrial processes requires a sound experience and a clear vision of their hydrodynamics since scale-up from laboratory experience is required.
The technological transfer from smaller to larger units is an important engineering aspect; it cannot be achieved only through a linear increment of the geometrical parameters, as the hydrodynamic stability has to be preserved.
The scale-up of a spouted bed has not consolidated criteria up to now; there are no established procedures for this (Grace J.R. and Lim C.J., 2011); a summary of industrial implementations appears in the recent book on spouted beds by (Epstein N. and Grace J.R., 2011) together with general criteria, though the issue remains open.
Spouted bed reactors have been developed with a cylindrical geometry; literature is full of laboratory experiments, with typical diameter of the column ranging between 80 to 200 mm. The key point is to know whether it is possible to predict spouting behaviour in larger columns using only dimensional similitude or if the wall-effects and the ratio between the particles and column diameter play an essential role for the scale-up.
From literature review (Nemeth J. et al., 1983) it appears that the column diameter should not exceed 12 times the gas orifice size to be far from the region of instability characterized by dead zones; additionally it is suggested to maintain the ratio between the particles and gas orifice diameter less than 25 (Chandnani P.P. and Epstein N., 1986). Considering the most common particles processed in spouted bed, the column diameter should not exceed 1 m. Nevertheless, few works in literature have been performed by means of columns with such a size of diameter, but in some of them (Lim, C.J. and Grace J.R., 1987 and He Y.L. at al., 1992), it is clearly evident that the possibility to have dead zones increase with larger columns.
Furthermore, as mentioned before, the solid hold-up cannot be increased without limits due to the hydrodynamic limitation given by H_m.
For the sake of completeness, a geometrical configuration, which helps scaling-up, is given by the so called slot-rectangular spouted beds, name suggested by Freitas et al. (2000), following the concept of two-dimensional spouted beds promoted by Mujumdar (1984). This configuration has a planar configuration, in which two parallel faces are

connected at the bottom with a sloping lower section; the gas is injected through a slot at the bottom. In comparison to the cylindrical configuration, the increment of the volume can be achieved by extending the bed in transversal direction.
For large columns, another possibility is to provide several gas feed ports; in this configuration it is possible to arrange a plenum chamber under the bed to connect all the orifices or arrange a single piping for each entry point. This configuration leads to consider the overall system into several spouted bed reactors in parallel. An evolution of this concept has been developed by means of vertical baffles installed between adjacent module in order to approach a plug flow residence time (Beltramo C. et al., 2009).
In conclusion, the scale-up a spouted and spout-fluid beds can be tackled according two approaches:

- increasing the size of a single unit, or
- repeating side by side several units.

Both routes must be discussed in terms of advantages and drawbacks. The first approach implies a simple geometry and mechanic construction: some doubts arise on the validity of the existing correlations and the overall hydrodynamics in the unit (gas distribution between spout and annulus, solids circulation, etc.). The use of the existing correlations up to a unit diameter (D_c) of about 0.6 m is generally thought fully safe. If a continuous operation is considered, this arrangement gives the solid particulate material a well-mixed behavior with a broad distribution of particle residence time at the exit of the unit.
The first approach for multiple spouting geometries, essentially divides the overall system into modular units in parallel. The bottom plate, conical or flat, presents several opening from which the gas enters in the reactor; it can be fed from a common plenum chamber or each entry point is independently regulated. When the orifices are connected all together, the stability may be difficult, since the local pressure drop can create instability and some orifice may become inactive (Chen Z.W., 2007).
Conversely, if a sequence of multiple beds is realized, achieving a complete non-interaction of the units becomes the fundamental goal. In other words a non-interfering system must be designed, so that it is up to the operator decide which unit has to be started-up or shut-down, first according to process needs. Due to the complexity of a multiple system, each unit must mandatorily replicate the foreseen behavior of the basic component. In this case, the residence time distribution of the solids approaches closely a plug flow to meet most of continuous process requirements.
The design and the construction of a multiple unit implies a careful geometrical optimization to minimize heat loss, investment and operating costs, assure a straightforward start-up, guarantee stability and process performance. According to this key requirement, squared-based units could replace a standard round section geometry, according to an account presented in literature (Beltramo et al., 2009 and Rovero at al. 2011). A correlation between cylindrical and square-based units is also needed.

From this point of view, the use of a square section geometry makes the apparatus more compact. Conversely, some doubts can arise by using this type of geometry, the hydrodynamic features must be checked and the literature correlations verified.
For all these reasons, the geometry taken into account for this PhD work is the square one; therefore it is necessary to lead a carefully study in terms of hydrodynamics, stability and possible technological performances.

3.2 Laboratory equipments

All the fluid dynamic experiments at room temperature have been performed in DISAT laboratories, the Department of Applied Science and Technology of Politecnico di Torino.
A simplify block diagram of all the rigs and piping available for the tests is shown in the following Figure 3.1:

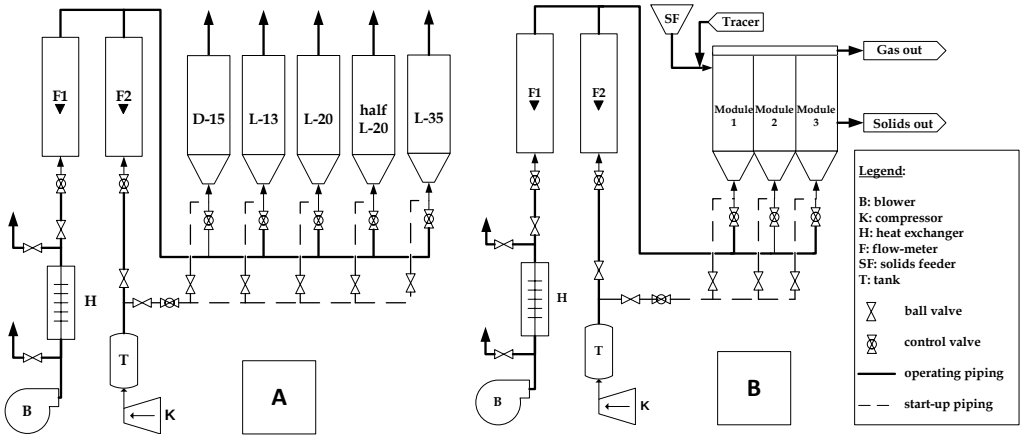

Figure 3.1 – Block diagram of the laboratory facilities. A) Batch units; B) Continues unit.

The experimental apparatus can be divided in four macro areas:

- air supply;
- spouted bed vessels;
- gas cleaning;
- continuous solid feeding.

- Air supply

The spouting gas can be taken from two sources: a blower or a set of compressors; if necessary, by providing a proper pressure regulation, the two streams can be merged.
The compressed air is directly provided by the department facilities, by means of two compressors and a 3 m^3 vessel in which the gas is stocked at 8 barg; a regulating valve is set to give an outlet pressure of 1.2 barg. Spouting gas can be provided even through a centrifugal pump, which gives a downstream pressure of 1.2 barg; due to compression

work, the air is heated to about 80°C, so that a water heat exchanger is used to maintain the air temperature at room conditions.
Three flow-meters, placed on a rack, measure the volumetric flow rate of the spouting gas and, thanks to a series of valves, it can be routed to each units as desired. Additionally, each flow-meter is connected to a manometer in order to properly calibrate the readings.

Table 3.1 – Working range of the installed flow-meter.

Flow-meter I.D.	Lower limit, Nm^3/h	Upper limit, Nm^3/h
F-a	25	250
F-b	30	150
F-c	8	50

- Spouted bed units

The air coming from the flow-meters, thanks to a sequence of sphere valve set in parallel, can be send independently to any spouted bed unit installed in the laboratory.
The field of fluidization on spouted bed reactors has been carried on in Politecnico di Torino from many years, but since the research on square based spouted bed is almost recent, most of the units taken into account for this PhD work were expressly built for this research.
The experimental units (Figure 3.2) arranged in the laboratory are listed below, additional details will be given later:

- D-15: following the standard guideline, this is a cylindrical spouted bed, made in Perspex with 150 mm internal diameter;
- L-13: squared-based spouted bed, made in wood and Perspex with 130 mm side;
- L-20: square-based spouted bed, made in wood and Perspex, with 200 mm side;
- L-26: square-based spouted bed, made in wood and Perspex, with 266 mm side;
- L-35: square-based spouted bed, made in carbon steel, with 350 mm side;
- HsL-20: this is an half-section 200x100 mm unit, characterized by several peculiarities; extra feeding points for gas at the base, turn it in the so called spout fluid bed; a gas distributor at the pyramidal frustum wall modify this unit into a spout-fluid bed
- MsL-20: this unit includes a cascade of three reactors L-20 in series; the possibility to introduce continuously the solids inside the reactor makes this unit suitable for continuous operations.

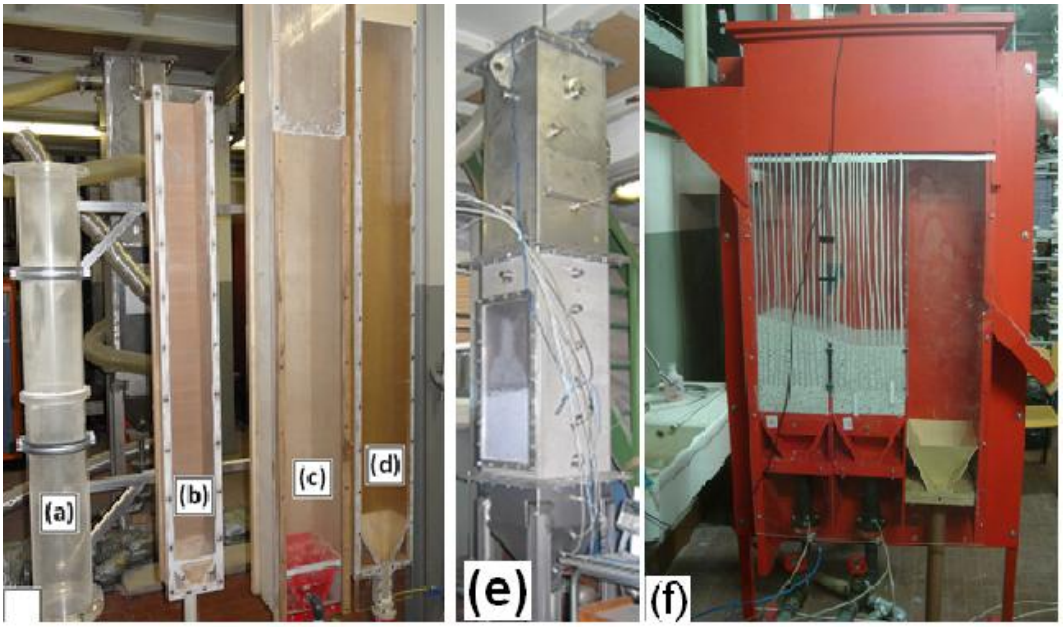

Figure 3.2 – Experimental units: A) D-15, B) L-13, C) L-20, D) HsL-20 E) L-35 F) MsL-20.

Several pressure probes are applied to each reactor to define the pressure drop across the bed, or through a cross section of it. As shown in Figure 3.3, the pressure probes are made by a water U-manometer, composed of a couple a steel capillaries staggered of 25 mm; each side is connected to a U-tube filled with water so that it possible to measure the pressure drop along 25 mm of bed. A frame installed at the top of each vessel can hold up to six probes and gives the possibility to move them up and down in order to complete the pressure mapping inside the reactor. If necessary, any U-manometer is connected one side only, determine the local gauge pressure, i.e. the pressure drop relative to the bed free surface.

Figure 3.3 – Water manometers and detail of the pressure drop sampling system.

- Gas cleaning system

An aspect intrinsic to any fluidization process, is the particle comminution, due to three different mechanisms: impact, crushing and attrition (Khoe at al., 1984); the spouted bed reactor is affected by this inconvenience. Therefore, for cleaning and for safety reasons, downstream the spouted beds, a gas cleaning section has been designed.

A swinging collector can reach to of each spouted bed to draw away by suction, and filter in a bag, the outgoing air. As an ultimate operation, water spray scrubbing allows to re-introduce the air into the environment.

- Continuous solid feeding

The spouted bed unit named MsxL20, works in continuous fashion and the particles are feed through a system that allows a good regulation and suitable.
The particles stocked in a 1 m^3 vessel placed over the unit under investigation, flow by gravity through several calibrated orifices to set the desired flow rate.

3.3 Comparison between cylindrical and square-based geometry

Spouted bed reactors have been developed with a cylindrical geometry and most of the correlations mentioned in the literature were obtained and consolidated for this configuration. Ahead of considering a scale-up realized by repeating several squared section units in series, it is important to evaluate the hydrodynamical behaviour of a single square based unit.
The first step is to compare two identical cross-sectional area reactors, to check the validity of the fundamental literature correlations, as well all the stabilities requirements. Two spouted bed units, named *D-15* and *L-13*, were built and operated for this purpose.
The first vessel is characterized by a circular section, with an internal diameter of 150 mm, while the second unit has a square section, where the length of the sides was set at 130 mm. Both units bases have an included angle of 60°: in the first case it is a truncated cone, while in the other unit the base is a pyramidal frustum. Since the experiments were planned at room temperature, these modules were built with plywood and a Perspex frontal face. The transparent wall was fundamental to detect trajectories, velocities and the global behaviour as well.
The ratio between gas inlet and the base has been taken between 1/2 and 5/6, balancing the pressure drop and the stability (M. Olazar at al., 1992). Furthermore, as specified in the literature works (Crudo at al., 2008), the spout orifice, extend up 1 mm from the base to improve the solids circulation at the bed bottom. The vessels are as high a 1.5 m to allow the measurement of the maximum spoutable bed depth. Table 3.2 provides additional geometrical features of these units.

Table 3.2 – Geometrical parameters of *D-15* and *L-13* units.

Geometrical parameters			*D-15*	*L-13*
Section			Cylindrical	Squared
Material			Perspex	Wood + Perspex
Column diameter / side	D_c	mm	150	130
Section	A_c	m^2	0.017	0.017
Inlet diameter	d_i	mm	14	14
Included angle at the base	γ	deg	60	60

Several solid types have been used to analyze and compare the spouting conditions in both cylindrical and square-based units, in a wide range of hydrodynamical conditions; for this set of tests, the solids used are defined in Table 3.3 and shown in Figure 3.4.

Table 3.3 – Physical properties of solids, (*) Source: Hayakawa and Oguchi, Evaluation of gravel sphericity and roundness bases on surface-area measurement with a laser scanner.

Material	Equivalent mean diameter	Bulk density	Sphericity	Repose angle
	d_p	ρ_s	Φ	α
	mm	kg/m^3	/	deg
PET chips	3.04	1336	0.87	35
Turnip seed	1.5	1081	1	27
Corn	7.82	1186	0.8	27
Soya beans	7.23	1144	0.99	29
Sunflower seeds	6.16	696	0.87	37
Sand	1.84	2510	0.85 (*)	30

Figure 3.4 – Solid particles used in the reactors

The set of experiments conceived to compare the behaviour of the two geometries were based on a single composition of solids, according to the features given in Table 3.3, i.e. all the particles have the same geometrical features. The selection of solids was done in order to minimize the size distribution (less than 1%); the evolution of these properties follows a careful and representing sampling.
The sphericity has been calculated in according to F.A. Zenz and D.F. Othmer, 1960, while the repose angle following the instruction given by Metcalf, 1965.

$$\emptyset = \left(\frac{Surface\ Sphere}{Surface\ Particle}\right)_{of\ same\ volume}$$

Equation 1

The bulk density was obtained by a pycnometric analysis, measuring the mass of material and its volume, given by the mass of given solvent displace by the material itself.
The goal at this set of experiments was to evaluate the amount of air required to induce spouting from a static bed (spouting velocity onset, U_{os}), and the minimum value that allows stable spouting (minimum spouting velocity, U_{ms}), increasing progressively the bed depth, up to reaching the so called maximum spoutable bed depth, H_m. Finally, the experimental results between cylindrical and squared were compared, upon considering the consolidated correlation.
Many empirical correlations are given in literature and summarized in the following tables:

Table 3.4 – Correlations for U_{ms}.

Author	Correlation for U_{ms}
Mathur and Gishler	$U_{ms} = \frac{d_p}{D_c} \cdot \left(\frac{d_i}{D_c}\right)^{1/3} \cdot \left(\frac{2 \cdot g \cdot H \cdot (\rho_s - \rho_f)}{\rho_f}\right)^{1/2}$
Wu et al.	$U_{ms} = 10.6 \cdot (2 \cdot g \cdot H)^{0.5} \cdot \left(\frac{d_p}{D_c}\right)^{1.05} \cdot \left(\frac{D_i}{D_c}\right)^{0.266} \cdot \left(\frac{H}{D_c}\right)^{-0.095} \cdot \left[\frac{(\rho_s - \rho_f)}{\rho_f}\right]^{0.256}$
Olazar et al.	$U_{ms} = \left(\frac{d_p}{D_c}\right) \cdot \left(\frac{D_i}{D_c}\right)^{0.1} \cdot \left[2 \cdot g \cdot H \cdot \frac{(\rho_s - \rho_f)}{\rho_f}\right]^{1/2}$

Table 3.5 – Correlations for H_m.

Author	Correlation for H_m
Malek and Lu	$\frac{H_M}{D_C} = 418 \cdot \left(\frac{D_C}{d_p}\right)^{0.75} \cdot \left(\frac{D_C}{d_i}\right)^{0.40} \cdot \left(\frac{\lambda^2}{\rho_s^{1.2}}\right)$
McNab and Bridgwater	$H_M = \frac{D_C^2}{d_p} \cdot \left(\frac{D_C}{d_i}\right)^{2/3} \cdot \frac{700}{Ar}\left(\sqrt{1 + 35.9 \cdot 10^{-6} \cdot Ar} - 1\right)^2$
Thorley et al.	$H_M = {U_{mf}}^2 \cdot \left(\frac{d_c}{d_p}\right)^2 \cdot \left(\frac{D_c}{D_i}\right)^{2/3} \cdot \frac{\rho_f}{2 \cdot g \cdot (\rho_s - \rho_f)}$

Table 3.6 – Other empirical correlations.

Author	Empirical correlation
Fountain height, H_f (Grace and Mathur)	$H_f = {\varepsilon_{spout}}^{1.46} \cdot \frac{v_{p,max} \cdot \rho_s}{2 \cdot g \cdot (\rho_s - \rho_f)}$
Spout diameter, D_s (Bridgwater and Mathur)	$D_s = \frac{0.0071 \cdot G^{1/3} \cdot {D_c}^{3/4}}{{\rho_s}^{1/4}}$
Maximum pressure drop, ΔP_{max} (Malek e Lu)	$-\Delta P_{max} = H \cdot (\rho_s - \rho_f) \cdot (1 - \varepsilon) \cdot g$
Operative pressure drop, ΔP (Mamuro and Hattori)	$-\Delta P = \left(\frac{3}{4} \cdot H_M\right) \cdot (\rho_s - \rho_f) \cdot (1 - \varepsilon_{mf}) \cdot g$

3.3.1 Spouting on-set and minimum spouting velocity

In an industrial operation, the installed blower power is an important cost issue that must be estimated carefully to minimize the investments, but assuring a full and reliable functionality.

This concept is strictly linked to the U_{os} (spouting on-set velocity) and U_{ms} (minimum spouting velocity); which were considered in the following set of experiments.

These gas velocities are strictly linked to operating conditions (solids properties and bed depth).

In a sequence tests the solids load was progressively increased by 50 to 100 mm steps, to record the minimum and on-set velocity.

The following graphs depict the results comparing the U_{ms} and the U_{os} for each solid; the diagrams on the left show the results obtained in the cylindrical unit, while the results from the square one are given on the right.

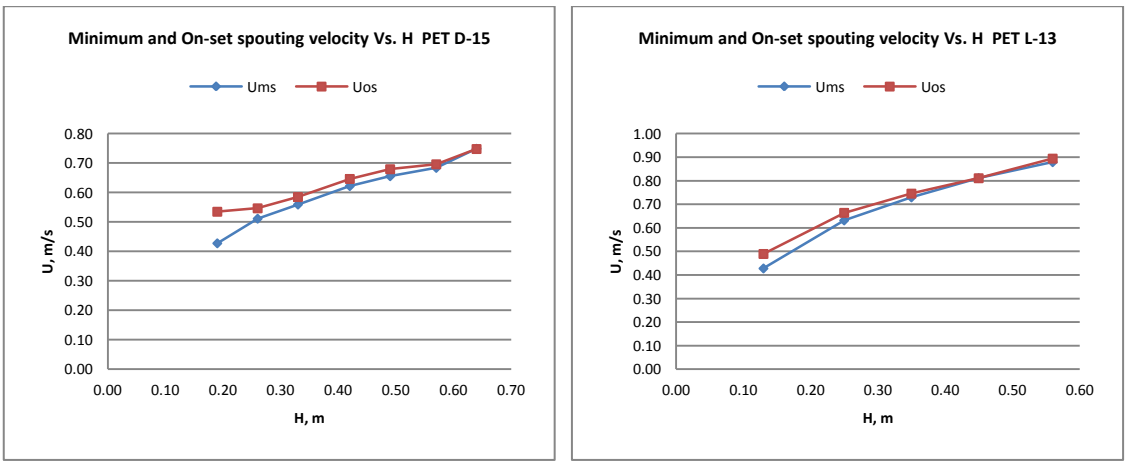

Figure 3.5 – Minimum and Onset spouting velocity in the two geometries for PET.

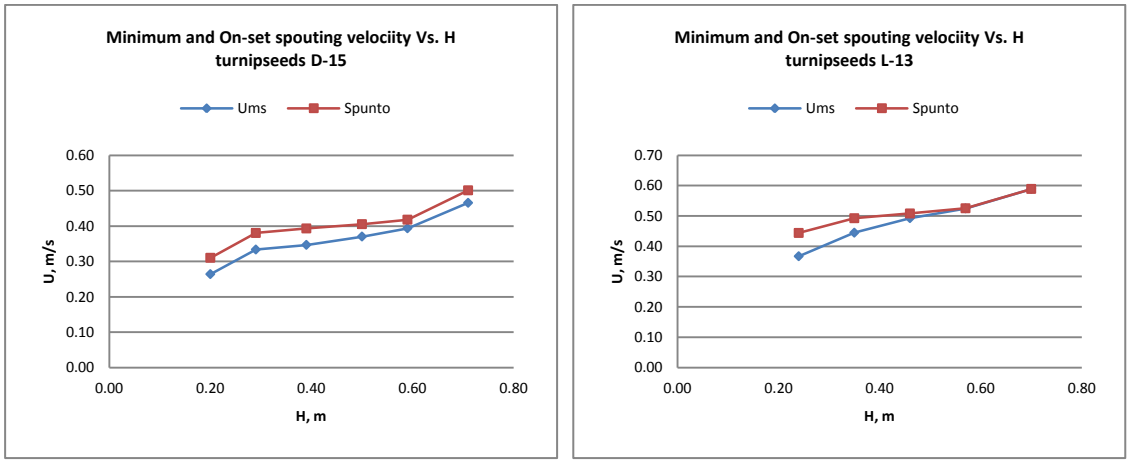

Figure 3.6 – Minimum and Onset spouting velocity in the two geometries for turnip seeds.

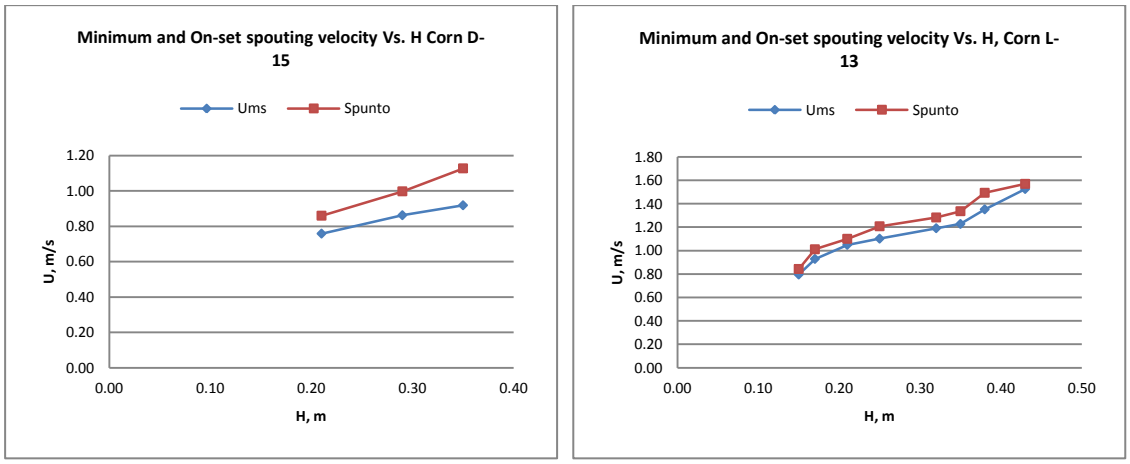

Figure 3.7 – Minimum and Onset spouting velocity in the two geometries for corn seeds.

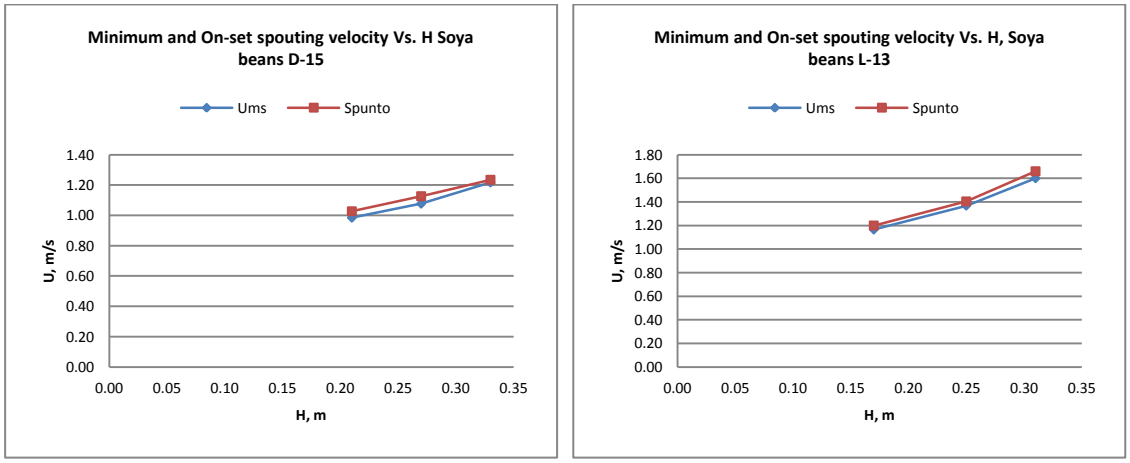

Figure 3.8 - Minimum and Onset spouting velocity in the two geometries for soya beans.

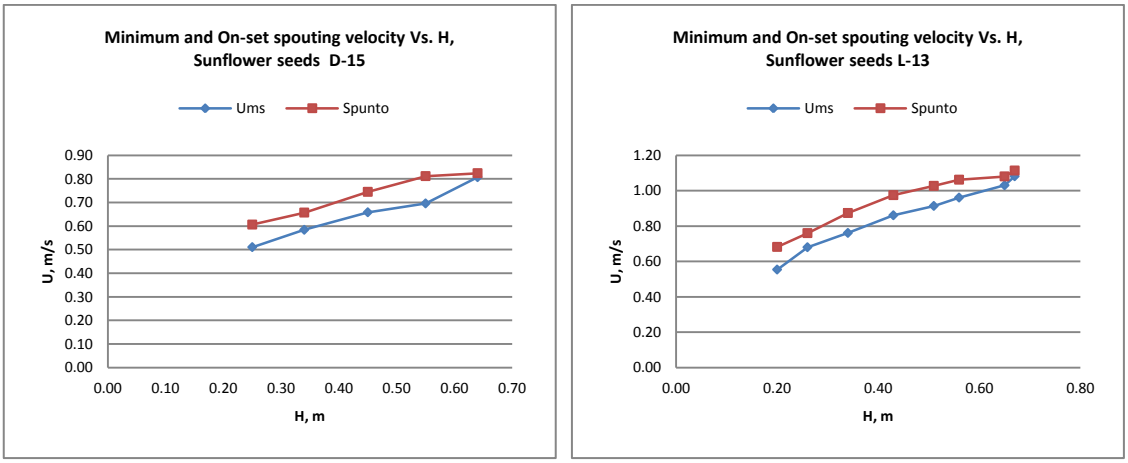

Figure 3.9 – Minimum and Onset spouting velocity in the two geometries for sunflower seeds.

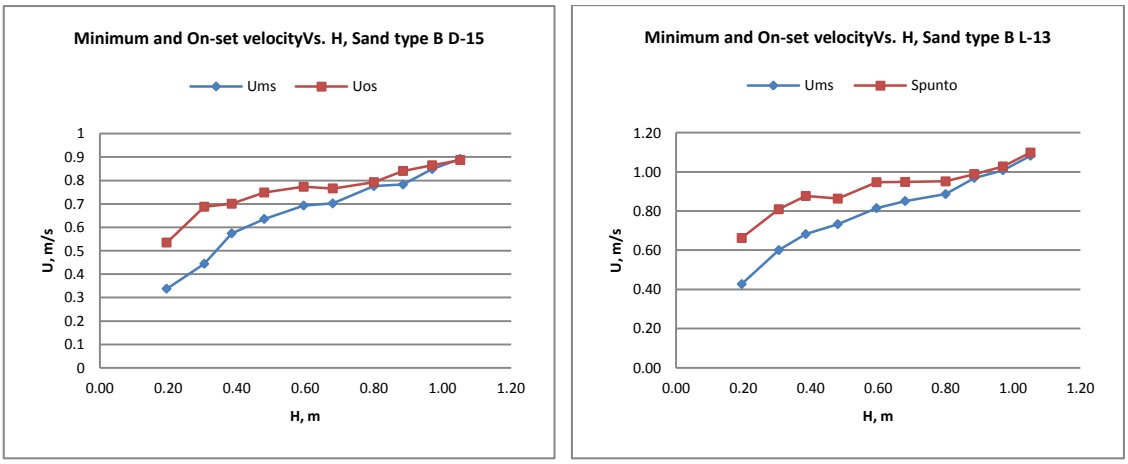

Figure 3.10 – Minimum and Onset spouting velocity in the two geometries for sand type B.

All of the graphs show that the onset velocity curve lays always above to the minimum spouting velocity curves; this is in agreement with the hysteresis phenomenon typical of this fluidization regime. Starting from a packed bed condition, the rate of gas needed to induce spouting is always greater than the necessary to maintain stable spouting. A key feature is that those two curves tend to overlap increasing the bed depth and this gap tends to zero at the maximum spouting bed dept.

This can be explained since the gas velocity in the annulus increases with the distance from the base to approach the minimum fluidization velocity at the bed top, which is not affected to any hysteresis behaviour.

3.3.2 Maximum spoutable bed depth

Beside the gas velocity, the maximum spoutable bed depth represents a fundamental parameter that must be taken into account for stable operations: spouting regime cannot be reached if the bed depth is deeper than H_m.
The front transparent wall of a vessel allows to evaluate easily this parameter, even though it is important to know that the transition between stability and instability is not that neat and the experimental evolution is up to an operator criteria to some extent.
The following Table 3.7 compares the maximum spoutable bed depth values obtained with the two geometries; the repetition of the experimental tests suggest that experimental errors and uncertainly could be estimated in ±5%. Moreover, the same table presents the foreseen values of maximum bed depth from two of the most common literature correlations.

Table 3.7 – Comparison of the maximum spoutable bed depth between cylindrical and square based, for different materials.

Maximum spoutable bad depth, m				
	D-15	L-13	Malek & Lu	McNab & Bridgewater
PET chips	0.69	0.65	0.39	0.65
Turnip seed	0.84	0.85	1.13	0.71
Corn	0.41	0.46	0.19	0.31
Soy beans	0.37	0.36	0.32	0.33
Sunflower seeds	0.68	0.69	0.5	0.37
Sand (B type)	1.08	1.11	0.35	0.93

The key point from the experiments is that the two geometries shown an identical behavior in terms of H_m, as the difference is negligible for all the solids testes. The transparent wall allows to assess that no dead or stagnant zones build up in both the equipments employed.
Malek and Lu and McNab and Bridgewater equation outputs were compared to the experimental data, since they appear to be the more reliable correlations for the solids tested; however, the first works pretty well with some solids and the latter with the others. This can be ascribed from the fact that these empirical correlations are typically optimized for solids as glass spheres or anyhow identical one to each other.

3.3.3 Pressure drop and gas distribution in the annulus

Beside the direct observation of solids trajectories and stability, the distribution of gas has been determined defining the pressure drop across the bed at different elevations. The squared section L-13 has been chosen for this analysis with a solid hold-up of 0.5 m; this test has been performed with PET chips and sand.
In the free-board a fixed frame holds six pressure probes, as depict in Chapter 3.2; these probes are placed along the diagonal and the apothem an connected to some water U-

manometers that give the pressure drop between 25 mm; see Figure 3.11 for more details.

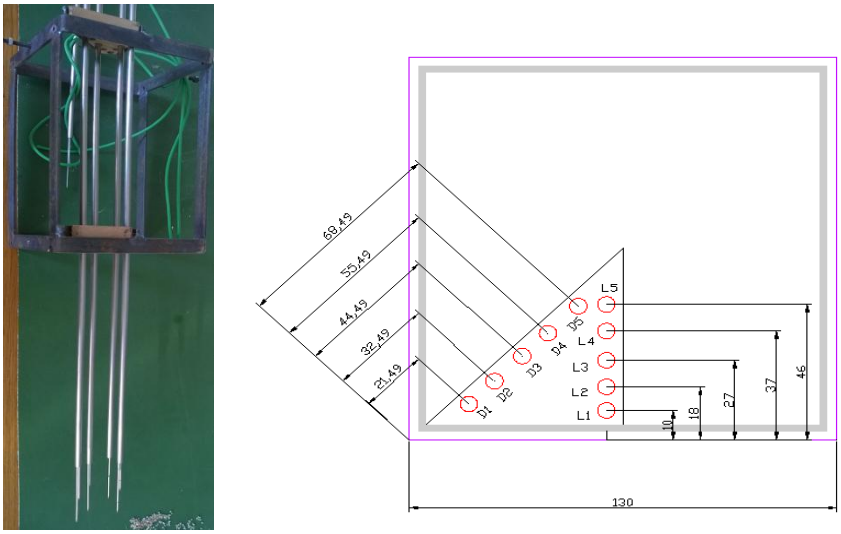

Figure 3.11 – Particular to gas contactor with a similar overall geometry. The sites D1, D3, D5 and L1, L3, L5 are connected to the water manometers giving respectively: ΔP1, ΔP2, ΔP3, ΔP4, ΔP5, ΔP6.

The pressure drop cannot be immediately linked to the gas velocity without a calibration curve. Accordingly, the spouted bed vessel was then modified by means of a gas distributor given by a performed plate, fixed at the frustum vessel, which supplies the gas homogenously.
The calibration curve is obtained by gradually increasing the gas flow rate, to give the flow-meter ready to the pressure drop calibration.
As the gas velocity is constant at different axial coordinates, the six probes, gave always a value included in the sensitivity range (1 mm), independently of their vertical position. To obtain the most reliable calibration, avoid misdistribution from bottom distributor or preferential channelling in the bed upper portion, the probes were set at half bed depth, and the maximum flow rate was set at 0.8 U_{mf} in order to keep the bed packed.

Table 3.8 – Pressure drop across 25 mm in a packed L-13 bed, with PET chips.

PET - Bed depth 0.53 m; Hold-up 7.64 kg								
Air flow		ΔP-1	ΔP-2	ΔP-3	ΔP-4	ΔP-5	ΔP-6	ΔP-Mean
Nm^3/h	m/s	cm H_2O						cm H_2O
23.1	0.4	0.8	0.8	0.7	0.8	0.8	0.8	0.8
27.8	0.5	1	0.9	0.9	0.9	0.9	0.9	0.9
32.6	0.5	1.2	1	1.1	1.1	1.2	1.1	1.1
37.4	0.6	1.5	1.3	1.4	1.5	1.5	1.4	1.4
42.3	0.7	1.9	1.7	1.7	1.7	1.8	1.8	1.8
47.2	0.8	2	1.8	1.9	1.9	1.9	1.8	1.9
52.2	0.9	1.9	1.9	1.9	1.9	1.8	1.9	1.9
57.3	0.9	1.8	1.7	1.8	2	2	1.9	1.9
52.2	0.9	2	1.9	2	2	2	1.9	2.0
47.2	0.8	2	1.9	1.9	2	1.9	1.8	1.9
42.3	0.7	1.8	1.8	1.7	1.8	1.7	1.8	1.8

37.4	0.6	1.6	1.5	1.6	1.6	1.5	1.6	1.6
32.6	0.5	1.4	1.3	1.3	1.4	1.2	1.3	1.3
27.8	0.5	1	1	1.1	1.1	1.1	1	1.1
23.1	0.4	0.9	0.9	0.9	0.9	0.9	0.8	0.9

From the results listed in Table 3.8, it is possible to correlate the mean pressure drop with the gas velocity, to obtain the following correlation:

$$U = 0.365 \cdot \Delta P + 0.124$$

Equation 2

where the gas velocity is expressed in m/s, while the pressure drop between 25 mm is given in cm of water.
The same procedure was followed to originate the calibration curve for sand, and the expression is:

$$U = 0.232 \cdot \Delta P + 0.197$$

Equation 3

The above equations can be used in the annulus of spouted bed where the gas permeates through the particles as in a fixed bed system.
Several data have been recorder by changing step by step the probes vertical position, so that it is possible to define the gas velocity profile across the annular section at different elevations.
This profile has been drawn for three different gas flow rate, namely the ones corresponding to U_{ms}, 1.2 U_{ms} and U_{os}.

<u>Pressure profile using PET:</u>

Table 3.9 – Gas flow and velocity for the experiments planned.

Velocity	Flow rate	Velocity
	Nm^3/h	m/s
A) U_{os}	53	0.88
B) $1.2U_{ms}$	57	0.94
C) U_{ms}	51	0.84

Table 3.10 – Pressure drop across the annulus at different bed depth and for different total gas flow.

Probes elevation, m	Velocity	ΔP-1	ΔP-2	ΔP-3	ΔP-4	ΔP-5	ΔP-6
Probe mean depth:	m/s	cm H_2O (±0.1)					
0.12	A	0.3	0.2	0.3	0.3	0.3	0.3
	B	0.3	0.2	0.3	0.3	0.3	0.3
	C	0.4	0.2	0.4	0.4	0.3	0.3
0.14	A	0.5	0.4	0.4	0.5	0.4	0.4
	B	0.4	0.3	0.4	0.4	0.5	0.4
	C	0.6	0.3	0.5	0.6	0.5	0.4
0.16	A	0.6	0.5	0.5	0.6	0.5	0.6
	B	0.6	0.5	0.5	0.6	0.5	0.5
	C	0.9	0.3	0.6	0.9	0.8	0.6
0.18	A	0.9	0.8	0.8	0.9	0.8	0.8
	B	0.9	0.8	0.8	0.9	0.8	0.7
	C	1.2	1.2	1.2	1.2	1.1	0.9
0.20	A	1	0.9	0.9	1	0.9	0.8
	B	1	0.9	0.9	1	0.9	0.8
	C	1.6	1.9	1.5	1.6	1.4	1.4
0.22	A	1	1	1	1	1	1
	B	1.1	1.1	1	1.1	1	1
	C	1.6	2	1.9	1.6	1.9	1.9
0.24	A	1.1	1.2	1.2	1.1	1.1	1.2
	B	1.1	1.2	1.2	1.1	1.1	1.1
	C	1.1	1.5	1.6	1.1	1.6	1.8
0.26	A	1.2	1.1	1.2	1.2	1.1	1.2
	B	1.2	1.2	1.2	1.2	1.1	1.2
	C	1.6	1.6	1.6	1.6	1.6	1.7
0.28	A	1.3	1.3	1.3	1.3	1.3	1.3
	B	1.3	1.3	1.3	1.3	1.3	1.3
	C	1.6	1.6	1.5	1.6	1.5	1.7
0.30	A	1.4	1.3	1.3	1.4	1.4	1.4
	B	1.4	1.3	1.4	1.4	1.3	1.4
	C	1.6	1.7	1.7	1.6	1.7	1.6
0.32	A	1.4	1.4	1.4	1.4	1.4	1.3
	B	1.4	1.4	1.5	1.4	1.4	1.4
	C	2.1	2.1	2	2.1	2.1	2.1
0.34	A	1.6	1.4	1.4	1.6	1.5	1.5
	B	1.5	1.5	1.5	1.5	1.5	1.4
	C	1.6	1.5	1.5	1.6	1.6	1.7

Pressure profile using sand:

Table 3.11 – Gas flow and velocity for the experiments planned.

Velocity	Flow rate	Velocity
	Nm^3/h	m/s
A) U_{os}	56	0.9
B) $1.2U_{ms}$	51	0.8
C) U_{ms}	43	0.7

Table 3.12 – Pressure drop across the annulus at different bed depth and for different total gas flow.

Probe elevation, m	Velocity	ΔP-1	ΔP-2	ΔP-3	ΔP-4	ΔP-5	ΔP-6
Probe mean depth:	m/s	cm H_2O (±0.1)					
0.12	A	0.6	0.6	0.6	0.6	0.6	0.6
	B	0.6	0.6	0.6	0.6	0.7	0.6
	C	3	1	1.6	1.2	1.6	2.5
0.14	A	0.6	0.7	0.7	0.7	0.7	0.7
	B	0.7	0.7	0.7	0.7	0.7	0.8
	C	2.5	2	2	2.5	2	2.3
0.16	A	1	1.1	1	1	1	1
	B	1	1	0.9	1	0.9	1
	C	2.3	2.3	2.3	2.3	2.3	2.4
0.18	A	1.2	1.2	1.2	1.1	1.2	1.2
	B	1.2	1.2	1.2	1.1	1.2	1.2
	C	2.4	2.1	2	2.2	2.3	2.5
0.20	A	1.2	1.3	1.2	1.3	1.2	1.3
	B	1.2	1.3	1.3	1.3	1.3	1.3
	C	2.2	2.2	2.3	2.4	2.2	2.4
0.22	A	1.5	1.5	1.5	1.5	1.4	1.5
	B	1.4	1.5	1.4	1.4	1.5	1.5
	C	2.2	2.2	2.2	2.2	2.3	2.3
0.24	A	1.5	1.6	1.5	1.5	1.5	1.6
	B	1.5	1.5	1.5	1.5	1.4	1.5
	C	2.4	2.5	2.6	2.6	2.5	2.5
0.26	A	1.6	1.7	1.6	1.6	1.6	1.6
	B	1.5	1.6	1.6	1.6	1.7	1.7
	C	2.3	2.3	2.3	2.3	2.4	2.4
0.28	A	1.7	1.8	1.7	1.8	1.7	1.8
	B	1.7	1.8	1.7	1.7	1.7	1.7
	C	2.4	2.4	2.7	2.4	2.5	2.6

0.30	A	1.9	1.9	1.8	1.8	1.9	1.9
	B	1.8	1.8	1.8	1.8	1.7	1.8
	C	2.5	2.5	2.5	2.5	2.5	2.5
0.32	A	2.2	2.2	2.2	2	2.1	2.1
	B	2	2.1	2	2	2	2.1
	C	2.4	2.6	2.4	2.4	2.5	2.5
0.34	A	2.2	2.1	2	2.1	2.1	2.2
	B	2.2	2.1	2	2	2	2.1
	C	2.7	2.8	2.6	2.7	2.5	2.6
0.36	A	2.1	2.1	2.1	2	2	2.1
	B	2.1	2.1	2.1	2.1	2	2.1
	C	2.1	2.1	1.9	2.1	1.8	2.2

Some considerations could be drawn for what concern the gas profile in the annulus at different bed elevation, total flow rate and relative position of probes.
At first, the total flow of gas that enters in the reactor (A, B or C), splits from the spout to the annulus, and the quantity of gas that passes in the annulus is correlated to this value.
It is easy to see that for each bed elevation and for the three velocities taken into account, the value of pressure drop is quality the same for all the probes, this demonstrate that also the velocity and the flow rate of gas that permeate across the reactor is homogeneous.
In addition, considering the mean pressure drop, the results show that the quantity of air that permeate in the annulus increases with the elevation, due to the continuous transfer of gas from the spout to the annulus.
The above considerations are valid for both PET and sand.
It is important to remark that one of the mechanisms of instability is given by the velocity of the gas in the annulus when approaches the velocity of minimum fluidization: in a spouted bed reactor, the annulus work as a standard fluidized system in which the gas permeates through the particles, the stability is given if the velocity of gas is lower than the minimum fluidization velocity, above which unexpected phenomena for spouting fluidization may occur like bubbling or slugging.
Figure 3.12 for PET and fig Figure 3.13 for sand, show that the gas velocity is always lower than U_{mf}, indeed no instabilities are remarked.

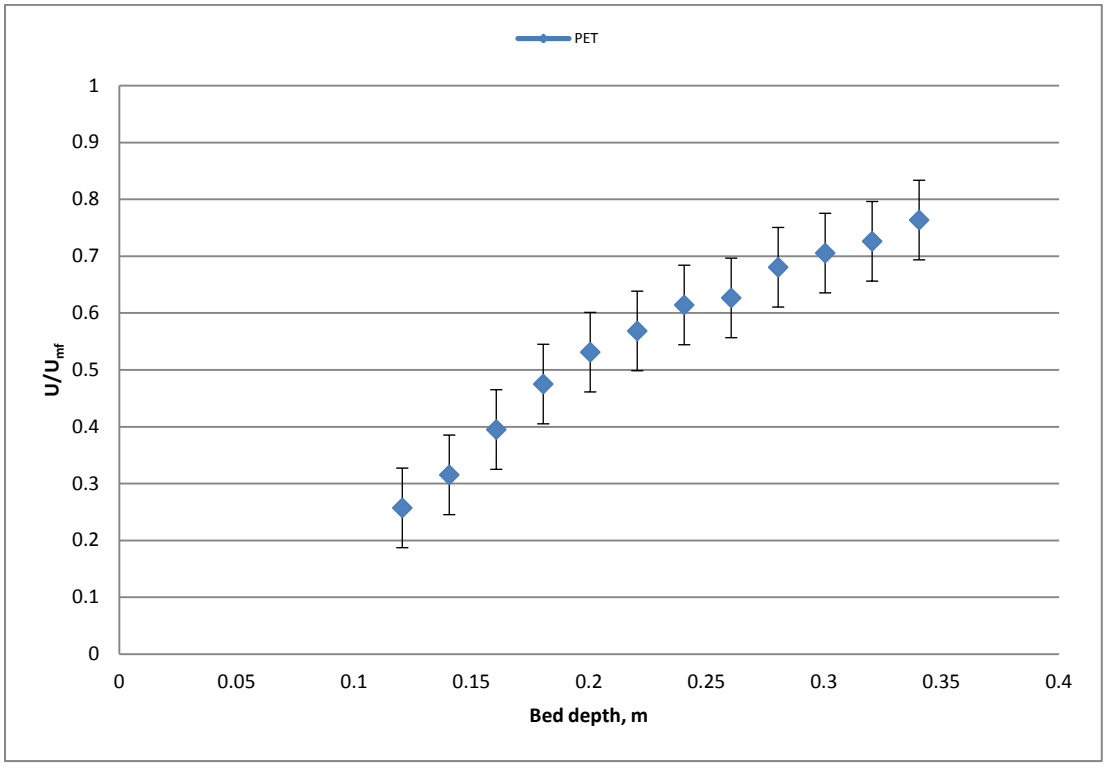

Figure 3.12 – Velocity in the annulus at different bed elevation, compare with the minimum fluidization velocity (PET).

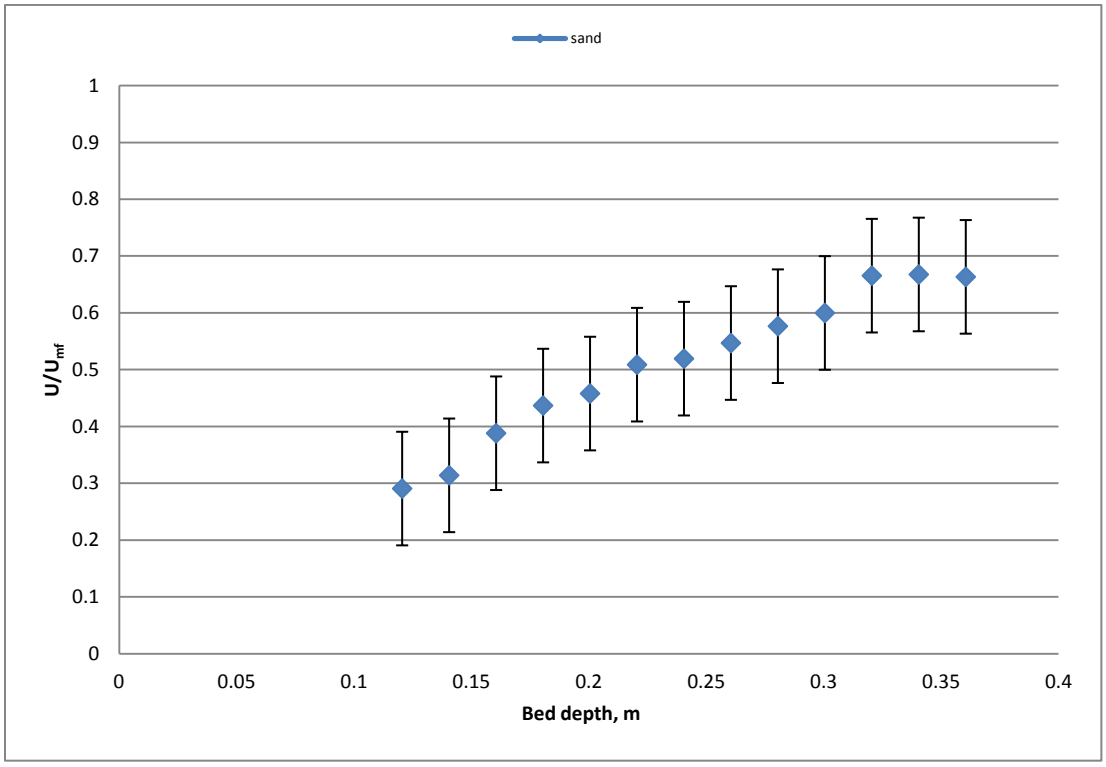

Figure 3.13 – Velocity in the annulus at different bed elevation, compare with the minimum fluidization velocity (sand).

In conclusion, the fluid dynamic behavior of squared units do not move away from the cylindrical ones, since the most important parameters are verified, both through the direct observation than the measurements.

3.4 Additional devices for improvements

The fluid dynamic proper of a spouted bed reactor, can be substantially modified by means of two devices: the draft-tube and the secondary fluidization.
The draft-tube is a pipe placed vertically respect the gas orifice at few centimetres from the base, it aims to channel the gas that enters in the reactor; this configuration could be widely applied since aids the control of fluid residence time and solid cycle distributions.
The secondary fluidization is a geometrical configuration in which several openings at the base feed additional air to the reactor, which can be considered as an hybrid between a spouted bed and a fluidized bed.
These equipments were built and equipped in the half section spouted bed, the most suitable unit for this set of experiments.

3.4.1 Draft tube

One of the first comprehensive work on this equipment, was provided by Grbavčić at al. (1982), but further investigation must be done in the squared section units. Grbavčić demonstrate that the ratio H_d/H, where H_d is the gap between the draft tube and the base, is an important parameter. Even though, from a geometrical point of view, it can ranges from 0 to 1, the inlet section H_d should be greater than a certain value to allow solids circulation, but less than the bed depth, at which the pneumatic transport can't be achieved. Furthermore, the minimum flow rate to produce spouting increases as H_d increases.
The half section spouted bed unit, has in the front a small removable wall which can be replaced with an equivalent one equipped with a draft tube, in this case an half pipe.
Five different types of draft tube can be equipped, see Table 3.13. For three of them (A B C) the difference lies in the distance from the base, while the summit is always set at 450 mm. Draft tube P has the same geometrical features of B, but it is a porous draft tube, in which a series of holes (5 mm diameter and total porosity of 10%) limits, but allows, the cross flow of air from the spout to the annulus; finally draft tube type M is a mobile draft tube, iron made, that can be fix magnetically at the desired bed elevation. All of the draft tubes have an internal diameter of 36 mm.

Table 3.13 – Geometrical feature of the draft tubes.

Type	H_d, mm	L_d, mm	D_{dt}, mm	Note
A	30	420	36	non-porous
B	70	380		
C	115	335		
P	70	380		porous
M	/	330		non-porous

- Maximum bed depth

As previously discussed, H_m represents a fluid dynamic limit that cannot be overcome in a standard spouted bed reactor: the gas injected from the inlet into the spout flows gradually in the annulus, therefore the amount of gas increases with the height; as it reaches a value close to the minimum fluidization velocity, the instability generated denied the spouting regime. A non-porous draft tube limits this cross-flow, since the amount of gas is linked to the gap between the draft-tube and the base (H_d) and does not change any more along the height.
A series of analysis were done in order to verify the influence of a draft-tube, limited in length, in the maximum bed depth. PET chips have been used as solid hold-up and the result have been compared with the situation without draft-tube.
In the following Figure 3.14 the H_m in absence of draft-tube is compared with the result achieved by the implementation of this device.

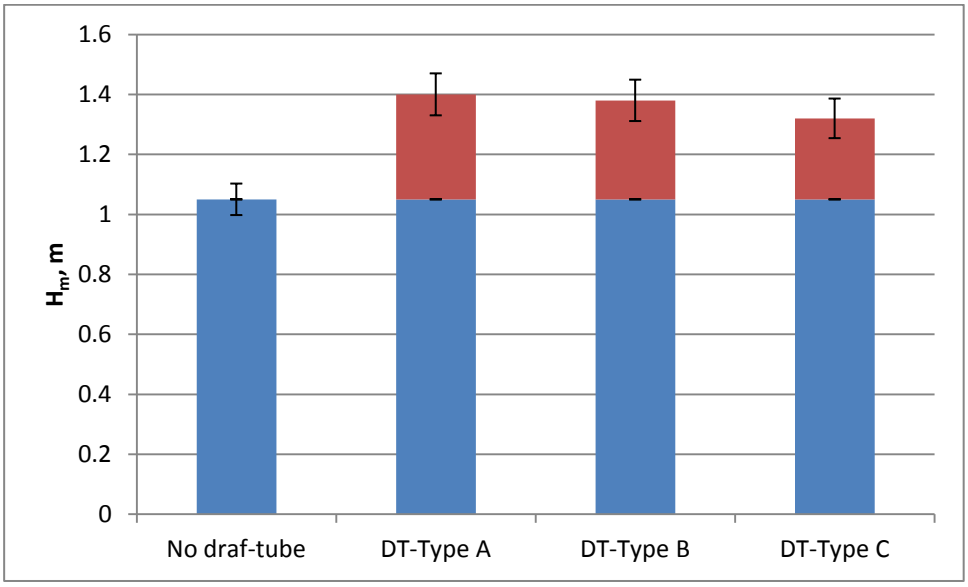

Figure 3.14 – Maximum bed depth, red area represent the increase compared to the absence of draft-tube.

From the Figure 3.14, it is evident that this device increases the maximum bed depth (blue plus red area). Furthermore, it can be established a relationship between the H_m and the length of the draft-tube: from the experimental data, the increment (red area) is equal to the draft-tube length used.

To confirm this aspect, a mobile draft-tube, with a fixed length of 360 mm was adopted and placed at different bed depth; it is a metallic device that can be place as needed and blocked by means of some magnets.

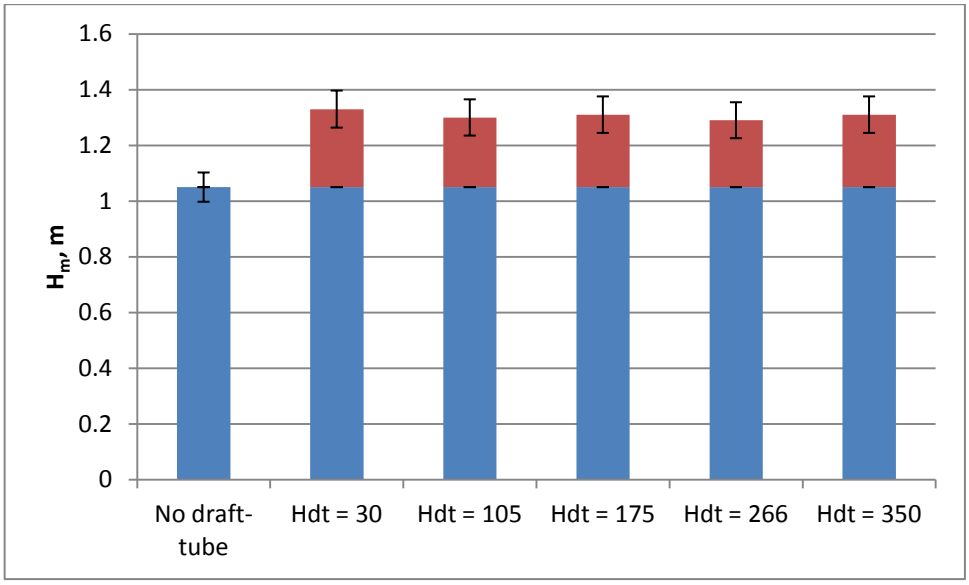

Figure 3.15 – Influence of the positioning of a mobile draft tube on H_m.

By adopting a mobile draft tube, as Figure 3.15 shows, the increment of the maximum spoutable bed depth is lined to the draft tube length, but it is independent from the vertical position of this device: among all the H_d adopted, the values range in less than 30 mm from the average value.

It is important to know that even though the previously results show that H_d does not affect the H_m by keeping constant H_{dt}, some considerations must be done in terms of the management of the start-up phase.

It is know that the hysteresis proper of the spouting regimes entails a boost gas velocity grater then the operative value; however, the start-up with a draft-tube may results problematic, especially if for some reasons, some particles have filled the draft tube. From the experiments performed in this chapter, only the draft-tube type A allows a safety start-up, while is almost impossible with the others.

The experience suggests performing the start-up from an empty reactor and the solids must be carefully charged only if a high gas velocity is granted, about 1.3 U_{os}. Many factors can influence this aspect, like the draft-tube, the solids diameter or the porosity of the draft tube, so that careful investigations must be done for the sizing of this type of device.

As soon as the operative conditions are reached, no problems of stability have been remarked; the use of this device can reduce drastically the air consumption, since the gas flow to maintain spouting, ranges between 35 to 45% compared to the absence of this device. Conversely, no results will be shown concerning the porous draft-tube, since among all, it shows the worst features for start-up, as well as during operative condition.

- Gas and solids flow in presence of a draft tube

The draft-tube is suitable to regulate the solid flow in the annulus, as well as the gas flow rate. The draft tube also reduces the intermixing of solids across annulus and spout; thus reduces the residence time spread of the solids in continuous processes.
As previously discussed, the quantity of gas the passes through the annulus increases with the bed depth, due to the cross-flow from the spout to the annulus. A non-porous draft tube, denied this phenomenon so that the gas velocity is constant along the annulus. The L-13 unit, equipped with a draft-tube and the mobile probes has been used to consider the pressure drop and the gas velocity as well.
A mobile draft tube can be placed at different levels namely 25, 40, 55 and 70 mm from the base (i.e. position A, B, C and D), while the gas velocity can be monitored from 100 to 350 mm. Since the pressure drop across the section is constant, the medium value was considered, while the calibration curve for PET was used to determinate the gas velocity. The air flow rate was kept constant, equal to 1.2 U_{ms}, for all the tests.

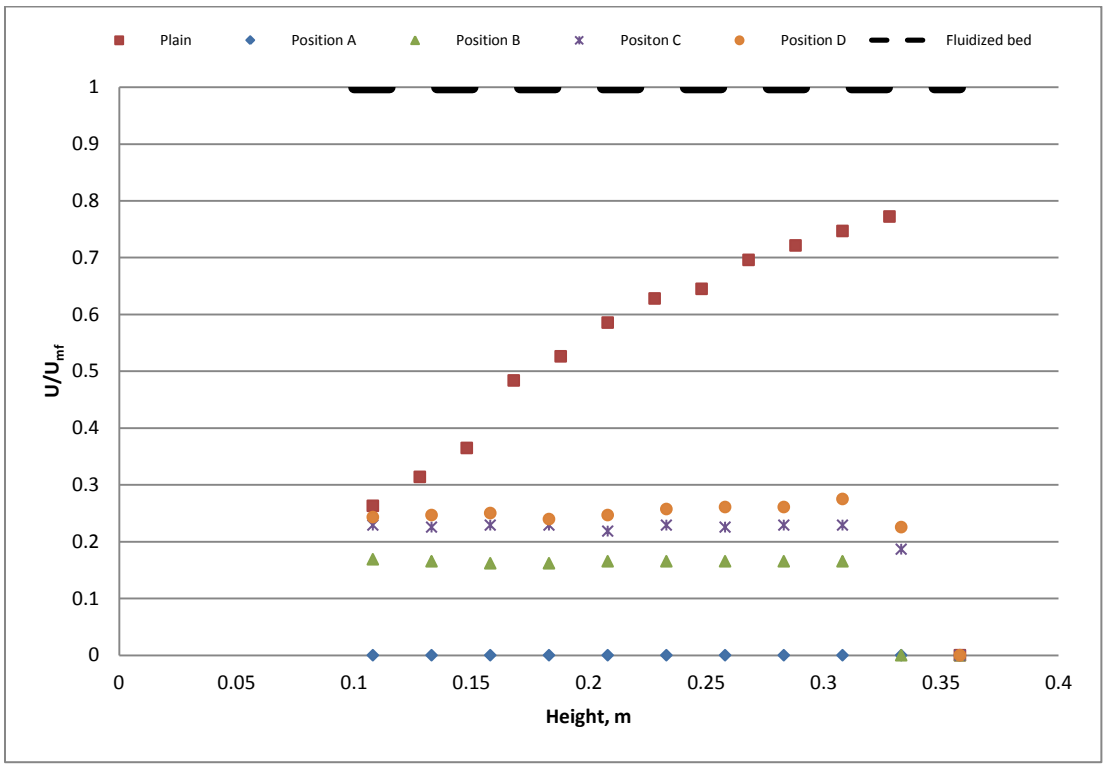

Figure 3.16 – Gas velocity in presence of a mobile draft-tube, compare with the standard configuration.

Figure 3.16 shows clearly that the presence of the draft tube reduces drastically the gas velocity in the annulus, keeping it constant along the bed height. A peculiar behaviour was recorded with position A, the closer to the base, in which the pressure drop across the probe was inferior to the sensitivity of the instrument. Furthermore it is possible to remarks again that the air velocity for the spouting regime, even without draft tube is always lower compared to an equivalent standard fluidized bed.

The use of a draft tube regulates and reduces the inner RTDf of solids in the annulus. To describe this phenomenon, the half-section spouted bed was used to define experimentally the mean residence time of PET chips.
The annulus was equally divided in three areas, corresponding to the solids path: zone A is the closer to the wall, zone B is in the middle section while zone C is the near the spout; each of them has a width of 27 mm.
Figure 3.17 compares the mean residence time of solids in these zones, in presence or absence of the draft tube. In a standard spouted bed, there is an important deviation among the three zones; this can be ascribed as path A is longer respect to the others but even because the particles cross flow between spout and annulus (zone C) drastically reduces the mean residence time in this area.
When the draft tube is employed, the solids residence time in the annulus is similar among the three zones; zone C still remains the faster as the path length is shorter.

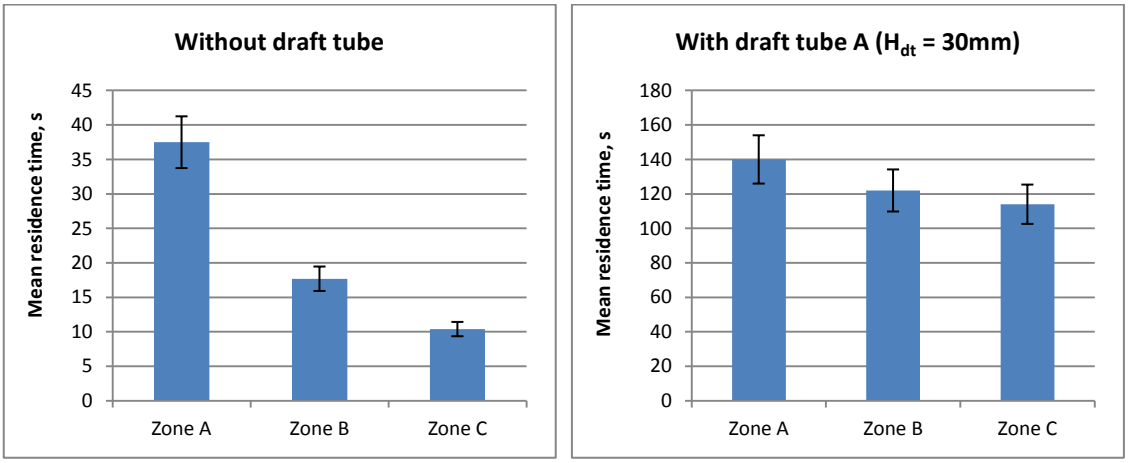

Figure 3.17 – Comparison of the solids mean residence time in the annulus without or with the draft tube.

In addition, the draft tube reduces the solids velocity in the annulus; this reduction is lined to the distant from the base, as shown in

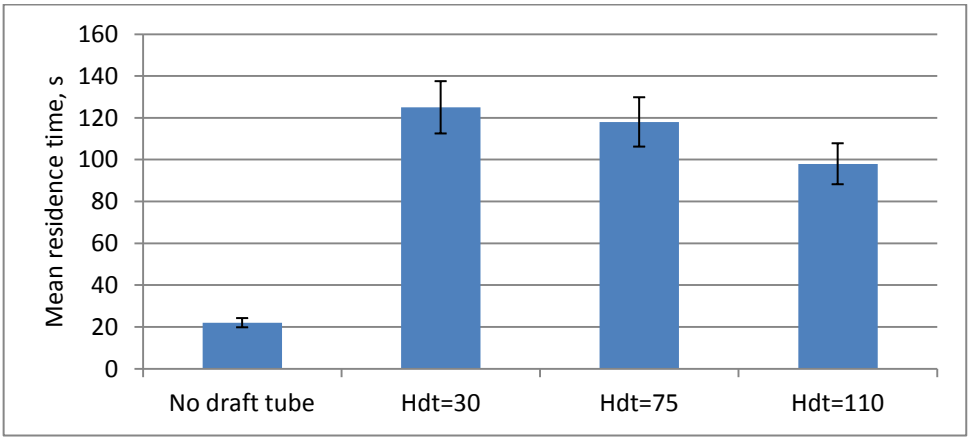

Figure 3.18 – Influence of H_{dt} on the solids mean residence time in the annulus

3.4.2 Secondary fluidization

The secondary fluidization, rather than a real device, is a structural configuration in which an auxiliary fluid flow, through a series of holes, enters tangentially in respect to the main stream. This configuration makes a hybrid reactor that shares some characteristics of both spouting and fluidization, which is especially useful for coarse, sticky or agglomerating solids (Epstein and Grace, 2011). Often, the auxiliary fluidization works together with a draft tube since it allows a fine regulation of fluid in the annulus.
The experimental unit used to investigate on this aspect is the half-section, in which several openings have been placed at the base. In particular six independent layers with holes of 2 mm diameter have been realized drilling the three tilted walls, as shown in Figure 3.11; each layer present a number of openings that depending on its perimeter. The air flow is controlled by an additional flow-meter, while a manifold sends air independently to each layer; pipes are sized in order to balance the pressure drop and assure the same gas flow rate at each opening.

Table 3.14 – Layers for the secondary fluidization.

Layer	n° openings	Distance from the base, mm
A	4	5
B	8	15
C	12	30
D	16	60
E	20	90
F	24	120

The secondary fluidization, besides improving the solid circulation at the reactor base, plays an essential role coupled with the draft tube, since it provides a good regulation of the gas in the annulus. A set of experiments performed with PET chips aims to improve the knowledge on the relationship between the gas velocity in the annulus, solids cycling time and trajectories as a function of the ration between primary and secondary fluidization as well as the type of draft-tube adopted (A, B or C, see Table 3.13)
Tests have been performed at three different hold-up, namely 350, 450 and 600 mm, with a total flow rate (primary plus secondary) kept constant at 1.2 U_{ms}; the results obtained from draft-tube A, B and C have been compared with the configuration without the draft-tube. It must be considered that the pressure drop (and the gas velocity) across the bed, without the draft-tube, depends on the vertical position, anyway for these experiments, the pressure probe was placed at 250 mm from the base.
The trajectory of several particles along the wall was taken into account to estimate the vertical velocity of the solids.

Without draft tube

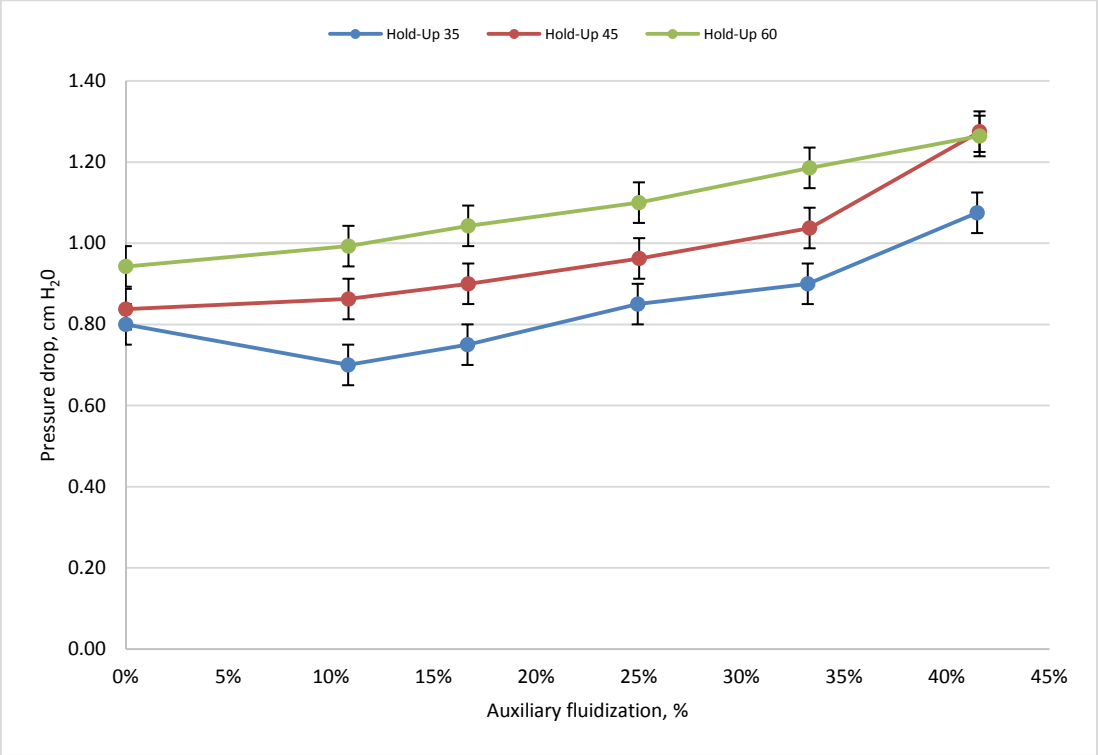

Figure 3.19 – Pressure drop profiles in the annulus as a function of the auxiliary fluidization, without the draft tube

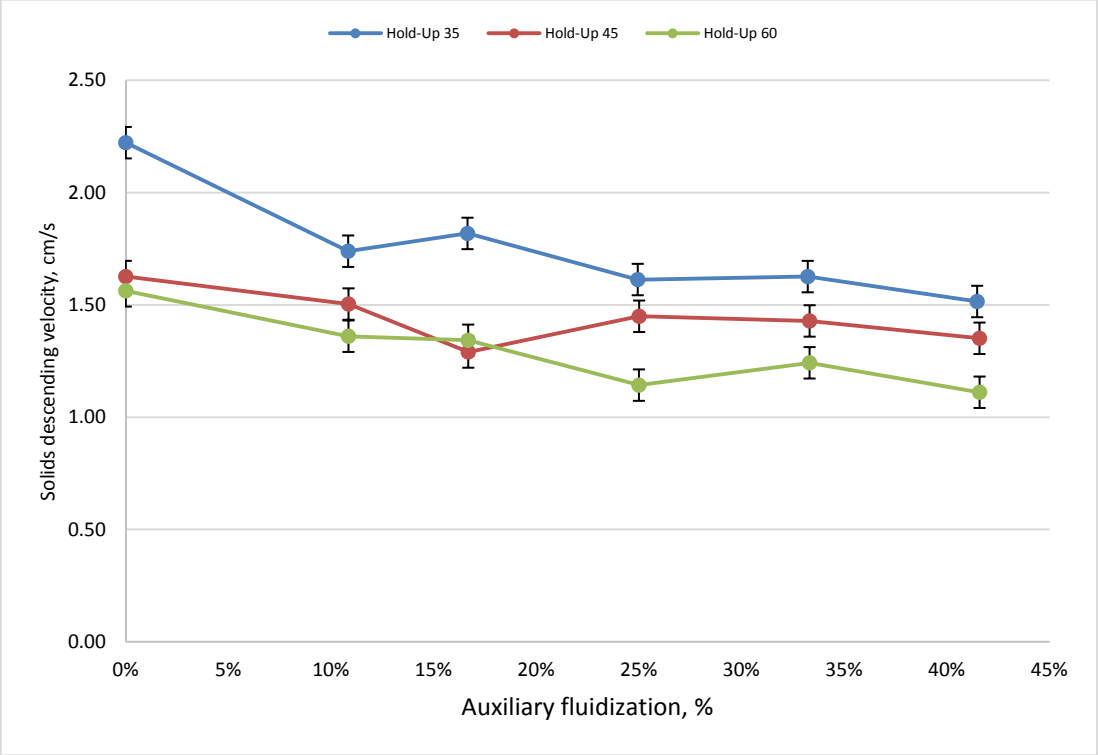

Figure 3.20 – Solids velocity in the annulus as a function of the auxiliary fluidization, without the draft tube

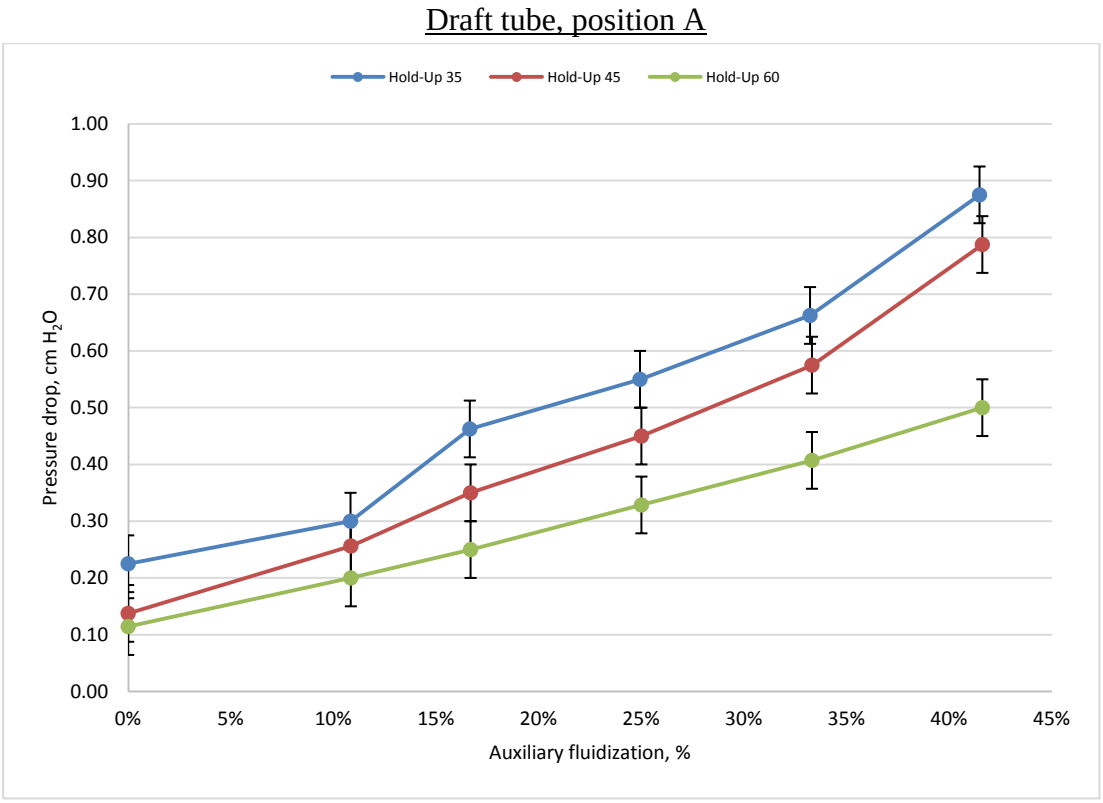

Figure 3.21 – Pressure drop profiles in the annulus as a function of the auxiliary fluidization, draft tube position A

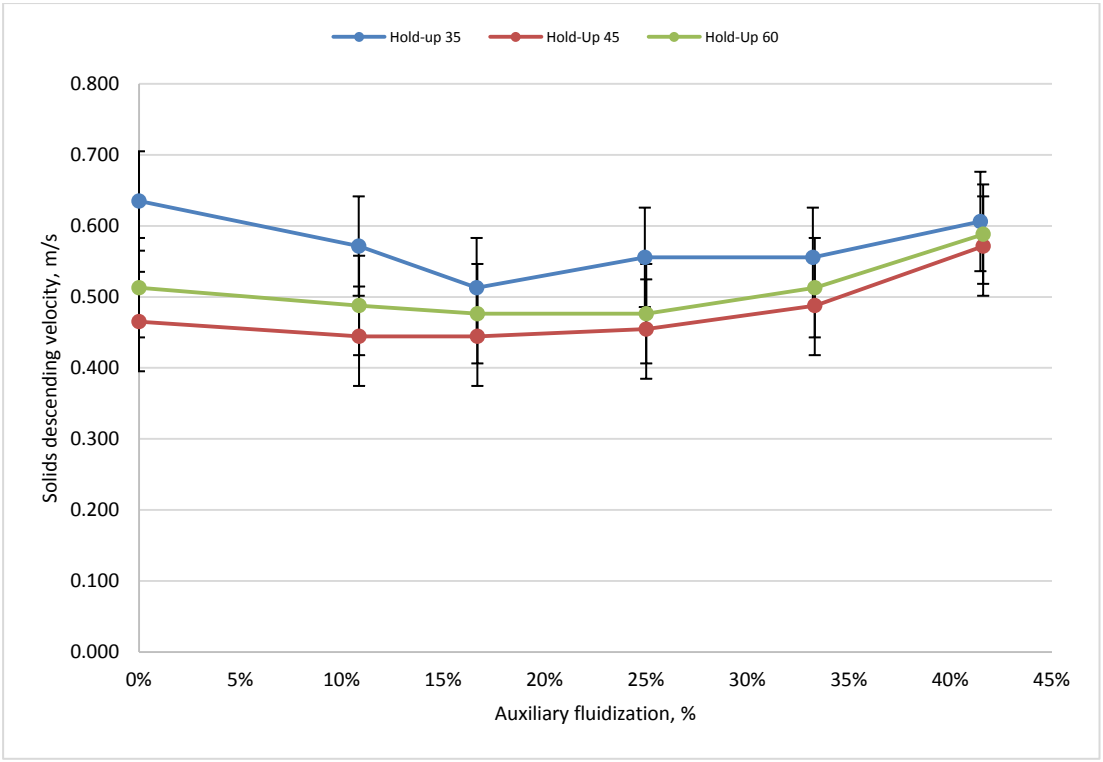

Figure 3.22 – Solids velocity in the annulus as a function of the auxiliary fluidization, draft tube position A.

Draft tube, position B

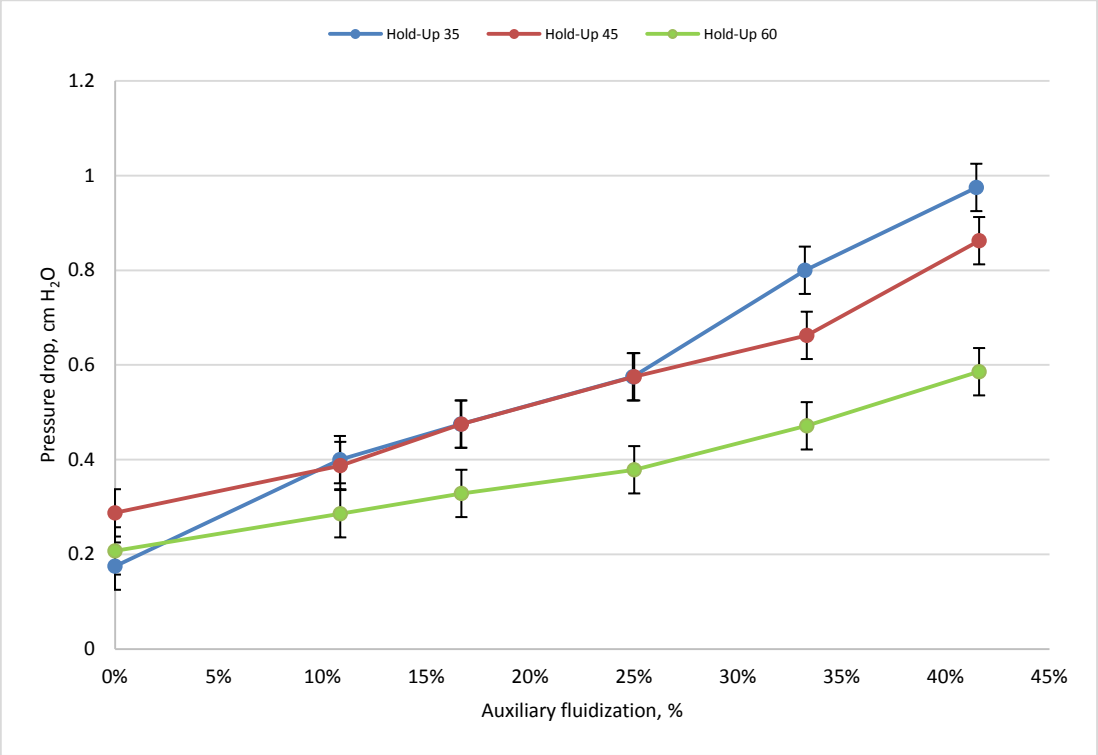

Figure 3.23 – Pressure drop profiles in the annulus as a function of the auxiliary fluidization, draft tube position B.

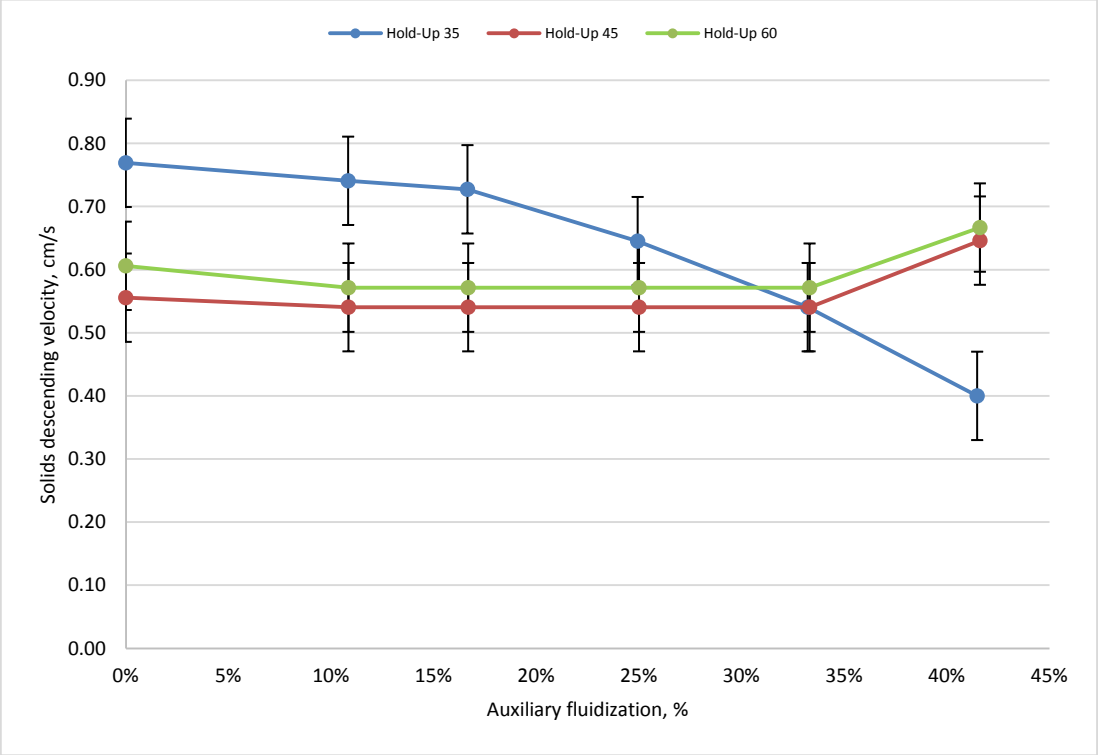

Figure 3.24 – Solids velocity in the annulus as a function of the auxiliary fluidization, draft tube position B.

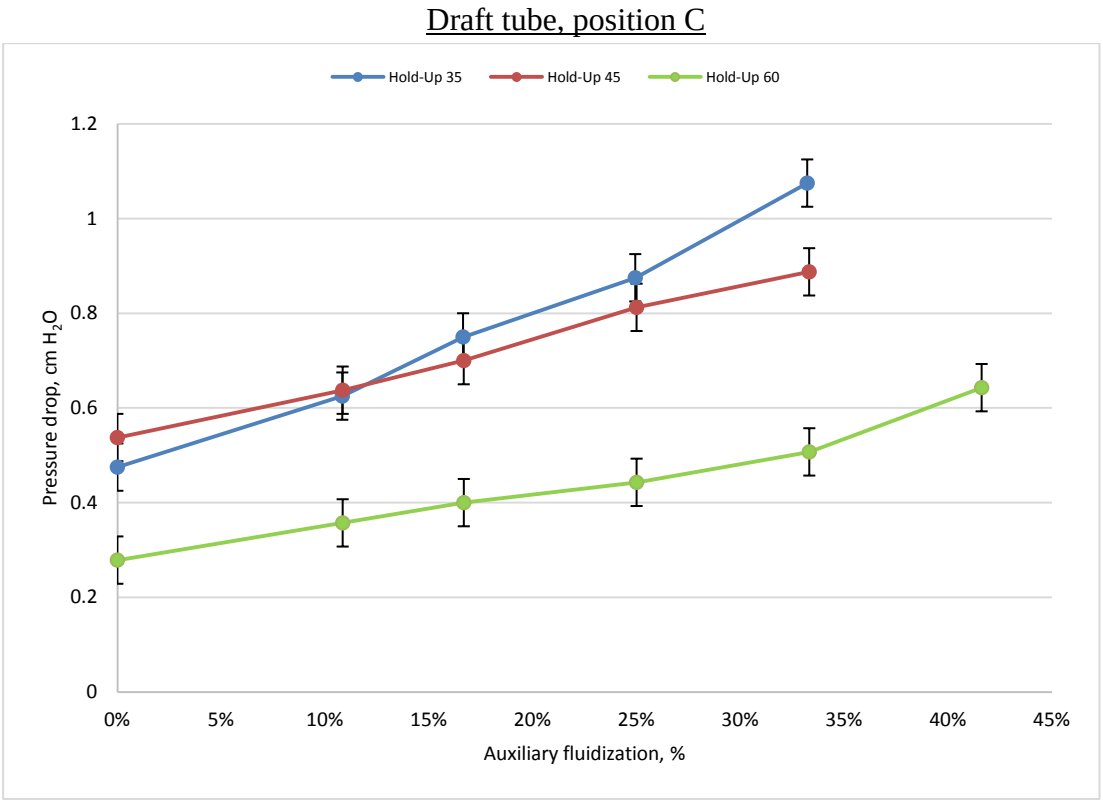

Figure 3.25 – Pressure drop profiles in the annulus as a function of the auxiliary fluidization, draft tube position C.

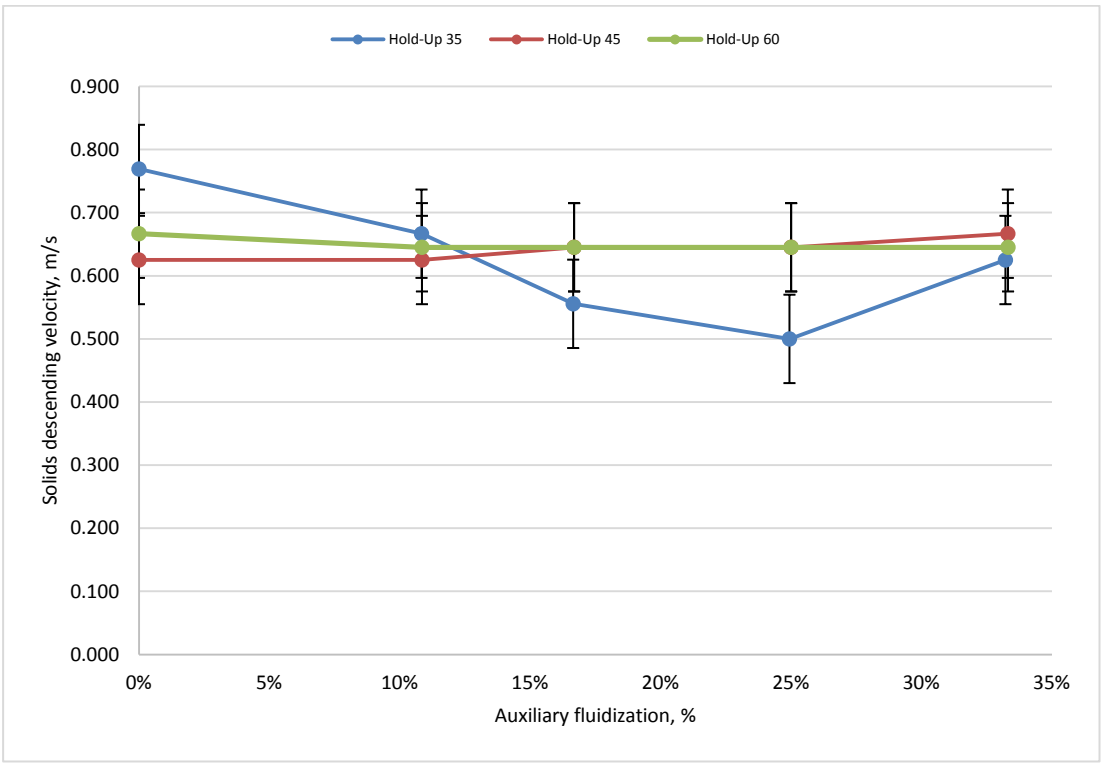

Figure 3.26 – Solids velocity in the annulus as a function of the auxiliary fluidization, draft tube position C.

The auxiliary flow is spread among all the layers, in order to understand better the global behaviour in presence of the secondary fluidization. The results show that the secondary fluidization can be used to regulate the amount of air that pass across the annulus without any negative effects on the stability as long as the primary fluidization is higher than 70%. The gas entering from the secondary fluidization splits between the annulus and the spout, the latter depending on the gap H_d. It is known, (Mamuro and Hattori, 1968), that the pressure drop close to the reactor base is negative, because the high gas velocity from the main inlet creates a sort of depression as Venturi effect; this merges part of the secondary fluidization directly into the spout. As depict in the Figure 3.16 the gas velocity in the annulus is mainly due to H_d, but the effect of the secondary fluidization is grater if the draft tube is positioned close to the base and the Venturi effect minimized.

The solid ascending velocity is not modify at all by the secondary fluidization, even though for a small increment of the auxiliary fluidization, and consequentially the gas velocity, a slightly reduction in velocity was remarked. When the ratio between secondary and primary fluidization approaches the fluid dynamic limit, the particles vertical velocity increase, together with some irregularities in the down flow.

All the results can be summarized in Figure 3.27, which compare the actual gas velocity with the standard configuration i.e. without draft tube and auxiliary fluidization.

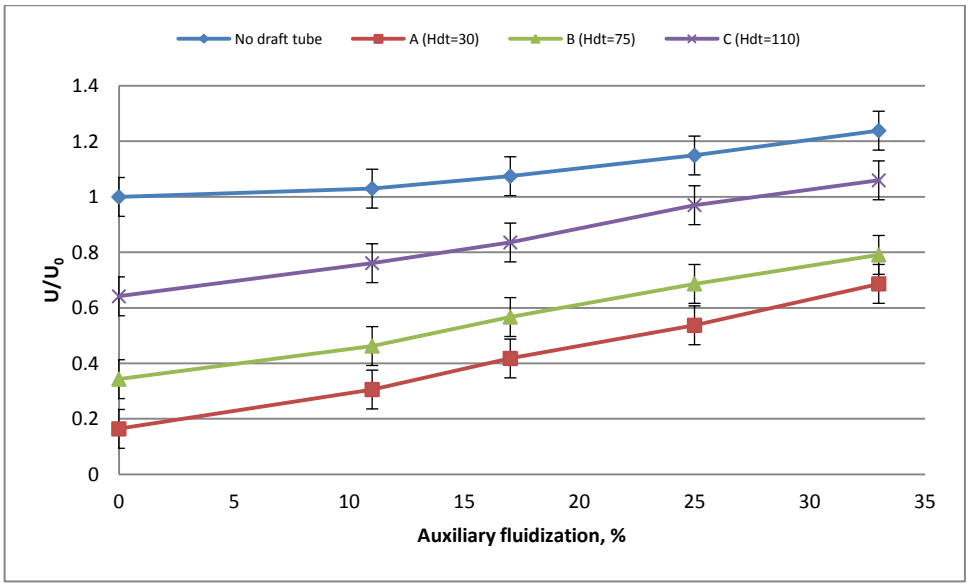

Figure 3.27 – Hydrodynamic effects of secondary fluidization and draft tube on the gas pressure drop in the annulus.

3.5 Hydrodynamics of solid mixtures

Several experimental tests were performed on the L-13 unit to determine the influence of a secondary solid phase in the spouted bed. Segregation is an important aspect to take into account in thermal processes, as the reacting phase is generally drowned in a stationary and inert phase, generally different in shape and density. In a standard fluidized system, the two phases tend to migrate at different bed levels, compromising the global behaviour.
In a first experimental campaign, two cuts of silica sand and wood chips were used to determine the influence of the mean size on the maximums spoutable bed dept and the gas velocity (minimum and onset spouting velocity). A series of sieves were adopted to sift solids; results are summarized in Table 3.15.

Table 3.15 – Mean size of sand and wood particles.

SAND	Diameter, mm	
	min	max
Type A	2.00	/
Type B	1.68	2.00
Type C	1.40	1.68
Type D	1.00	1.40

WOOD	Diameter, mm	
	mean	deviation
Type A	14.9	± 2
Type B	8.7	± 2
Type C	6.5	± 2

This set of experiments makes use of different mixture obtained with Sand B or D together with wood A or C at different concentrations.

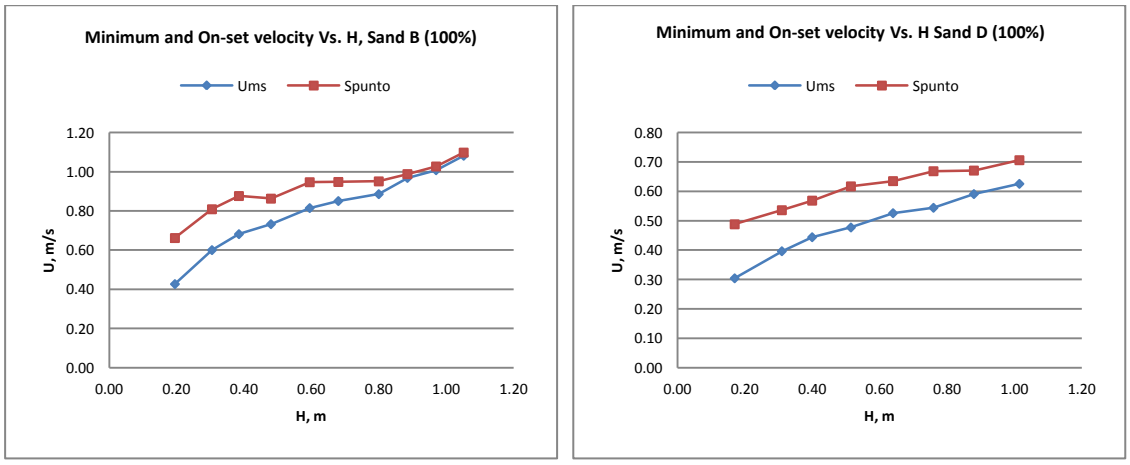

Figure 3.28 – Minimum and Onset spouting velocity with sand at different mean diameter.

As expected, the mean diameter influences the hydrodynamics of the spouted bed, as a reduction in size decreases the quantity of air both for minimum and for onset spouting: this reduction lies between 30 to 40 %. The maximum spoutable bed depth increases with the smaller cut of sand i.e. 1.11 m for sand B and 1.20 for type D.
The results on the maximum spoutable bed depth are summarized in the following table.

Table 3.16 – Effects of bed composition on H_m.

	H_m, m	
	Sand B	Sand D
Sand %	1.05	1.2
Wood C - 3% b.v.	0.97	0.95
Wood C - 10% b.v.	0.87	0.82
Wood C - 30% b.v.	0.8	0.67
Wood A - 3% b.v.	0.57	0.39

The direct observation of the spouting regime, allows confirming the absence of segregation for all the condition tested. However, a noticeable difference in size of two solid phases mainly affects the H_m, as well as the composition of the mixture. The deviations from the one phase composition are depicted in the Figure 3.29

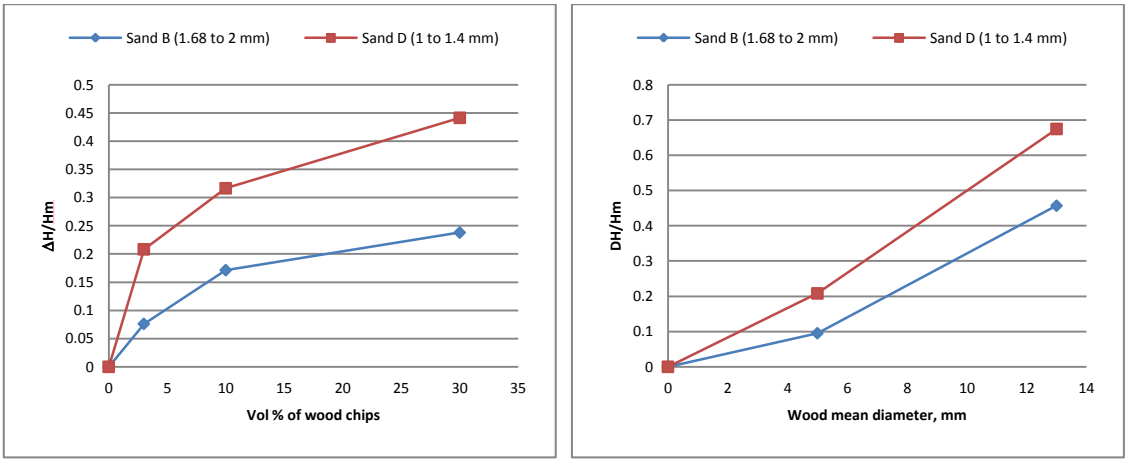

Figure 3.29 – Influence between inert and reacting phase.

3.6 Multiple square based spouted bed

The scale up is an important aspect in the design and operation for physical and chemical processes, especially when an increment on productivity is request through the increment of the solid hold-up. It is possible to conceive a multiple discrete entry points for the incoming spouting gas, dividing the entire system in small units. As remarked by J.R Grace and C.J. Lim (2011), multi-orifice spouted bed can be used to provide scale up, however instabilities and interferences between adjacent modules can lead to serious operability issues.

This configuration is suitable especially when the solid phase is homogenous and segregation is not expected. The scaling-up performed through the repetition of several units increases the plug flow behaviour of the total apparatus.

When the scale-up approach is performed by this last concept, the reactor geometry that gives the more compact rig, with the easiest way to pour solids from unit to unit, is the squared based section.

A continuously operating unit was tested to devise a guideline to design, start-up and gain in stability in multiple square-based spouted beds.
A picture of the rig is present in Figure 3.30A, while a 3D scheme of the same unit is shown on the side Figure 3.30B.

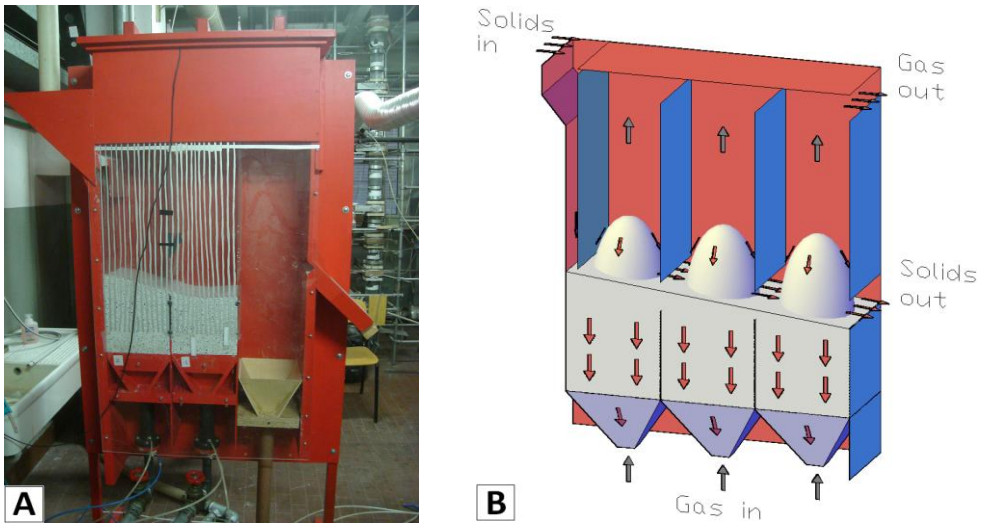

Figure 3.30 – A) Picture of the three-module experimental rig; B) 3D diagram of the same continuously operating unit with a horizontal layout stages

Designing a multiple spouted bed system does not represent a "black art", though may be more complex than other gas/solids contactors. In particular the following design aspects were focused in this project:

- diverting baffle at solids inlet,
- fountain height regulators,
- freeboard baffles between units,
- submerged baffles between units,
- overall layout of a multiple spouting unit

The following paragraphs illustrate the progressive tuning of a multiple stage spouted bed up to achieve safe know-how and run continuous operations.

3.6.1 Solids inlet design

Solid particles were stored in an elevated drum, from which they could flow by gravity, being metered by a rotary valve, a screw feeder or a simple calibrated orifice. The particles were distributed along one entire side of the spouted bed, addressed down by a vertical baffle protruding to a small distance from the bed free surface. This simple device avoided any solids bypass promoted by the fountain. Residence time distribution measurements quantified a bypass as high as about 20% of the total flow rate, in case of

baffle absence. The elevation of the baffle over the bed may require some regulation, depending on solids feed rate.

3.6.2 Fountain height regulators

A spouted bed fountain can be defined underdeveloped, developed or overdeveloped, depending on whether its geometrical margins reach the side of the spouting vessel. Since the volumetric solids circulation through the spout/fountain system can be estimated to range to a few percents of the spouting gas flow rate, the fountain alone can pour very noticeable flows of material onto contiguous stages; then, its action should be limited by some mechanical devices to restrain its hydrodynamic effect. Some devices, the so-called “Chinese hats” were presented in the sector literature (Mathur K.B. and N. Epstein N., 1974) and tested in this unit. The experimental output was entirely disappointing, as these regulators failed in sufficiently defining the fountain shape, acted as a target for the particles propelled by the spout and interfered hydrodynamically with the gas flow in the freeboard, either when they were made of solid steel plates or wire mesh screen. To conclude, these devices are not advisable as internals in multistage spouted beds.

3.6.3 Freeboard baffles between stages

Each stage was segregated from its adjacent ones by side vertical baffles protruding down from the vessel top to a very short elevation over the bed free surface. The gap left had to assure solids flow only, depending on the continuous throughput rate; this gap between the submerged and the freeboard baffles has to be regulated to allow solids transfer by overflow, with restricted particle bounces from the fountain. In addition, bypass was minimized by this precaution. These flat and inexpensive devices were chosen to separate completely the freeboard into as many stages as the spouted bed design required. As a result, the action of each fountain (independently of its shape, thus gaining in spouting regime flexibility) was limited to its own stage, while still allowing transfer of solids among adjacent modules. The use of these simple baffles repartition was observed to be fundamental for minimizing any interference between stages and enormously gain in stability.

3.6.4 Submerged baffles between stages

In principle, according to the fundamentals of fluidization, a multiple orifice spouted bed does not require a repartition between the annuluses. This consideration is also compatible with the particle vertical streamlines and the side-to-side homogeneous percolation of gas from a spout into the corresponding annulus. This assessment can be

fully accepted when the system is operated batchwise and no net solids flow from one stage to the downstream one has to be steadily maintained. Practical reasons (easy start-up, spouting stability over time, independent gas flow rate regulation in each spouting module) have demonstrated that submerged baffles greatly help in defining the solids holdup in each stage. The separation of contiguous annular regions contributes in properly distributing the gas rate and giving origin to fully independent spouts. Conversely, if the hold-up of solids is out of control, all the system stability may be affected.

3.6.5 Overall layout of a multiple spouting unit

In the recent past, in the frame of industrialization of a novel process was patented for polyethylene terephthalate solid state polymerization (Cavaglià, 2003), where polyester beads with low intrinsic viscosity are heated in one equipment. Such unit was conceived as a series of n-fluid beds (where n>5), operated in turbulent fluidization; as an alternative, a sextuple spouting demonstration unit was built and operated as a prototype equipment for PET chips upgrading (Beltramo et al., 2009). The six modules were placed at identical elevation and positioned according to a 2x3 layout; the solids moved following a chicane path without being hindered by any internal repartition. The multiple spouted bed appears advantageous in term of heat transfer efficiency (higher gas temperature at the inlet, thanks to a very short contact time between gas and heat sensitive solids) and generated good property polymers. However, the overall operation was troublesome because of difficult control on solids holdup and gas flow rate regulation.
From that study sound design hypotheses were drawn to construct the experimental rig appearing in Figure 3.30A, whose main difference with respect to the previous industrial equipment consists in the possibility of positioning each stage at the desired elevation to facilitate the solids overflow to the downstream stage, as represented in the schematic of Figure 3.31. The final version of this experimental rig had the possibility of testing all the internals described above.

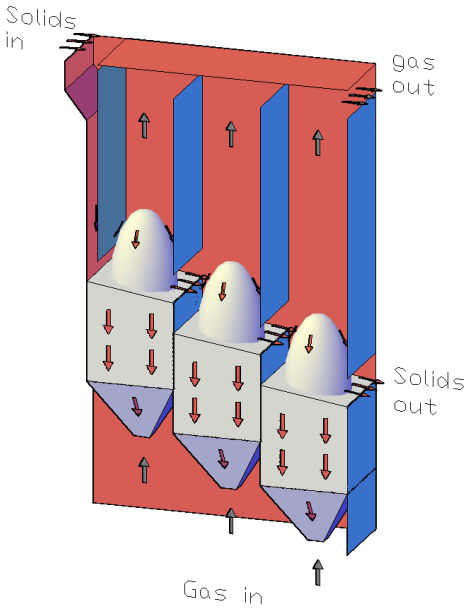

Figure 3.31 – 3D diagram of a continuously operating unit with a sloped layout of stages.

The difference of level between units suitable for continuous and stable operations was evaluated both by running specific tests and by comparing these results against a simple correlation originated by estimating the angle of internal friction of the solids used in the experiments. The tests performed in the triple spouted bed unit aimed at devising the effect of increasing solids feed rates on bulk mass transfer from stage to stage, by measuring the angle of the bed surface with respect to the horizontal level, as well as the effectiveness of the internal baffle positioning. Figure 3.32 shows three different operating conditions at a mean (snapshot A, corresponding to a mean particle total residence time τ = 13.5 min), high (snapshot B, τ = 4.5 min) solid rates and at a solids throughput far exceeding the nominal system capacity, as required by any foreseen process (snapshot C, τ = 2.5 min). The bed free surface slant increased to a maximum slope (about 15°, as a mean value between inlet and overflow sides) by increasing the flow rate. This angle is in the range of 1/2 to 1/3 of the solids repose angle, which can be measured following literature recommendation (Metcalf, 1965-66). By further enhancing the feed rate, the downcomer flooded unless further raised. The hydrodynamic slope that builds up at the bed surface caused the first stage to work with a solids depth quite higher with respect the last one, this difference increasing with the number of stages. It follows that the fluid dynamic control was much trickier and the overall spouting stability impaired.

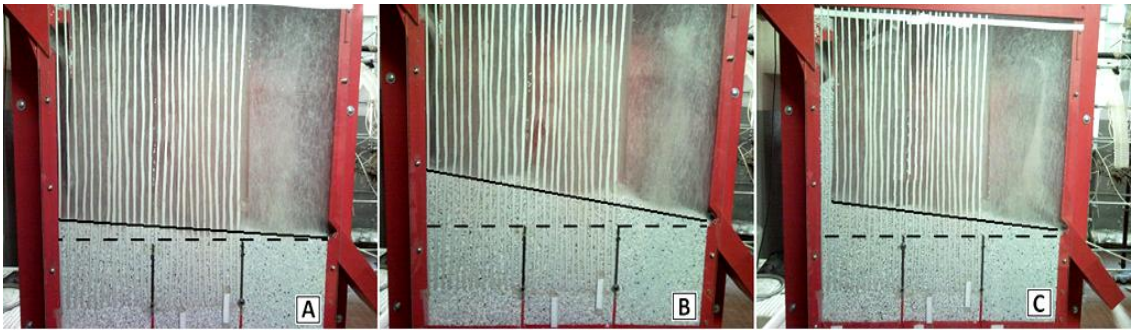

Figure 3.32 - Continuous operation in the three-module 0.20 m side spouted bed: – – – ideal solids free surface; —— actual solids surface at various solids flow rates: a) 2 kg/min, b) 6 kg/min and c) 10 kg/min, as given in the scheme of Figure 3.30B.

This geometrical limitation was overcome by setting each bed at a minimum difference of level equal to:

$$\Delta H = D_c \tan \alpha$$

Equation 4

where α is the angle formed by the actual solids surface with the horizontal level.
A rule of thumb suggests to determine the progressive vertical distance between adjacent spouted beds at:

$$\Delta H = 0.5\ D_c$$

Equation 5

which, compared to the output of Equation 4, leaves a safe operating margin.
As a conclusion, stable operations in a multiple square-based spouted beds require three types of flat internal baffles: one for properly addressing the solids feed to the bed surface, intermediate baffles in the freeboard to confine each fountain action, submerged baffles, each of them setting the solids overflow level from the upstream to the downstream stage. A non-interfering condition between stages was provided by generating a sloped cascade of independent spouting units.
One of the main goals of a spouted bed cascade is to control the mixing degree of the overall system and possibly generate a piston flow of the solid phase to guarantee identical residence time to all particles. These evaluations are carried out by means of stimulus-response techniques after attaining steady state in a continuously operating unit. Since each individual spouted bed appears to have about 90% of its volume in a perfectly mixed state (Mathur and Epstein, 1974), the recycle ratio (ratio of internal circulation in the spout referred to feed rate) leaves a small volumetric fraction of the annulus to operate as plug flow. Residence time distribution (RTD) studies in multiple spouted bed were presented in the literature (Saidutta and Murthy, 2000) in small rectangular columns having two or three spout cells. The absence of internals in this system brought to fountain wandering and excessive fountain heights that caused overall mixing higher than the one corresponding to the number of mixed units in series. A detailed RTD study on stable systems and the correlation of the experimental results

with respect to the ones predicted by a model can give a relevant contribution in designing these units. Models have gained increasing importance by making use of direct measurements in the half-sectional unit, thus becoming fully predictive.

3.7 Residence time distribution function

The RTD curves represent an effective way to interpret the fluid dynamics of the solid phase in a multiphase continuously operating reactor. These functions describe the elapse of time spent by individual solids fractions in the system and can be modelled by a relatively simple combination of ideal systems, each of them describing a basic element (mixed or plug flow system, dead zone, bypass, recycling).
Two types of curves can be studied. The *E(t)* function describes what a system releases instant after instant, i.e. the volumetric (or mass) fraction of particles whose residence time is between t and t+dt. The *F(t)* function provides the integral of *E(t)*·dt and represents the fraction of elements whose residence time is lower than t.
The most direct way to trace an *E(t)* curve makes use of a physical tracer, whose characteristics are identical or very close to the ones characterizing the bulk of solids travelling the system.
Usually, two types of stimulus are adopted, a pulse (given by a definite amount of tracer introduced into the system in the shortest time) or a step (an abrupt change from the normal feedstock to an identical feed made of tracer only). The first one is generally the prompter to use. Right away after the introduction of the pulse, samples are taken at the system exit with a proper scrutiny degree and the tracer concentration is measured and recorded.
The two *E(t)* and *F(t)* functions are defined below:

$$E(t) = \frac{C(t) \cdot \dot{M}}{M_{tr} \cdot \rho_b}$$

Equation 6

$$F(t) = \int_0^t E(t)dt$$

Equation 7

with *C (t)* being the concentration of solid tracer in the discharge, M_{tr} the mass of tracer injected, ρ_b the bulk density of tracer, $\dot{M}$ the mass flow rate of solids travelling the system.
A pulse function (called Dirac function, δ(t)) is given by an instantaneous but finite entity (equal to unity) entering a system at t=0. The Laplace transforms of these functions allow the use of simple algebraic input/output relationships.

In our experiments, the pulse was obtained by quickly introducing in the feed a small amount of tracer (150 to 300 g, equivalent to about 1.5% of the total solids hold-up) made of PET chips doped with some ferromagnetic powder. After sampling, the ferromagnetic PET chips were sorted out from the PET bulk by a magnet and their concentration calculated in each sample.

An example of RTD curves is given by Figure 3.33 which comparatively reports two *E(t)* curves obtained at steady state from tests in the 3-module spouted bed operated with and without submerged baffles, according to the configuration appearing on Figure 3.30B. The two curves overlap almost perfectly to demonstrate that internal baffles do not alter at all the solids circulation in a multi-unit cascade. The same test also demonstrates that the external solids streamlines do not have any transversal (horizontal) component, as also visible from half column monitoring. The slope of solids at the free surface was modest in these runs, due to a very low throughput (2 kg/min). Thus, it is straightforward assessing that batch operations do not require any repartition between modules. From these considerations, the use of submerged baffles is beneficial to the start-up phase of continuous processes only and becomes fundamental as geometrical boundary to generate the configuration given in Figure 3.31.

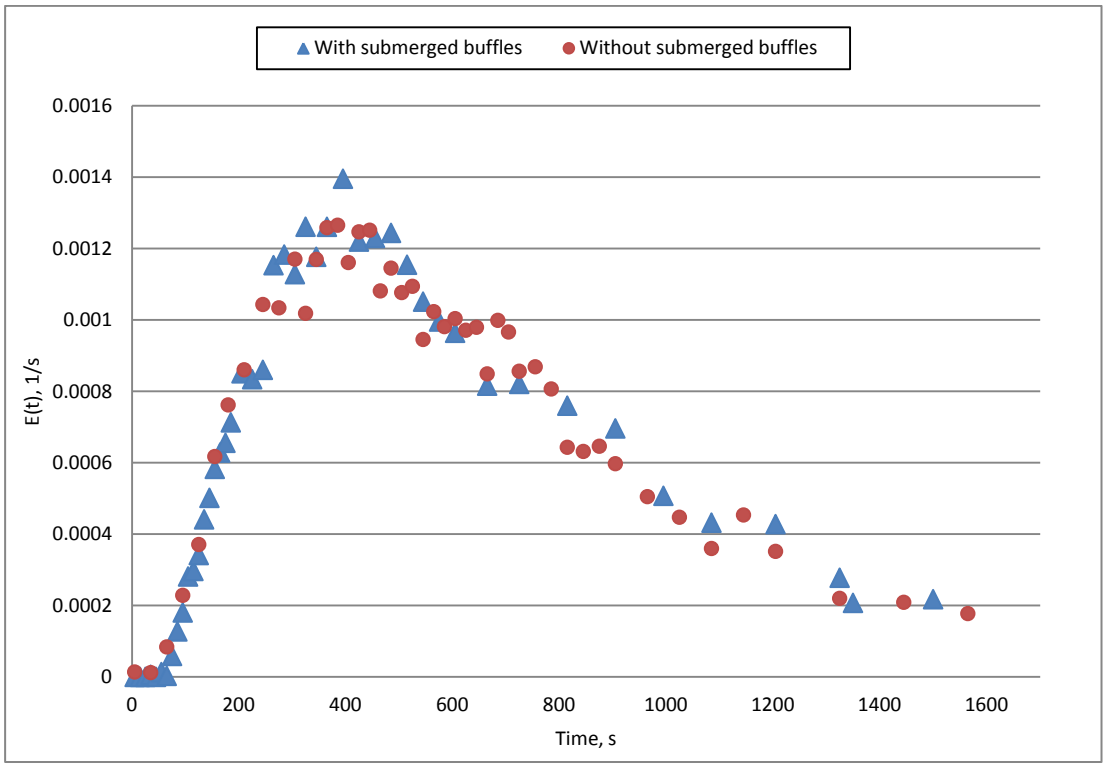

Figure 3.33 – Comparison between the RTD curves in the 3-module spouted bed with H/D_c=1.72 with and without submerged baffles.

3.8 Modelling

The theoretical description of continuous units combines basic elemental models, whose combination gives origin to a system capable of generating an overall response to match properly the actual behaviour of the real system studied. A descriptive model can produce an output without having a strict link with the actual hydrodynamic behaviour and then has to make use of fitting parameters. This approach does not allow sound predictions or extension to more complex reactor structures. A much powerful tool is produced by conceiving a phenomenological model based on experimental observations. These models become fully predictive since all parameters are based on actual measurements. Then, a model interacts with scale-up procedures through the validity of the correlations used rather than its structure.
Dynamic responses were obtained by making use of a Matlab Simulink tool by generating model schemes as given in the below Figure 3.34 and Figure 3.35. The fundamental modelling was based on a one-stage spouted bed; a multiple-cell system was then given by a cascade of basic units.

3.8.1 Descriptive model

The initial modelling started by considering an early dynamic description of spouted beds, where the overall behaviour can be portrayed by a well-mixed system with a minor (8 to 10%) portion of plug flow. The corresponding scheme given in Figure 3.34A) includes the feed rate F_1, the bypass to fountain F_3 (which become negligible when the inlet diverting baffle is considered, as a consequence $F_2 \equiv F_1$ and $F_5 \equiv F_4$), the total circulation from spout F_4, the net discharge rate $F_7 \equiv F_1$ (for continuity) and $F_6 = F_4 - F_1$. From the experimental conditions, F_1 is known and F_4 can be estimated by measuring mean particle velocity at the frontal wall of half-column. As far as the other parameters than appear in Figure 3.34B) are concerned, t_d is estimated from particle circulation, $\tau_{annulus}$ follows from holdup in the annulus and $\tau_{spout+fountain}$ is calculated by difference from the known bed holdup.
Accepting this description, also this model does not contain any fitting parameter, once the constitutive elements are assumed. Since the F_4 (internal circulation) to F_7 (net flow) ratio is very large, the overall system approaches a well-mixed unit and in this view the modelling is scarcely sensitive to the hydrodynamic description given to the annulus.

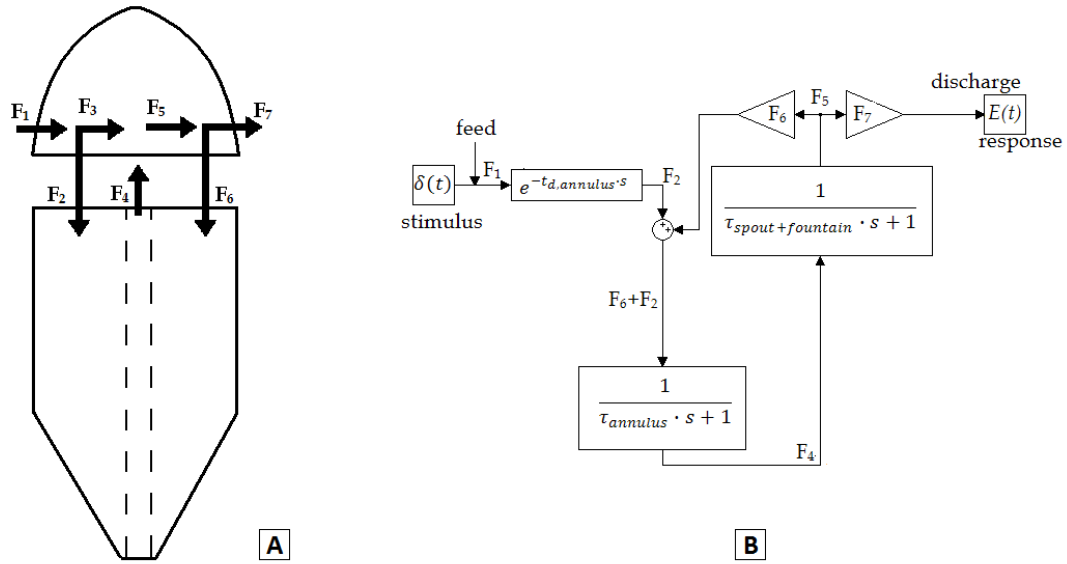

Figure 3.34 - Descriptive model of one stage two-zone continuously operating spouted bed: A): schematic of flow circulation between annulus and spout/fountain regions; B) Simulink model including pulse stimulus, delay at annulus entrance, two perfectly mixed regions for annulus and spout/fountain volumes and recirculation to bed surface.

Figure 3.35 presents the comparison between experimental and modelling results for $H/D_c = 1.72$. The fitting is excellent, considering the time delay given by the minimum residence time of particles (t_d) and the well-mixed key dynamic component brought by spout recirculation.

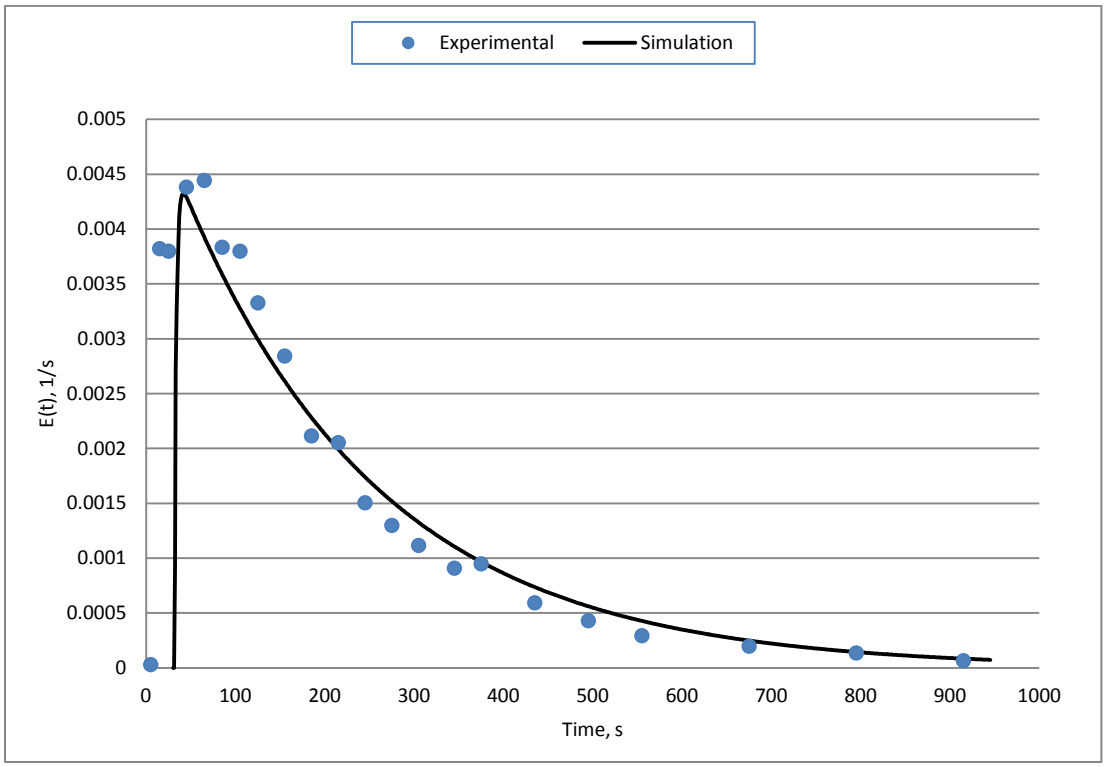

Figure 3.35 - Comparison between experimental data and the descriptive model

3.8.2 Phenomenological model

The relevant limitation contained by the above model consists in the fact that the annulus, representing the massive part of a spouted bed, has not been given a proper description. By observing it through the flat transparent wall of semi-cylindrical columns, particles show well-defined trajectories with scarce intermixing, according to consolidated findings (Mathur and Epstein, 1974).
The phenomenological description adopted in the updated model assumes that the squared-section of the annulus (with a cylindrical spout D_s) is divided into three axis-symmetric zones, each of them having the same width according to the scheme given in Figure 3.36A. Each of these regions receives from the fountain a solids flow rate proportional to its cross sectional area (F_{6A}, F_{6B} and F_{6C}, respectively moving from outside towards the spout). The flow fashion in each region is a piston with particle residence time $t_{d,A}$, $t_{d,B}$ and $t_{d,C}$, from the bed surface down to the cylinder-frustum junction, according to experimental observations. The mixing component acting in the annulus was concentrated in the frustum, which progressively discharges solids into the spout, depending on local streamline length. As a whole, this section was assimilated as far as its dynamics is concerned to a well-mixed volume, accounting to about 20% of the total holdup of the spouted bed. Also in this case, the effect of the F_4/F_7 ratio overcomes the sensitivity of other variables on the model, so that the ratio between frustum to parallelepiped volumes (i.e. plug to well-mixed volume ratio) is not relevant at all.

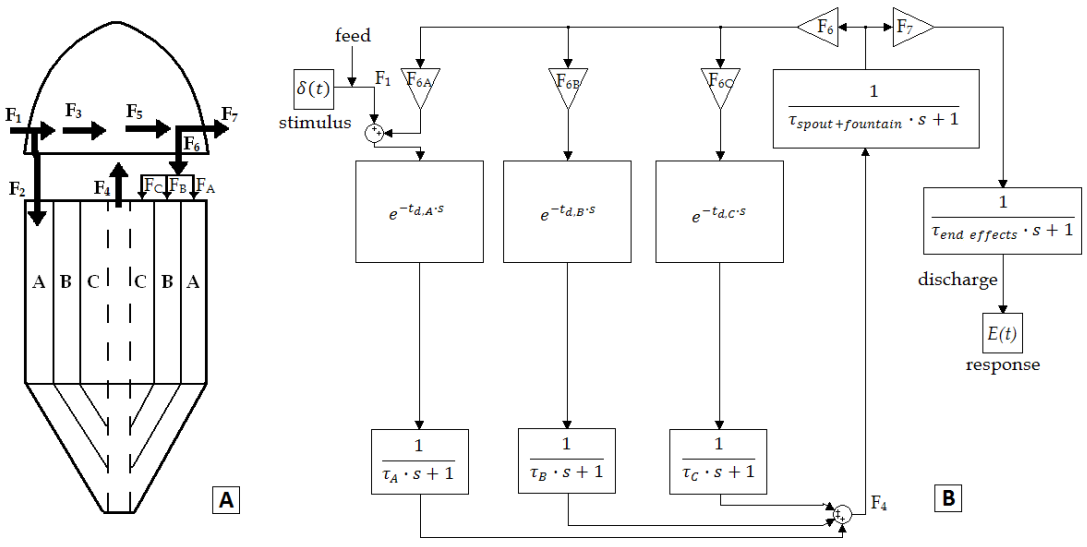

Figure 3.36 – Phenomenological model of one stage four-zone continuously operating spouted bed: A): schematic of flow circulation between annulus and spout/fountain regions; B) Simulink model including pulse stimulus, three parallel delay times in annulus, followed by three perfectly mixed regions in bottom frustum, one perfectly mixed zone in spout/fountain region and recirculation to bed surface. Small well-mixed volume accounts for sampling end effects.

Figure 3.36B) presents the Matlab Simulink scheme, where the RTDF is generated by introducing the pulse into the sector A of the annulus (due to geometrical constrain of the inlet baffle). The overall solids flow rate from fountain travels three parallel annulus

pistons, then each portion of solids enters the corresponding well-mixed portion of frustum, respectively characterized by a mean residence time estimated by observations at the flat frontal wall. The spout collects particles from the annulus and mixes them in the fountain. A small well-mixed volume characterizes the solids sampling operation to account for end effects.

Figure 3.37 compares experimental results to the output of the phenomenological model. Any difference can be hardly noted with respect to the previous descriptive model output. Due to plug flow effect, a certain oscillation matching the cycle time frequency is observed. A short sampling time $\tau_{end\ effects}$ was sufficient to damp the greatest part of oscillation.

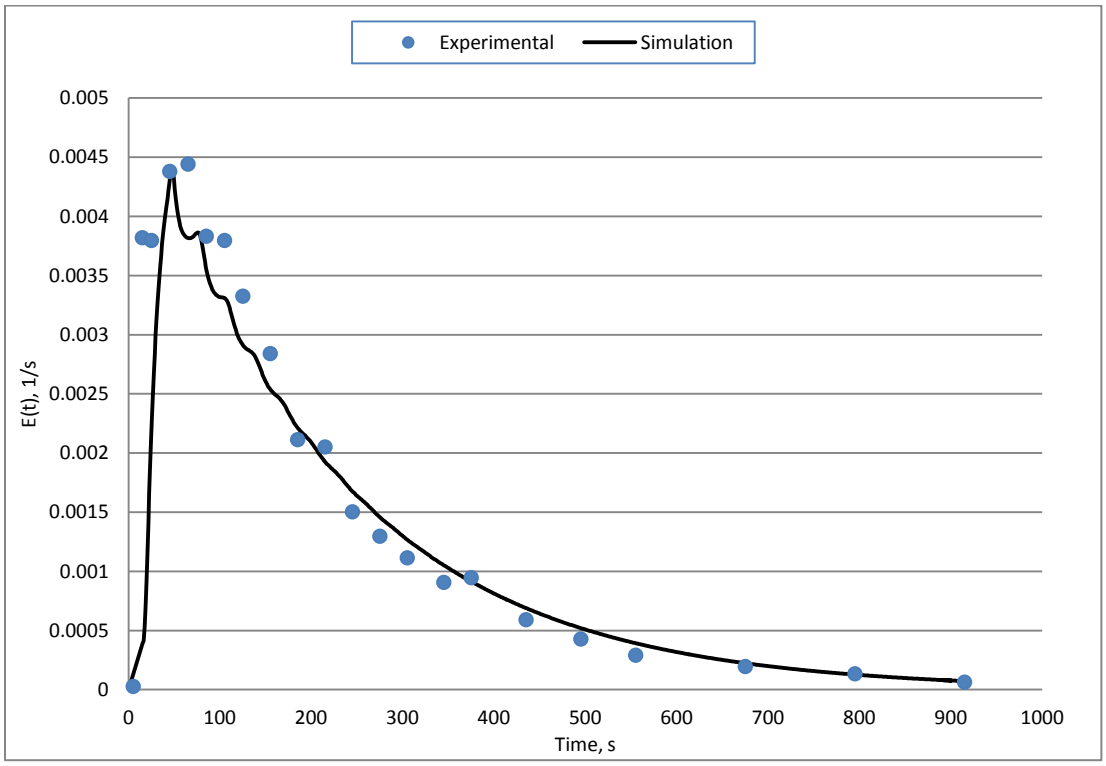

Figure 3.37 - Comparison between experimental data and the phenomenological model

3.8.3 Model validation for multiple units

The Matlab Simulink description conceived for the phenomenological model of one-stage spouted bed can be replicated a number of times corresponding to the number of cells included in a multistage system. An example is given in Figure 3.38 for a three-module spouted bed. The agreement is fully satisfactory, even though it may appear that experimental data anticipate the model output moderately and then a tail slightly higher than expected is displayed. This analysis could require to consider some direct bypass from fountain to downstream stage through the gap between submerged and freeboard vertical baffles and a small partially stagnant backwater, possibly existing along edges of frustum walls.

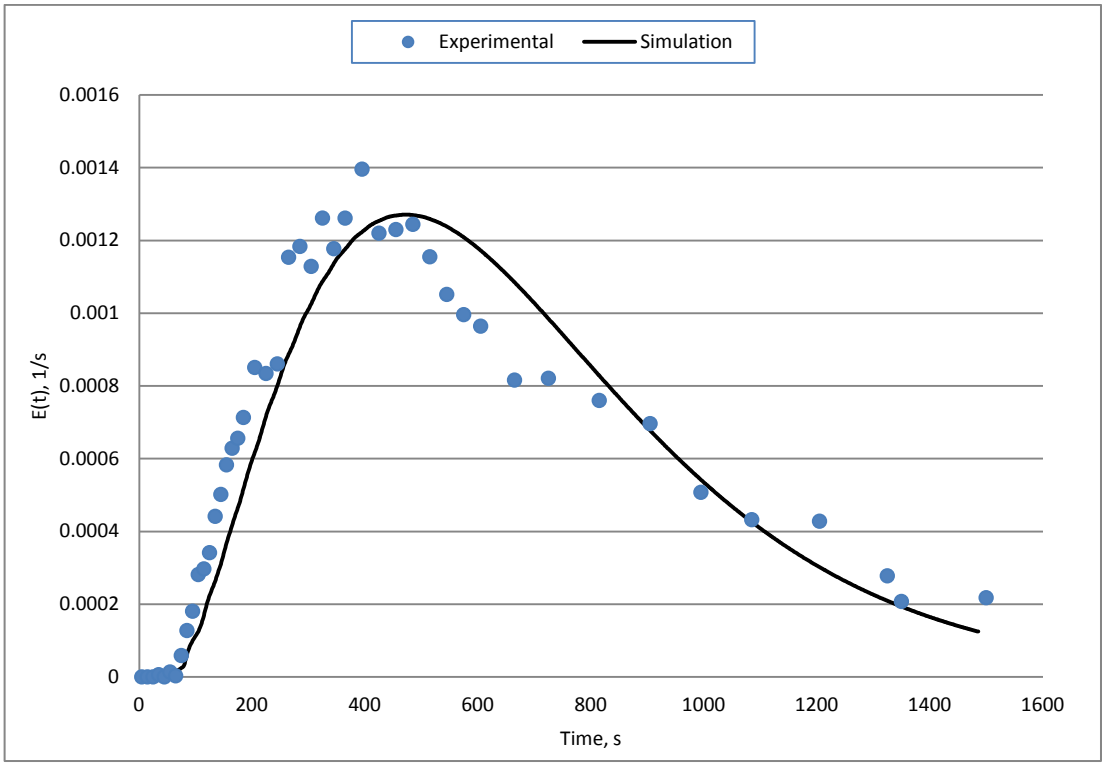

Figure 3.38 - Comparison between experimental and model RTDs in the 0.20 m side squared-based three-module spouted bed

4 Textile waste valorisation

4.1 Gasification, pyrolysis and combustion

Gasification, pyrolysis and combustion are a set of reactions, which occur when a carbonaceous solid undergoes a thermal process. The operative conditions, in terms of temperature, pressure and content of oxygen, can favour one over the others but in general, somewhere in the reactor all of them occur; Table 4.1 summarizes the most common reactions that take place in the reactor.

Combustion is a high-temperature exothermic reaction, in which the fluid phase, rich in oxygen, oxidise carbonaceous compounds and the reaction will primarily yield carbon dioxide and water. Further applications are not generally foreseen for these products, since combustion is generally considered a process to produce only heat.

Gasification is an endothermic reaction that is carried on by the heat generated either by some external equipment or by other exothermic reaction. Furthermore, the process of gasification generates, at a high temperature, hydrogen and methane and other CO mixture or what is generally called syngas. Pyrolysis reaction occurs in absence of oxygen, at a temperature lower than gasification, and it is a process that generates useful tars.

Gasification plants can be classified according to the gas-solid contacting system, properties of the carbonaceous feedstock or to the physical and chemical characteristic of the gas fed.

An important performance parameter is the heating value of the syngas produced and it is strictly linked to the fluidization agent, usually a stream of air, air-steam or oxygen-steam.

Air-steam gasification gives a low or medium-calorific value gas, since the nitrogen present in the air does not participate to the thermal reaction and dilutes the products. The steam or oxygen-steam gasification is suggested to increase the calorific value, as well as the quality of the syngas, to the detriment of overhead. Low tar production is generally beneficial and the carbon conversion, excluding CO_2, is an important factor too.

Table 4.1 – Main chemical reactions in a thermal process.

Pyrolysis	$Solid \rightarrow Char + Tar + Gases$	$\Delta H \approx 0$
Gasification	$C_{char} + H_2O \rightarrow CO + H_2$	$\Delta H = +131\ kJ/mol$
	$C_{char} + CO_2 \rightarrow 2CO$	$\Delta H = +172\ kJ/mol$
	$C_{char} + 2H_2 \rightarrow CH_4$	$\Delta H = -75\ kJ/mol$
Combustion	$C_{char} + O_2 \rightarrow CO_2$	$\Delta H = -394\ kJ/mol$
	$C_{char} + \frac{1}{2}O_2 \rightarrow CO$	$\Delta H = -111\ kJ/mol$
Gas phase	$CO + H_2O \rightarrow CO_2 + H_2$	$\Delta H = -41\ kJ/mol$
	$CH_4 + H_2O \rightarrow CO + 3H_2$	$\Delta H = +206\ kJ/mol$
	$CO + \frac{1}{2}O_2 \rightarrow CO_2$	$\Delta H = -284\ kJ/mol$

4.2 Gasification in spouted bed reactor, state of the art

Watkinson and Lisboa (2011) provided a comprehensive presentation on the state of the art about the use of spouted bed reactors for gasification processes. Spouted beds have been used for thermal treating several feedstocks, namely coal, coke, sludge and municipal wastes. The reactors usually are operated at atmospheric pressure and the agent used for gasification is a mixture of air and steam. However, several works presented in literature describe plants operating at high pressure or with an oxygen/steam mixture. As an example, Quan (1991, 1995) illustrated a pressurized spouted bed reactor of 0.1 m in diameter, working at 1.8 MPa. Yet, in this case, no significant effects on the gas composition were remarked.

Considering small units research, an electrical furnace may provide the heat necessary to reach the gasification temperature. Nevertheless, it is possible to combine exothermic and endothermic reactions to obtain an process independent of external heat sources. Rovero and Watkinson (1990) developed a vertical auto-thermal process, composed of two stages, where the pyrolysis takes place in the upper part and the heat needed for the reaction comes from the exhaust gas of combustion/gasification carried out in the lower stage.

As described in the literature (Gale and Bower, 1989; Arnold et al., 1992), spouted bed reactors have typically cylindrical shape, with an internal diameter that usually ranges between 100 to 350 mm, while larger units, up to 1 m in diameter, may give origin to some scale-up concern.

Tsuji and Uemaki (1994), working with an oxygen-steam spouted bed gasifier, 200 mm diameter and fed with coal at 10 kg/h, demonstrated that for a shallow system (H/Dc ≈ 2) and high gas velocity (up to 1.8 m/s), the operating temperature shows a uniform axial profile and ash agglomeration does not occur. Coal particles, with a size ranging from 0.5 to 3.5 mm, were used as a reacting phase fed from the reactor top, through a side port or transported pneumatically by the entering gas. The inert phase is composed mainly of silica sand with a size ranging from 1 to 3.5 mm. Considering the option where solids inventory is composed only by the reacting phase, the resulting bed of char presents instability and a significant variable behaviour over time. Usually at high gas velocity, a relevant solids throughput corresponds. The oxygen-to-coal ratio is an

important process parameter: by increasing this variable, the reactor temperature increases and reduces H_2/CO ratio in the syngas produced.
Various configurations such as standard spouting, spouting with secondary fluidization were considered with the insertion of a draft tube as an additional internal; in this case, the auxiliary fluidization is expected to provide advantages for large units in terms of reaction control.

4.3 Wastes from textile industry

Textile industry production generates different solid waste, depending on the processes carried out in a given factory: fibres of various length, card webs, fabric waste, selvage and dust can be identified both in terms of type and quantity. Dust is composed out of broken fibres, namely shorted than 1 mm, collected in various points of machinery and in the aeration and conditioning system filters.
A reasonable percentage of fibre can be recycled back into certain textile operation, while short fibres are not useful to generate textile intermediates.
A textile factory is commonly composed of several working areas in which the by-product has well defined characteristics, as presented below.

- *Spinning*: from spinning, fibres and powders represent the common waste. Fibres come from the carding and combing processes, while powders come from the air treatment filters. The waste fibres resulting from this process have different lengths, where the longer ones are re-used or sold like a secondary raw material, while the others, together with powders, are compacted and disposed in landfill.
- *Weaving*: fibre scraps are produced during this operation; sometime the by-products can be sold, but rarely these operations are performed; therefore, the waste scraps are disposed of.
- *Finishing*: a common waste coming from dry finishing, like shearing and raising, is composed of powder and even in this case the re-use is not possible.

In order to evaluate the feasibility of a thermal process, it is strictly necessary to characterize and define most of the properties of the textile waste, in terms of chemical composition and physical structure.
An environmentally responsible behaviour leads to assess that any textile good should find a proper final destination as an alternative to landfill. Textile waste management involves recycling, reuse, up cycling, landfilling, or incineration, with a possibility to recover partially the energy. A novel approach to industrial waste management of textiles processes is given by thermal valorisation. In order to evaluate the appropriateness of a thermal process, it is strictly necessary to characterize and define

most of the properties of the textile waste, considering handling and in terms of physical properties and chemical composition.
From the production of finished or semi-finished goods, from yarn to garments and household products, the percentage of textile waste relative to the production volume ranges between 1.9% in the knitwear production and 12% in the carpet production industry.

Table 4.2 – Production and waste from production processes by categories of textile goods. Source: based on the FATM-Unternehmensbefragung and STBA.

Categories:	net production	total amount of waste	share of textile dust	share of fibre waste	share of yarn waste	share of fabric in %Pts	gross production
	tons						
yarn	327942	16897	4828	8276	3793	-	344829
non-woven	181031	15102	7257	981	-	6669	196133
fabrics	300830	16501	1269	-	5395	9837	317331
carpets	243274	33174	4977	-	3317	24880	276448
knitted fabrics	81271	1574	83	-	414	1077	82845
Total	1134348	83248	18414	9257	12919	42463	1217586

According to "United Nations Industrial Development Organization", the textile industry is one of the ten most important manufacturing sectors in Europe, producing about 12 million tons of textile waste each year, 65% of which ends up as landfills and 18% is processed by incineration. A massive thermal valorisation on these refuses is then a promising solution to reduce the consequent environmental impact.
The textile companies dispose the textile waste in two ways. In one case, the waste can serve as a raw material for other companies that manufacture different types of technical and functional textiles products (generally non-woven). The second way of managing the waste is for the company to discard the waste either through incineration or as landfill. In the first instance, the manufacturing company gains revenue from re-using the waste, but in the later, it will sustain the costs of the disposal and receives back no benefits.
Incineration is a process during which the waste materials are burning in an oxygen-rich environment. The waste materials combust and produce heat, along with a variety of other end-products, usually described as polluting agents.
Gasification is an eco-friendly solution to convert any carbon containing material into synthesis gas (syngas). In contrast with incineration or combustion, the gasification process undergoes in chemical reduced conditions, i.e. with a great lack of oxygen.

4.4 Survey on textile waste in Biella's District

In order to evaluate the feasibility of the thermal valorisation process on textile by-products resulting from different manufacturing processes, a survey was conducted in

the textile district of Biella (Italy) with the support of Piemonte's Regional Government. Over a dozen of manufacturing companies provided accurate data about their solid textile waste together with the originating production department, namely:
"Filatura Godi Giuseppe", "Filatura Mello", "Filatura di Pollone", "Filatura di Trivero", "Lanificio Colombo", "Lanificio Ferla", "Maglificio Maggia", "Marchi & Fildi", "M.E.T.", "Stamperia Alicese", "Trabaldo Togna", "Yanga", "Zegna Baruffa".
The data collected from this survey is summarized in Table 4.3.The factories asked to reply to this statistical analysis represent about the 50% of the total, so that it is possible to double the quantities in order to estimate the total amount of textile waste produced in Biella's District.

Table 4.3. Textile waste characterization in Biella's District. Source: final report of VALENTEX project.

Waste Textile	Un-recycled waste unsold from spinning, kg/day	Un-recycled waste unsold from woolen mill, knitwear and finishing, kg/day	**Total**, kg/day	%
Short Fibre	1819	231	2050	55
Long Fibre	88	0	88	2
Powder	111	0	111	3
Fibre and powder mixture	894	237	1131	31
Yarn and selvages	45	14	58	2
Others	0	256	256	7
TOTAL	2956	738	**3694**	100

As seen in the table above, it is easy to understand the high potential of a thermal valorisation performed over this textile scraps. The only pre-treatment required is a low compaction in order to reduce the volume and to size the particles to a final shape suitable for spouting and easy to regulate. It is important to know that actually all of these wastes before being disposed are pelletized, so that devising a low compaction pre-treatment for the thermal reaction does not weigh on the cost afforded.
Consequently, this new process applied to the textile waste can become added revenue for the company or a new method for reducing costs, by providing an additional source of thermal and mechanical energy.

4.5 Textile waste characterization

A feasibility study of gasification implies a careful evaluation of the properties of the solid waste addressed to the process. Physical properties must be defined to guarantee a stable hydrodynamic regime, easy handling and processing and, consequently, a suitable process control. Chemical features are investigated to define the waste heating value, thermal modifications, required treatment of the syngas produced and its potential environmental impact. The physical and chemical properties of the textile waste presented in this paragraph were obtained by analyzing a relevant lot of samples collected in various industrial sites at different periods.

- Physical properties

The raw material comes from Marchi&Fildi, a manufacturing plant placed in Biella, which provided some samples of waste coming from its producing area.
The powder and the short and long fibres, which result from different manufacturing areas, are collected and pelletized in small cylinders of 80 mm diameter and 200 mm length before they are disposed of. Each cylinder has a volume of 1 L and a weight of approximately 250g. Due to its size, the textile waste is unsuitable for introduction into the bed reactor at this stage, since, generally, the particle mean diameter in a fluidized system barely passes 10 mm (Mathur and Epstain, 1974). Therefore, the textile waste undergoes a pre-treatment process, which will be described further in chapter 5.3.

- Chemical properties

The waste material taken into account for this work is composed of a mixture of cotton and polyester fibres, considering that the main products manufactured by Marchi&Fildi contain mostly these two types of fibres. For safety reasons, no chloride compounds were present in the samples.
A calorimetric analysis, following the Mahler method, was performed for several textile waste samples to define the heat of combustion. The HHV (higher heating value) range was between 16.5 and 18 MJ/kg, which are values similar to wood or cellulose commonly used in thermal transformation processing. This result consolidates the hypothesis of considering textile wastes a promising material for a thermal treatment.
The TGA analyses, performed in collaboration with Genova University (DICCA) and the Universitat Politècnica de València (ITM), were carried out in order to evaluate the thermal degradation of textile waste, both in neutral and oxidizing atmosphere.
Results can be summarized in the following graphs:

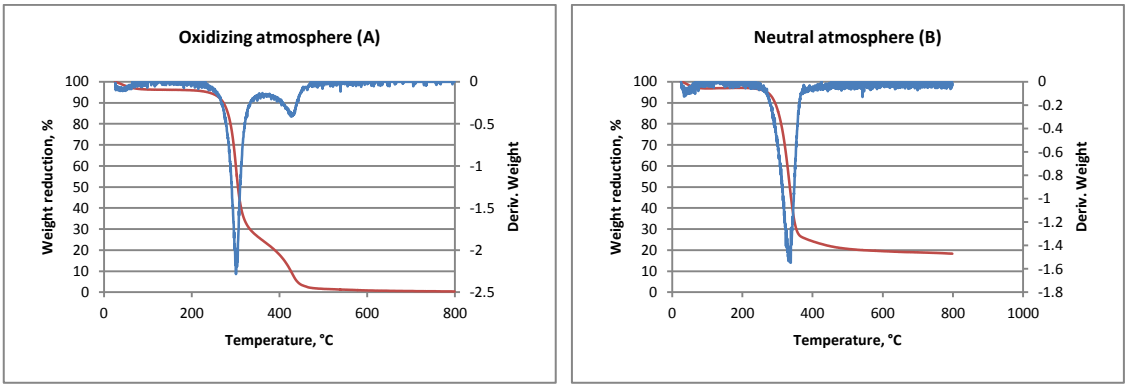

Figure 4.1 – A) TGA analysis in oxidizing atmosphere, elapsed time: 2h:30min ; B) TGA analysis in reducing atmosphere, elapsed time 2h:30min.

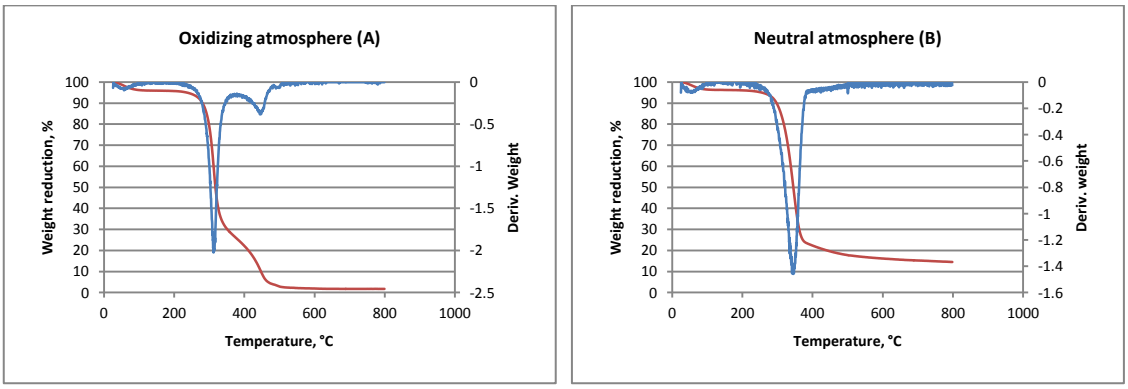

Figure 4.2 – A) TGA analysis in oxidizing atmosphere, elapsed time: 1h:15min ; B) TGA analysis in reducing atmosphere, elapsed time 1h:15min.

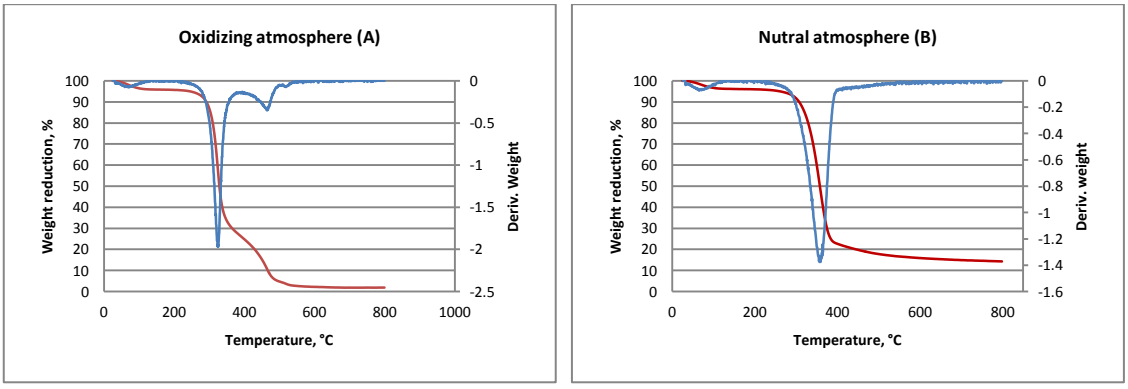

Figure 4.3 – A) TGA analysis in oxidizing atmosphere, elapsed time: 0h:40min ; B) TGA analysis in reducing atmosphere, elapsed time 0h:40min.

The experimental data are obtained considering the thermal degradation of 250 mg of textile waste. The temperature rises gradually from 25 to 800 °C with different levels of rising velocity. In the first analysis the rising velocity is set at 5 °C/min (Figure 4.1), in the second is set to 10 °C/min (Figure 4.2), while in the latter to 20 °C/min (Figure 4.3). By comparing the graphs obtained for the same atmospheric conditions (A-A-A and B-B-B) in Figure 4.1, Figure 4.2 and Figure 4.3, we can conclude that the incremental velocity of temperature does not affect degradation, since the reaction is very fast and the equilibrium condition is reached very quickly.

As an example, Figure 4.1A gives both the integral and differential weight loss in an oxidizing environment. The first peak in graph denotes a step of polymer decomposition occurring between 260 to 390 °C, while the second peak from 410 to 500 °C is relative to the combustion of the carbonaceous residual. The ultimate weight corresponds to the ash mass close to 2% of the initial weight. On the contrary, the TGA obtained at neutral conditions shows only a broader peak of devolatilisation between 270 and 400 °C, leaving a much higher final non reacted carbonaceous residue of about 15% by weight with respect to the initial fibre waste sample. In an atmosphere rich in steam also the residual carbonaceous material deriving from degradation of cellulose and synthetic polymers is expected to undergo transformation thanks to gasification and water-gas shift reactions.
Due to the seasonal production and the intrinsic concept of waste, the physical and chemical composition of solids, together with the presumed composition of the syngas, may vary; this is way is better to focus our attention on the holistic aspects of the textile waste treatments instead of one and well defined composition.
The physical and chemical properties of textile refuses discussed in this chapter are obtained over a wide batch of samples that were collected from various working areas and at different periods during the year.

4.6 Textile waste pre-treatments

The goal of this set of experiments detailed in this chapter, is to define which is the best solution in order to have stable fluidization, easy regulation and control of the thermal reaction.
Quite typically, combustion and gasification of particulate material in a fluidized system requires a relevant inventory of stationary inert material (e.g. silica sand), which acts as thermal capacity and regulates the overall hydrodynamic behaviour. This phase forms the major bed component, increases the heat transfer to the freshly fed reactant and avoids the onset of hot spots. Specifically, spouted beds show optimal features, considering pressure drop and gas flow rate, when this inert is characterized by a mean particle diameter of about 2 mm. Depending on the physical features (density and size) of the reactant pellets, a proper inert selection counters any phase segregation.
In order to find the best solution to introduce the textile waste inside the reactor we need to take into consideration the following three possible processes.

- The powders and fibres are fed in the reactor through the spouting gas.

This solution does not need any pre-treatment, as powders and small fibres are previously dosed in the spouting gas and then introduced in the reactor.

However, this option is not advisable, due to some aspects: first, textile fibres and powders enter in the reactor at high speed in a fluid dynamic area, the spout, which works as pneumatic transport. In absence of a draft tube, the spouting gas permeates easily in the annulus, but the gas bypassing the solid-reaction zone could carry out most of the fibres. Even thought the gasification could take place in the gas-phase, this could bring to hot-spots or irregularities in the gas composition.

- The mixing of silica and textile waste is done externally.

In this case, a defined amount of the inert sand continuously re-circulates out of the unit, through an external mixer, in which the reacting phase is added and mixed.
This solution avoids the carry-over of fibres, since the feeding port could be place immediately above the bad surface in a descending area for the solid phase. Even though it is not easy to manage the re-circulation of hot sand, circulating beds or riser configuration are present in several industrial sectors. For this solution, it is essential to minimize the heat lost in the external vessel and pipes or, on the contrary, to provide a heat exchanging to recover the thermal energy.
However, a serious problem is connecting the fibres that melt during the process: the external mixer is not a fluidized system and the contact between hot sand and textile creates agglomerates of melted textile, especially if synthetic fibres are present.

- Textile waste is pre-treated in small agglomerates and fed over the bed surface.

A light compaction creates small agglomerates of textile which can be dosed ad fed into the reactor directly through the wall, over the bed surface.
In order to avoid obstructions, the reacting phase is introduced through a tilted pipe: with a slope of 60°.
This does not represent an additional cost for the factories as the process of waste compaction is always performed before disposal.

The experimental rig adopted for textile waste gasification makes use of this last solution, due to the architectural simplicity and advantages in solids flow regulation.
An approach to process textile waste at high temperature was presented in the literature (Bjerle et al., 1995). Gasification of textile scraps was carried out by mixing this refuse with coal particles to generate the feedstock to a fluidized reactor. The fuel preparation was problematic mainly because of the difference in density between fibres and coal; a marked segregation between the two phase occurred during storing and metering, which generated irregular feeding and inappropriate reaction control. The technological conclusion was that a mixture containing more than 10% w/w of textile material cannot be handled.

Also the reaction kinetics is seriously affected by the different properties of the two phases: the fibrous material undergoes immediately primary oxidation reactions consuming largely the oxygen provided. Then, the remaining oxygen tends to react more easily with the gaseous reaction product instead of with coal particles, which undergo secondary reactions typical of slow pyrolysis.
The above authors carried out the gasification of mixed textile waste and biomass; a syngas very similar to that produced by biomass alone was generated, which is an additional consideration in favour of pure textile waste gasification.
The preparation of fibrous pellets is a critical step upstream of thermal transformation processes, as it may affect the whole reactor behaviour. A work presented in the literature (Shilde, 1995) aimed at comparing different preparation methods to obtain an optimal exergy output. The conclusions drawn by the author confirmed that the low bulk density of textile waste is disadvantageous for feeding, so that to maintain a continuous operation it is necessary to agglomerate fibres and fines, as a density increase plays in favour of good dosage.

4.7 Segregation, pressure drop and elutriation in spouted bed reactors

The proper fluid dynamic of a spouted bed reactor tends to avoid or minimize the segregation of phases. However, due to the high difference in density between sand and textile, some experimental tests were performed as detailed bellow.

- Pellets production

From the experience acquired, the spherical shape seems to be the best solution for spouting.
The first set of experiments aims to verify how a spouted bed is able to manage a hold-up of sand and textile. The starting material, as said before, comes from Marchi&Fildi and has a cylindrical shape. These blocks were crumbled by hands and, due to a rotary movement, some small spherical agglomerates were obtained, as shown in Figure 4.4.

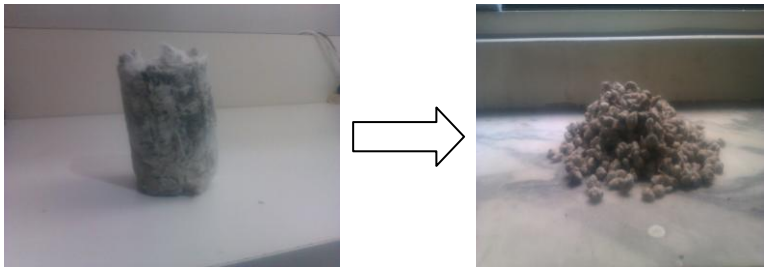

Figure 4.4 – Textile waste coming from the factory and after hands pelletisation.

Following different recipes, three lots of samples were prepared; the main goal is to obtain a sphere of about 1 cm of diameter, with a small deviation from the mean value.
After the mechanical disruption, the first set of particles were obtained only by mechanical movements, while for the second and the third samples, a solution of water and starch-water was used to help the sizing and to increase the density. Finally, the batches of samples were dried in an oven to remove the residual water.
Table 4.4 summarizes some geometrical details of the three batches of samples; the particles resembled a spheroid and the three diameters were measured for more than fifty particles. The equivalent diameter was chosen as characteristic length.

Table 4.4 – Size and density of textile agglomerates.

	Lot A) dry	Lot B) water	Lot C) water + starch
X-axis, mm	5.6	6.0	5.7
Y-axis, mm	7.9	7.9	7.8
Z-axis, mm	11.1	10.9	10.8
Equivalent diameter, mm	**7.9**	**8.0**	**7.8**
Bulk density, kg/m^3	**96**	**132**	**144**

- Pressure drop and global behaviour

Six pressure probes were used to measure the pressure drop across the bed section. The two pressure lines, staggered of 25 mm, are placed between 230 and 255 mm form the base. The bed dept was kept constant and equal to 450 mm.
Five different mixtures were compared to observe the global behaviour inside the rector and the gas velocity inside the annulus; Table 4.5 provides more information.

Table 4.5 – Differential pressure drop between 230 and 255 mm from the base. Different mixtures of sand (1.68÷2.00 mm) and textile waste agglomerates.

Textile waste Lot type	Textile waste % V/V	Spouting time, s	ΔP cm H_2O						mean ΔP cm H_2O	Superficial gas velocity, m/s
			D1	D2	D3	L1	L3	L5		
/	0	60	1.3	1.3	1.3	1.3	1.3	1.3	1.3	0.5
		300	1.1	1.1	1	1.1	1	1.1	1.1	0.45
A)	5	60	1.1	1.1	1	1.1	1.1	1.2	1.1	0.45
		120	1.1	1.1	1	1.1	1.1	1.2	1.1	0.45
		300	1.1	1.1	1	1.1	1.1	1.2	1.1	0.45
B)	5	60	1.1	1.1	1.1	1.1	1.1	1.2	1.1	0.45
		120	1.1	1.1	1.1	1.1	1.1	1.2	1.1	0.45
		300	1.1	1.1	1.1	1	1.1	1.1	1.1	0.45
C)	5	60	1.1	1.1	1	1.1	1	1.1	1.1	0.45
		120	1.1	1.1	1	1.1	1	1.1	1.1	0.45
		300	1.1	1.1	1	1.1	1	1.1	1.1	0.45
A)	15	60	1.1	1.1	1	1.1	1.1	1.2	1.1	0.45
		120	1.1	1.1	1	1.1	1	1.1	1.1	0.45
		300	1.1	1.1	1	1.1	1	1.1	1.1	0.45

The homogeneity of these results demonstrate that no remarkable hydrodynamic changes were caused by using sand/fibrous agglomerate mixtures instead of pure sand. The gas distribution in the annulus was uniform throughout (i.e. non affected by the corners of the square geometry) and governed by the prevailing dense phase. It is also worthwhile considering that the bed composition adopted in the tests includes the real conditions in a broad way, as the rapid gasification kinetics will give origin to low concentrations of textile material in the bed. Additionally, the progressive modification of the agglomerates over time did not affect the spouted bed hydrodynamics. Under a reactivity viewpoint it can be inferred that a low density fibrous material should be characterized by a high mass transfer, thus surface controlled reaction very fast.

Figure 4.5 – Particles of textile before and after spouting

From Figure 4.5 we can see than the shear forces given by the sand inside the annulus during spouting, tend to destroy the agglomerates; the final fibrous aspects is suitable for thermal reaction, as it increase the superficial area.

In addition, further consideration has been given for what concerns the air flow needed to induce spouting (U_{os}) and the minimum amount of air that grants spouting (U_{ms}). The following Figure 4.6 and Figure 4.7, compares these two parameters with and without textile (prepared as batch B), in the half section spouted bed reactor:

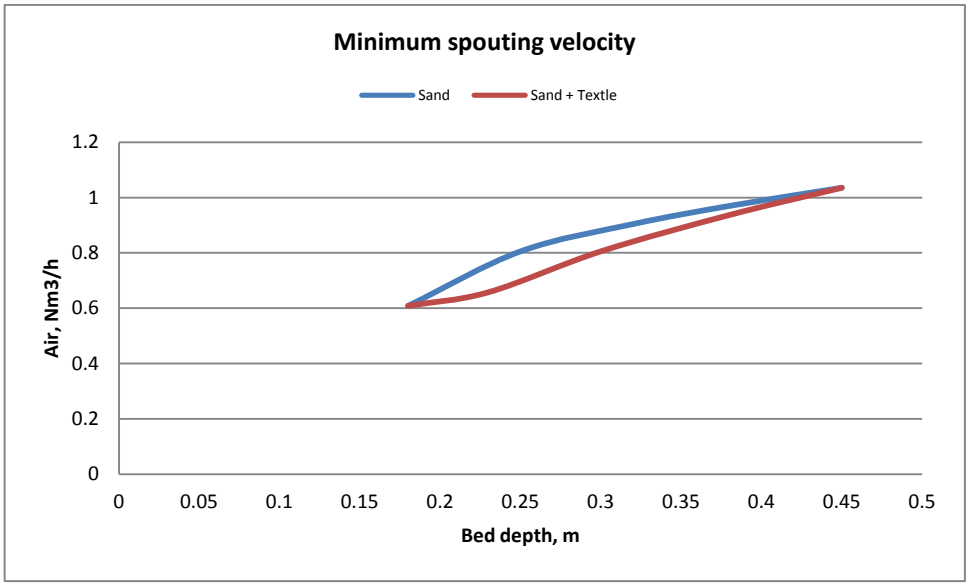

Figure 4.6 – Effects of textile agglomerate on Ums.

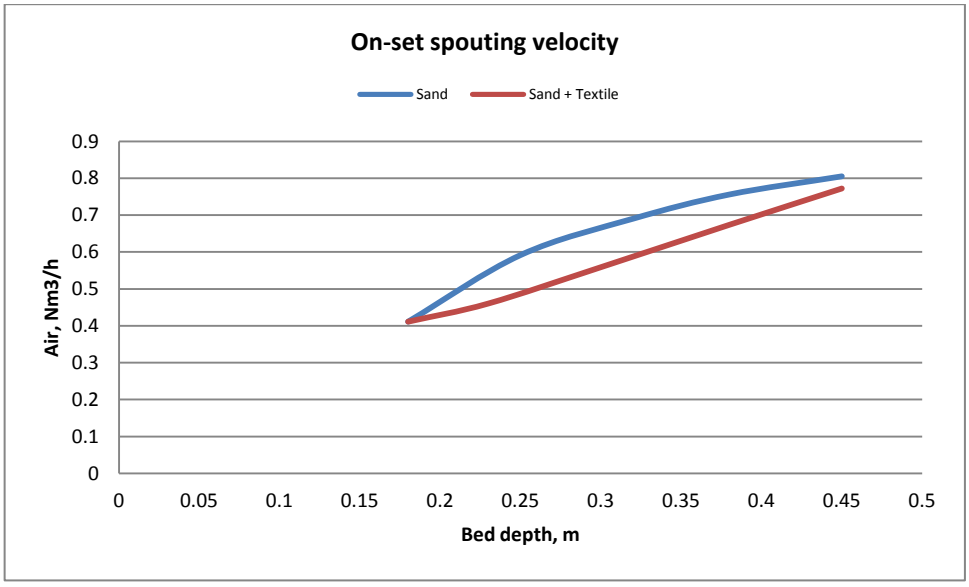

Figure 4.7 – Effects of textile agglomerate on Uos

- Elutriation

Solids that circulate in a spouted bed undergo repeated comminution actions, causing a progressive size reduction and fines generation. Following Khoe (1984), three different mechanisms contribute to the overall comminution process: impact, crushing and attrition. The comminution mechanism is dominated by attrition, while impact and crushing are relatively unimportant, unless additional devices like draft tube or target plates are installed. Additionally attrition, due to different density and size, is expected to prevail at the spout-to-annulus interface, as well as in spout acceleration distance
As short time intervals were considered, only the comminution of the textile material was considered, while the fines generation from the dense phase was assumed negligible. Also several tests at different gas rate were performed to account for different time cycles, frequency and inlet gas velocity. The comminution of textile agglomerates during spouting fluidization (see Figure 4.5) is not a problem from a thermal point of view. Indeed, it increases the superficial area and improves the mass transfer of the reaction. However, it must be verified that the way chosen to pre-treat and feed the solid waste inside the reactor avoids problem lined to the by-pass of the reaction zone, for example due to an untimely carryover through the exhaust gas.
To avoid fluctuations in the syngas composition or in the bed temperature, it is important to perform the chemical reaction inside the annulus, where the textile waste is surrounded by the inert medium and minimize the gas-phase reactions over the solid carbonaceous compounds.
Considering the contribution to the overall reaction in the three zones of a spouted bed, carryover in the freeboard could limit gasification efficiency, unless fines reactivity is very high (as expected at high temperatures) or elutriation non relevant. It should be pointed out that the control of gasification is easier at a constant and well defined temperature which is a characteristic of the annulus, where the highest holdup and longest residence time of the reacting phase occur.
Even though is demonstrated that the agglomerates stay inside the reactor, it is important to evaluate the quantity of fines the leave the reactor with the outgoing gas.
Fines carryover was measured by continuous isokinetic sampling of the dilute phase in the spouted bed freeboard. A 30 mm ID probe was positioned in the vessel top, connected to a 170 μm filter and to a gas meter (see Figure 4.8). Out of a 9 kg inventory of silica sand forming the spouted bed, 100 g of agglomerated particles were dropped on the annulus surface to simulate textile waste feeding. The result are given by the histogram of Figure 4.9, which denotes how the generation of fibre fragments is about linear with spouting time, while slightly increases with gas flow rate. It is quite evident that 5 minute spouting generated less that 3% of carryover by weight, while a complete fibre transformation to a gaseous product is expected to last few seconds only. This is a prove that gasification should occur in the most dense regions of a spouted bed (annulus, spout and fountain).

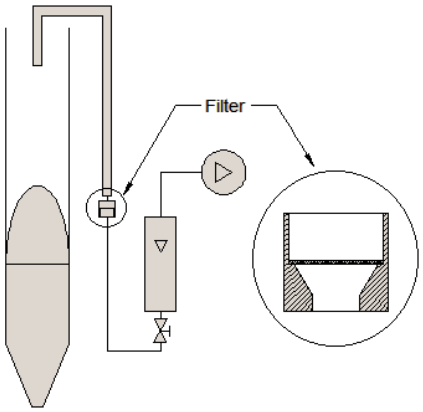

Figure 4.8 – iso-kinetic sampling equipment

The elutriation phenomenon was estimated at two different gas velocities: the test was performed at two different air flow rates, namely 50 and 60 Nm^3/h.

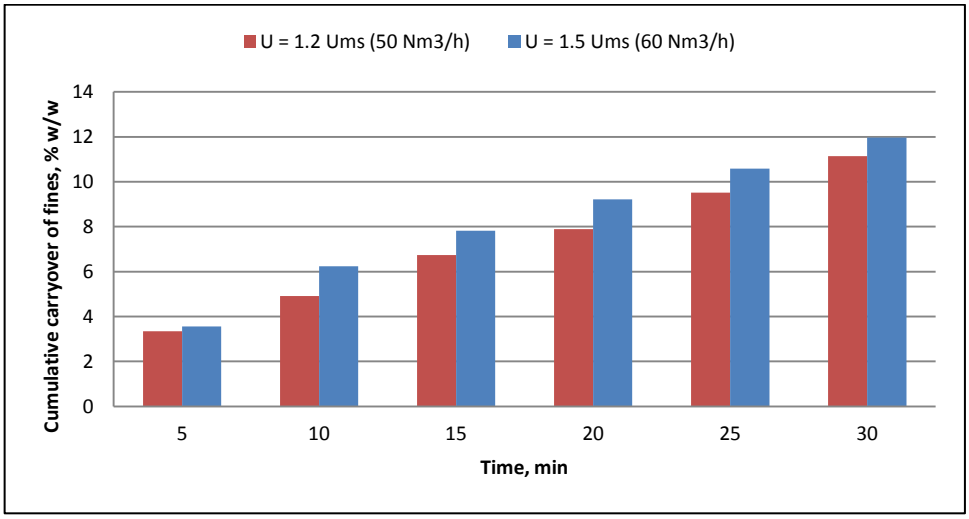

Figure 4.9 - Cumulative carryover of fines lost through the exhaust gas.

It is possible to conclude that the amount of fines lost in the exhaust gas is a function of the gas velocity and range between 10 to 15% b.w. in the field of 1.2 – 1.5 U_{ms}. This evaluation is however conservative, since the gasification reaction is foreseen to occur in few seconds and in the pseudo-homogeneous gas system in the free-board.

5 Pilot unit for gasification

All the knowledge acquired in the field of fluidization performed at room temperature has demonstrated that the spouted bed reactor gave advantages compared to other solid-gas contacting systems.
Furthermore, a light reacting phase, namely wastes from textile industries, can be easily managed in a spouted bed reactor and the resulting syngas is foreseen to have an adequate heating value.
Following a preliminary process description, Bernocco 2013, a 20 kW thermal power unit have been conceived and built, following all the tips to assure an easy and straightforward start-up, simply management during operations, stability and efficiency.
The core of the apparatus is a square based spouted bed unit; pre-heated fluidizing gas comes from a burner, while the exhaust gasses are cleaned from powders in a cyclone followed by a water scrubber to cool them and remove fines.
The reacting phase is previously prepared in an off-line apparatus, expressly designed to transform the textile scraps at the desired size and shape. The solids feed point in the vertical wall of the reactor is connected to a hopper from which the particles can be continuously fed in the reactor.
A block diagram of the apparatus, together with a 3D draft, is presented in Figure 5.1.

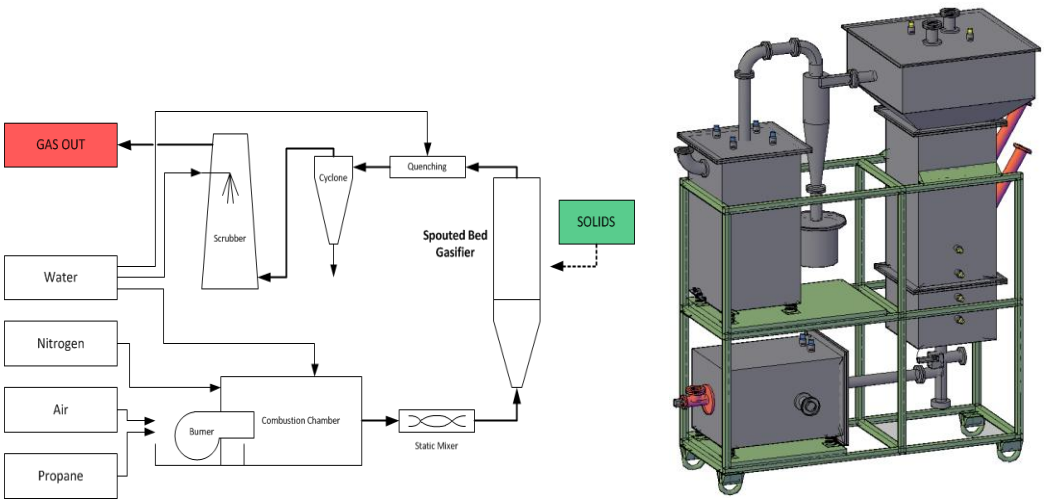

Figure 5.1 – Block diagram and 3D sketch of the pilot unit for gasification.

5.1 Process calculation

Spouted beds with squared section have a fluid mechanic behaviour that does not differ substantially from the standard cylindrical one. Literature presents several empirical correlations that are still valid on the squared section; for these reasons, some of them were used to foresee the working parameters and the fluid mechanic limits for the equipment.
The reactor is therefore a square based spouted bed reactor, with a side of 200 mm and a total high of 2.0 m; as always the base has an included angle of 60°, while the spouting orifice at its centre has a 21 mm diameter. From these geometrical features, it is possible to define the process parameters, considering the start-up temperature and the bed depth.
From the TGA analysis previously performed we can consider that the ignition temperature for textile ranges between 300 and 380°C; therefore, during the start-up phase, it is necessary to pre-heat the inert to a temperature sufficient to induce the auto-combustion which will cause a further increment of temperature till the desired value for gasification. An operative ignition temperature of 400°C seems to be appropriate. Due to the fluid dynamic limit given by the maximum spouted bed depth, following McNab and Bridgwater equation (see Table 3.5), the total height cannot exceed 0.8 m. The sequence of steps to define the mass and enthalpy balance is then shown:

- Input Parameters

A process calculation sheet was compiled to manage easily all the streams if the input parameters change.
Besides them, the process is constituted by a sequence of phases characterized by a different ratio between the flows and this tool is extremely useful.
Table 5.1 lists all the values that will be used to run the reaction.

Table 5.1 – Input parameters for process calculation

Geometrical features		
Column side, m	D_c	0.2
Bed depth, m	H	0.5
Inlet diameter, mm	d_i	21
Sand properties		
Mean diameter, mm	d_p	1.8
Density, kg/m^3	ρ_p	2510

Other input		
Ignition temperature, °C	T	400
Oxygen index	λ	1.05

The minimum spouting velocity was defined considering the sand as the only solid phase inside the reactor, sinc the quantity of textile inside the bad has demonstrated to modify the fluid mechanics not at all.
Mathur and Gishler equation was used to get this value, at the desired process conditions as previously defied.

$$U_{ms} = \frac{d_p}{D_c} \cdot \left(\frac{d_i}{D_c}\right)^{1/3} \cdot \left[\frac{2 \cdot g \cdot H \cdot (\rho_s - \rho_f)}{\rho_f}\right]^{1/2} = 0.99\, m/s$$

The volumetric flow can be easily retrieved knowing the section of the reactor, as well as the mass or mole flow.

$$Volumetrc\ Flow = 143\ m^3/h$$
$$Mass\ Flow = 0.014\ kg/s$$
$$Mole\ Flow = 0.578\ mol/s$$

The spouting gas is generated in the burner, which should be adequately sized in order to fulfil enthalpy and mass balance: the flue gas temperature must be able to heat the inert up to 400 °C; at the same time, the mass flow should be equal to 0.014 kg/s to maintain spouting.
A key point in a gasification reaction is linked to the composition of the gas inside the reactor that has to respects some chemical constraints. To convert partially the carbon of the feedstock in a syngas with a high chemical potential, it is important to maintain a mild reducing atmosphere; only a small amount of extra oxygen is present for safety reasons. The O_2 index (λ), represents the ratio between air and the stoichiometry propane at the burner, always maintained above 1.05 for safety reasons.
The burner works mixing air and LPG and, because of the last consideration, the ratio between this two gasses has to be kept constant. Three constrain have to be satisfied: temperature, mass flow and oxygen index. This problem can be solved performing the so-called “steam-air gasification”, adding water to the process. The air combustion in the burner provides the right amount of thermal energy to vaporize water nebulised in the combustion chamber; therefore, mass ad enthalpy balances are satisfied.
Even nitrogen could be used as inert, but water was chosen for its low cost and because it more easy to remove from syngas to increase its heating value.
A couple of nebulizers sprinkle water in the combustion chamber directly atop the flame and its vaporization allows reaching the mass flow required; obviously, the heat of

vaporization must be taken into account in the global enthalpy balance. All the constraints will be satisfied with the following streams:

$$Air = 7.7 \cdot 10^{-3}\ kg/s$$
$$LPG = 4.0 \cdot 10^{-4}\ kg/s$$
$$Water = 5.2 \cdot 10^{-3}\ kg/s$$

It is important to clarify that the process sheet makes use of iterative calculations, as the smokes composition in terms of density, viscosity, and temperature, changes continuously.
Depending on the holdup, the operative working parameters change, Table 5.2 summarizes some values of the main streams for four possible bed depths.

Table 5.2 – Possible working parameters to grant spouting regime and λ≈1.1.

	Bed Depth, m	Minimum spouting velocity, m/s	Air flow, m^3/h	LPG flow, L/min	Water, L/min
Set-up 1	0.2	0.61	14.75	9.2	0.19
Set-up 2	0.3	0.77	18.07	11.27	0.24
Set-up 3	0.4	0.89	20.84	13	0.28
Set-up 4	0.5	0.99	23.31	14.53	0.31

The gas post-treatment section was conceived and sized in a versatile manner as the syngas composition and temperature will vary depending on the reaction conditions.
A nebulizer before the cyclone acts, if it is necessary, a pre-cooling, while a water scrubber is able to bring the gas temperature at room conditions. The total water consumption ranges between 2 to 4 L/min.

The burner and the spouted bed reactor have an insulation layer that prevent as much as possible the loss of heat. As for the gas cleaning section, the temperature may vary depending on the reaction conditions; however, an insulating layer of 60 mm thickness has been evaluated to be the best solution in terms of cost-efficiency.

5.2 Construction and assembly of the components

The squared based spouted bed gasifier chosen for the thermal treatment of textile scraps, is a unique exemplar, this means that almost of all the components must be planned and built ad hoc.
The main geometrical features of the equipments were defined by the experiments at room temperature, and the previous chapter provided some information on the magnitude of the gas flows and the utilities consumption.
Executive drawings were prepared, discussed and modified until the final version, from which it was possible to begin the build up phase.
The mechanical work to realize a prototype needs a careful analysis over all the details and nothing has to be neglected.

5.2.1 Materials

The rig makes use of few row materials that are listed below, together with additional information.

- Carbon steel

The shell of all the equipments, such as the burner, the spouted bed reactor and the water scrubber is made of this material, as well as the framework that holds all of them together. High temperatures do not represent a serious problem since the insulation layer was conceived to have a superficial temperature less than 100°C; however, paint for high temperature, up to 400°C, coats all the structure to give a further protection against the atmospheric agents. The only critical area for steel is the connection between the burner and the reactor because, even though the operating temperature in that area is around 500°C, during the start up higher temperature may be reached, in any case a thermocouple monitors constantly the line avoiding values over 700°C.

- Concrete

The internal layers of the burner and of the reactor are made of a refractory concrete, which must hold out against the high temperature given by the burner flame or the heat generated by the chemical reactions inside the reactor.
The size distribution should be narrow with small particles in order to obtain a smooth surface after casting; in addition, a smooth layer prevents from the erosion acts by sand fluidization.
Table 5.3 provides additional information on the concrete named “F40” purchased from “LaRefrattaria”, a company specialized on high temperature materials.

Table 5.3 – Additional information on F40 concrete

High temperature concrete		
Operating temperature, up to	1350	°C
Density	1900 - 1950	kg/m^3
Size distribution	≈ 0 - 10	mm
Resistance to compression at 815°C	320	kg/cm^2
Resistance to compression at 105°C	280	kg/cm^2
Al_2O_3	42 - 44	% b.w.
SiO_2	40 - 43	% b.w.
Fe_2O_3	7 - 8	% b.w.
Application	pouring	

Before pouring, the concrete was divided in two groups, depending on the particle size; a sequence of sieves was used to split the concrete in particles smaller or greater than 5 mm; some particles greater than 1 cm were present and they were removed.
Thinner concrete was used in some critical areas, as for the reactor base and the medium section, since here it is important to have a smooth surface.
At the contrary coarser particles were adopted were the concrete is in touch only with a gas phase, like in the burner and in the top section of the reactor.

- Insulating

Insulating panels were used for the thermal insulation of the reactor, the burner and some pipes as well. For the reactor and the burner, this layer is placed between the metallic shell and the concrete wall; it plays an important role, since we need to reduce as much as possible the thermal dissipation, in order to reduce operative costs, utilities consumption and to get faster the thermal regime inside the rig. Due to the high temperature that can be reached, the insulating is based on silica oxides and can stand up to 1260°C; thank to the low conductivity factor the external temperature on the steel shell will be kept below 100°C.
As an example, Figure 5.2 depicts the axial temperature profile inside the reactor from an internal temperature of 800°C to the external shell.
Some physical and chemical properties are summarized in the following Table 5.4.

Table 5.4 – Properties of the thermal insulation

Thermal insulation		
Operating temperature (ENV 1094-3)	1260	°C
Melting point	>1400	°C
Density	128	kg/m^3
Mean fibre diameter	3.5	μm
Linear shrink 24H, 1100°C (ENV 1094-7)	1	%
Thermal conductivity at 200°C (ASTM C 201)	0.06	W/mK
Thermal conductivity at 400°C (ASTM C 201)	0.1	W/mK
Thermal conductivity at 600°C (ASTM C 201)	0.15	W/mK

Thermal conductivity at 800°C (ASTM C 201)	0.2	W/mK
Thermal conductivity at 1000°C (ASTM C 201)	0.27	W/mK
SiO_2	65 -80	% b.w.
ZrO_2	< 2	% b.w.
MgO+CaO	22 -40	% b.w.
Al_2O_3	< 1	% b.w.

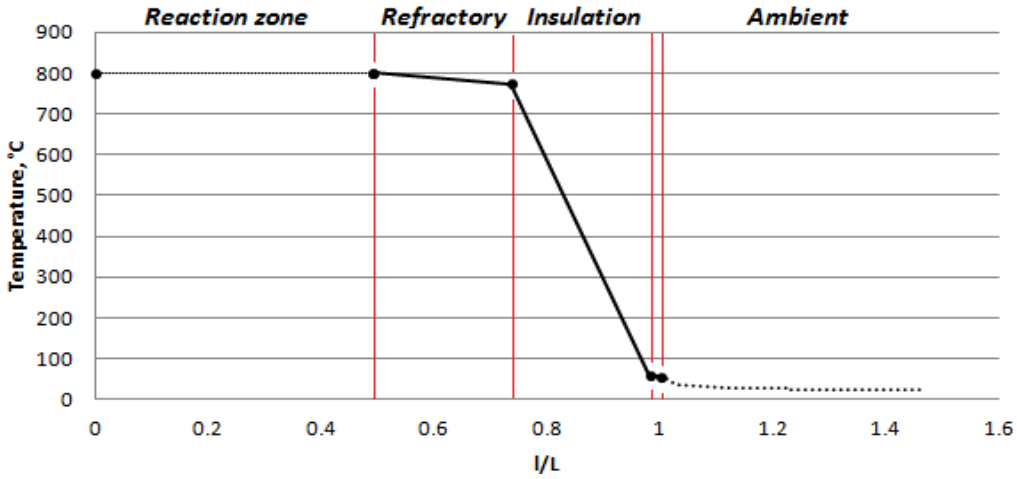

Figure 5.2 – Foreseen axial temperature profile across the gasifier wall

5.2.2 Building-up

The mechanical draws of all the equipments were prepared, discussed and modified together with a skilled carpenter, who realized the external carbon shell of all the equipments, as well as the framework. At the contrary, the on-line solid feeder and the pelletiser prototype for textile scraps were designed and built from one of our Partner in VALENTEX project.
The placement of the thermal insulation, the casting of concrete, and the realization of others devices is bounded to this PhD work; in the next pages, all the equipments of the pilot prototype will be described, focusing on the mechanical execution.

- Burner and burning chamber

The burner mixes air and propane at the desired ratio, in order to pre-heat the gas flow for fluidization.
The maximum thermal power that can be reached is 35kW, but the high rangeability more than 10 times allows an easy regulation at each working conditions.
The burner is composed of the following modules: burner housing, burner insert and ceramic tube. The burner is secured to the combustion chamber by the burner housing inside which the burner insert and the ceramic tube route the air inside the chamber in the right way, assuring a stable flame; the burner head is specifically designed for LPG.

The ignition electrode, close to burner head is used for the start up, while the ionization electrode checks constantly the presence of the flame and acts on security valves if necessary. A SiC ceramic tube, lightweight in design, serves as a pre-combustion chamber and ensures complete combustion. Detailed quotes are present in Figure 5.4.

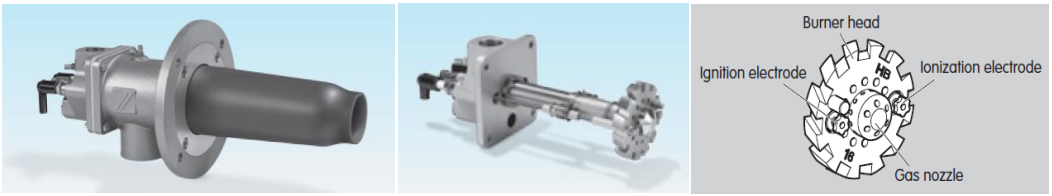

Figure 5.3 – Burner and constitutive elements

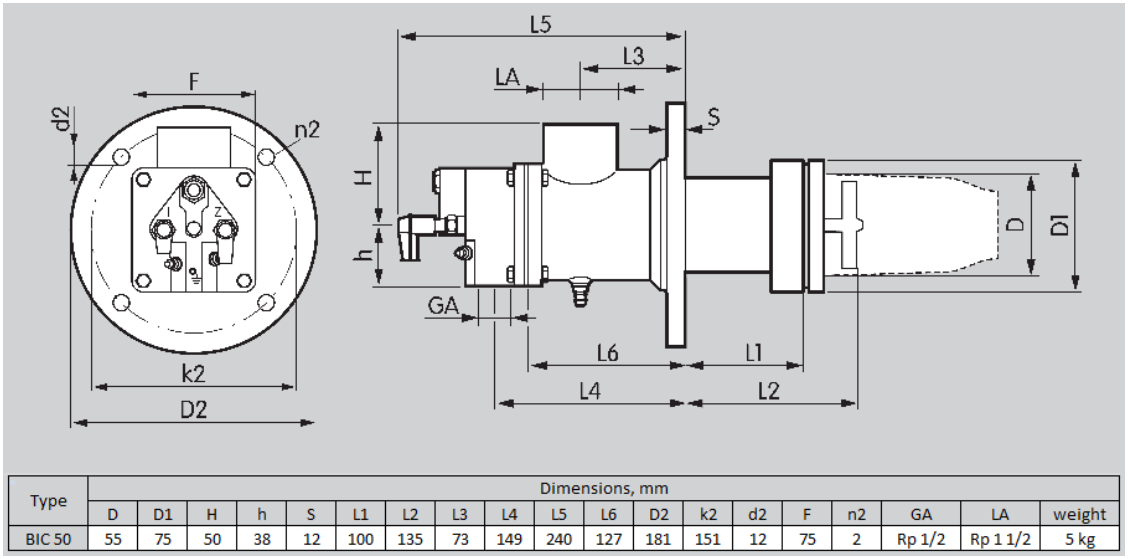

Type	Dimensions, mm																		
	D	D1	H	h	S	L1	L2	L3	L4	L5	L6	D2	k2	d2	F	n2	GA	LA	weight
BIC 50	55	75	50	38	12	100	135	73	149	240	127	181	151	12	75	2	Rp 1/2	Rp 1 1/2	5 kg

Figure 5.4 – Mechanical draw of the burner; ELSTER BIC-50

The burner can be switched-on through the control panel Figure 5.5 which ignites and monitors directly the burner status, displaying numerical information. In case of flame failure, a message of error appears and at the same time, two security valves in series on the LPG line Figure 5.5 are closed.

Figure 5.5 – Status panel and security valve

The burner chamber, see the below Figure 5.6, has an external shell in carbon steel 600x400x400 mm (LxHxW), 3 mm thickness.

Figure 5.6 – Burner chamber

The rear wall houses the burner, while laterally some openings are present for the introduction of the water nebulisers or thermocouples.
Depending on the control range, the burner flame ranges between 180 to 230 mm; to prevent a direct contact between the flame and the outgoing steel pipe and to assure a good mixing, a flame arrester in refractory concrete was placed in front of it.
Besides the ignition electrode, the presence of the flame can be checked through two tempered windows, the first placed in the burner housing, the other on the lateral wall of the burner chambers, as Figure 5.7 shows.

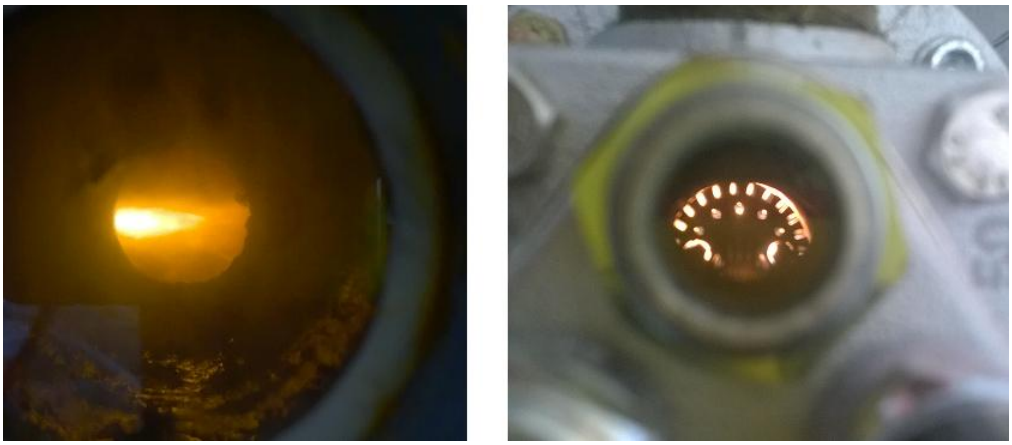

Figure 5.7 – Burner flame

- Wood framework and casting operations

This section is dedicated to the description of all the operations taken into account for the realization of the internals.
Casting operations need a framework to define the concrete shape. To do that, some panels of plywood were cut in the proper way ad put together.

The reactor is composed of three different elements, so that even the wood framework was prepared with three joinable pieces; this choice was made to help in the assembling and allows further modifications.
Figure 5.8 shows the internal silhouette of the entire reactor and the mechanical operations.

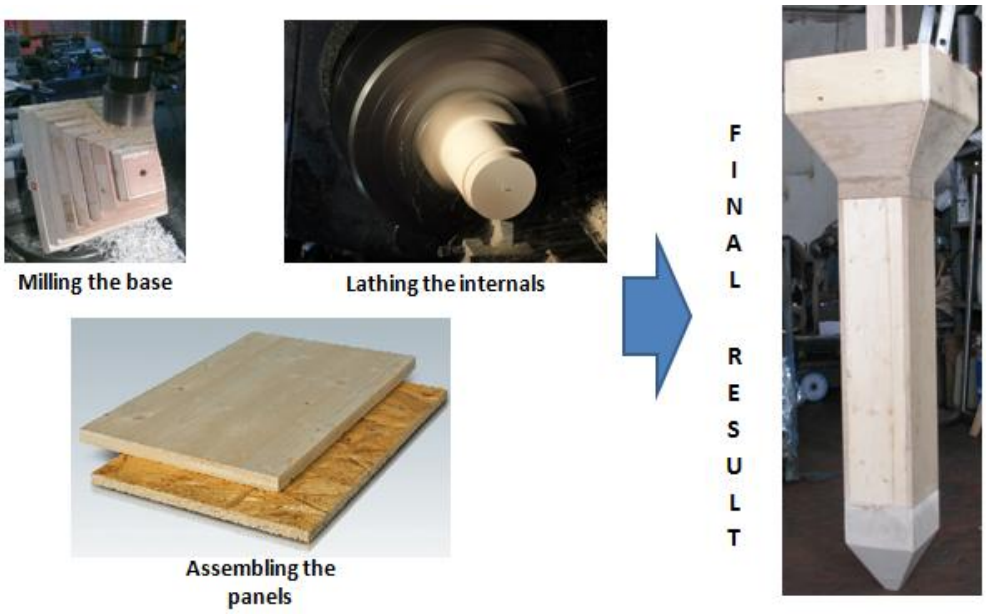

Figure 5.8 – Internal structure execution

As an example, is than described the sequence of the operation followed to prepare the central section of the reactor.
At first, a couple of layers of thermal isolating, cut in the proper way, were placed in contact with the steel wall, as Figure 5.9 shows.
Welded at the wall, it is possible to see several springs, which act as an anchorage for the concrete. In the outside portion of each spring, a plate fastens the concrete and holds all the structure, while the first portion surrounded by the insulating is free to move and damps the thermal dilatations.

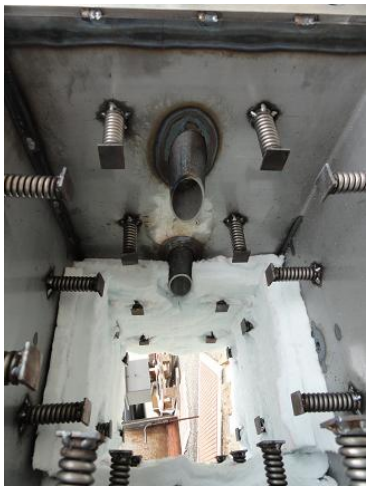

Figure 5.9 – Thermal insulation positioning

It is important to consider, before casting, that some additional devises, such as thermocouples, need a path to be introduced across the concrete. For this reason, wood elements that cross the space between the external shall and the framework, must be placed and removed after the solidification of the entire structure; most of them are placed to arrange tunnels for the thermocouples, by using wood cylinders of 6 mm diameter.
The preparation of the cavities connected to the feeding ports needed a preparation much more complex. Figure 5.9 shows two metallic pipes that partially protrude inside the structure; the key point is that it is not possible to put in touch the steel with the concrete as the thermal dilations will crack the pouring.
The solution adopted, makes use of a small refractory pipe that bridge the steel and the concrete; this pipe has a diameter slightly greater than the one in the steel section because of thermal dilatation. An intermediate wood structure with two different diameters is connected both to the steel and to the ceramic pipe, holding them together for the pre-casting phase.

Figure 5.10 – Refractory pipe and wood holding structure

As soon as the insulating is all over placed and all the internals positioned, the wood framework can be introduce carefully in the midpoint. Now it is possible to pour the concrete, with the right degree of viscosity, in the gap between the insulating and the wood. After few hours, the concrete solidifies, even though it is better to wait a couple of days before removing the internals. Some wood elements that cannot be removed easily do not represent a problem since they will be removed during the pre-commissioning phase at high temperature.

- Flanges and gaskets

Flanges and gaskets are used to guarantee a good connection between constitutive elements and pipes, avoiding leaks. All of the flanges were rebored after welding, in order to optimize the relative contact, than leaks are prevented by using three different solutions.
It is important to remark that the pilot unit was devised to work at atmospheric pressure; a slightly overpressure is caused by the pressure drop generated by the solid hold-up, pipes and the equipments as well; the overall pressure drop is evaluated less than 300 mbar.
For some flanges relatively far from the high temperature zones or in stagnant areas, fibre gaskets are sufficient to prevent leaks. These gaskets were used, as an example, for the small windows at the top of the reactors that will be described later.
For the connections at high temperature, metal gaskets were used to guarantee the seal.
A different solution was followed concerning the big squared flanges proper of some elements, like the burner cover, the top of the reactor or the different sections of the rig. In this case, a copper filament, placed as a spiral, stays between the two flanges and minimizes leaks; furthermore, powder deposition during operation will optimize the seal.

Figure 5.11 – A) fibre gaskets, B) metallic gaskets, C) copper seal

- Connection to the gasifier

The flue gas from the burner passes through a horizontal pipe of 450 mm length, followed by a vertical one connected to the reactor base.
A static mixer, composed of a series of tilted blades (Figure 5.12), is placed in the horizontal pipe.
Mixed gas, after a 90° turn, enters in the reactor across the inlet orifice, flanged to the bottom of the reactor base (Figure 5.13). A plate valve can be closed during the shut dawn in order to maintain solids inside the reactor or conversely a screw plug can be removed to unload all the reactor hold-up.

Figure 5.12 – Static mixer.

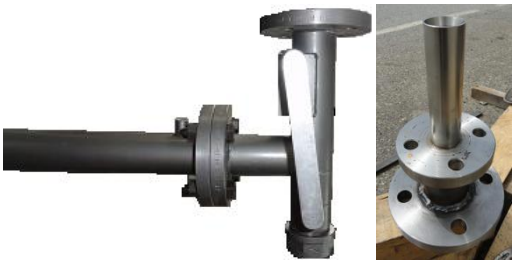

Figure 5.13 – Entrance for the fluidizing gas and central inlet.

The weakness of this area from a thermal point of view can be overcome with a proper insulation. As shown in Figure 5.14, three layers of insulation roll up the tube and a thermocouple gives information about the temperature of the gas entering the reactor; the drawback is the high temperature that can be reached by the steel but, as previously discussed, values over 700°C during the start-up are avoided. The final aspect taken by this section is given in Figure 5.14.

Figure 5.14 – Static mixer and gas entering point.

- Spouted bed reactor

The reactor body is divided in three sections: the base, the central and the top. This choice was done in order to simplify the construction, to allow further structural modification and even because these sections play different roles.

The base

The reactor base has a pyramid frustum shape; it can be considered the most complex part of the rig, since several openings are present besides the complicated geometry.
At the base of the structure, as depicted in Figure 5.15, four openings are presented: in the centre, a metallic cylinder replaces the gas inlet: it helps to place in the proper way the wood framework and creates the cavity for the inlet after casting. On the left, two channels are provided for a continuous solid discharge; even though this aspect will be not contemplate in this work, the unit gives the possibility to feed and discharge continuously the solids, thanks to two openings placed in the vertical wall of the reactor at 200 and 350 mm from the base. The last tilted opening accommodates a piston than

during operation maintains the surface of the pyramid smoothed and closed, if it is retracted, the opening in the pyramid allows the solid discharge.
Moreover, besides the anchoring, the vertical wall hosts some opening for thermocouples.

Figure 5.15 – Operation sequence for the preparation of the reactor base.

The median section

This section is placed above the base and it extends the bed depth of additional 1.5 m; it engages the upper part of the solid hold-up and contains the fountain for all its length. Two entrances for solid particles are present in this section, characterize by a slope of 60 deg to avoid obstructions; the feeding points are placed respectively at 500 and 700 mm from the base.
Embedded in the concrete, to be more precise at the corners, two pipes allow the discharge of solids in continuum and they pair vertically with the two openings previously depicted at the base. Since they are inside the concrete, the fluid dynamic is not affected and, if the exits are closed, they simply fill with solid and, like a dead volume, do not affect the process.
In conclusion, eight openings at the wall allow introducing thermocouples to monitor the temperature profile along the section.

Top section

Named also disengagement zone, it has a bigger cross sectional area, which passes from 200 mm to 400 mm side, with a 60° slope. This configuration, suggested by some literary works (Wotkinson, 1984), reduces the gas velocity and it consequently reduces the elutriation of powders and sand fragments.
The wall houses an additional manifold connected to a rupture disk of 3 inches, placed for safety reasons; additionally it is present a connection to a U-manometer to define the pressure inside the gasifier.
A series of openings at the top of the reactor allow placing additional devices; a thermocouple is used to monitor the gas flow temperature, while two temperate small windows are present to visually directly the spouting regime.

- Cyclone

The outgoing flue gas contains coarse particles resulting from the sand erosion or residues from the reaction. These particles are removed by means of a stainless steel cyclone placed downstream the top section of the gasifier. Solid fraction is stocked in a tank, while the cleaned gas is sent to a water scrubber.
A water sprayer is placed in the pipe that connects the gasifier with the cyclone, in order to cool slightly the temperature if necessary.

- Water scrubber

A water scrubber is used to remove the remaining fine particles from the exhaust gas, and to cool at room temperature the syngas in order to be safety discharged in the environment or to be sent to the analysis instruments.
It has a parallelepiped structure 400x400x600 (LxWxH) and on the middle of the vertical walls, four sprayers are placed to inject vertically nebulised water.
The hot gas enters in the scrubber through a vertical pipe that passes across the top cover up to few centimetres from the base; from this point, it has to raise the structure in counter-flow respect the water, since a water trap is present at the base. At the top, the water scrubber has again a demister, which is continually maintained wet by other four sprinklers.

- Off-line solids pelletiser

In Chapter 4.7 it was demonstrated that some textile agglomerates prepared by hands work in the proper way inside a spouted bed reactor. However, for industrial applications is obviously infeasible to follow this way, but it is necessary to conceive an apparatus able to prepare and to dose the textile waste in the gasification unit.
In the frame of VALENTEX project, an equipment able to solve this problem was designed and assembled.
This feeder is composed of a hopper where all types of wastes can be accumulated; it has a cylindrical shape and an internal agitator that prevents solids blocking. The bottom is connected to a cochlea that is used to dose and mildly compact the fibre scraps. At the end of the cochlea, the solids have the right degree of density and an iron disk with blades disrupts the aggregates and let them fall into another tank. At the end, these particles pass through two rotating asymmetric disks and they are sized at the final shape and density.
Even though the final aim of this project is to connect this apparatus directly with the reactor, at first, a different solution was considered for more simplicity: particles produced in this way are stocked and manually transferred to another equipment that doses and discharges automatically the agglomerates inside the reactor.

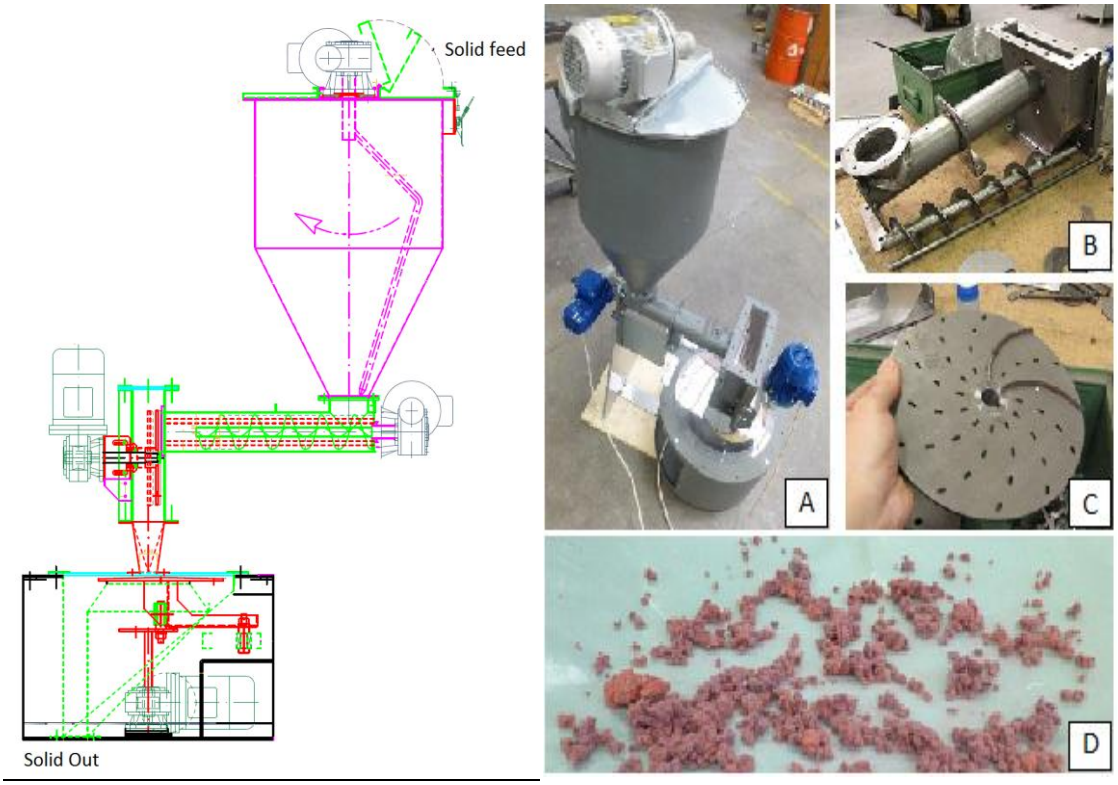

Figure 5.16 – Scheme if the textile pelletizer and Mechanical details of the pelletizer for textile scraps. A) Apparatus, B) Screw feeder, C) Bladed disk, D) Pellets of textile.

- On-line solids feeding

Solids particles can be fed continuously in the reactor through a system connected to the lateral wall of the reactor. The feedstock, previously prepared and sized, is charged in a hopper, with a conical shape to help in the discharge. Inside this vessel, a blade enlivens the particles in order to avoid obstructions; furthermore, a vibrating system gives an additional help.
Out of the hopper, the particles pass through a rotary valve that allows dosing the solids inside the gasifier.

- Sprayers

The experimental rig makes use of three different types of spryer: atomisers and nebuliser with empty or full cone.
For what concern the air-steam gasification, the water atomisers are essential to lead the reaction: two sprinklers are placed inside the burner chamber and they supply the right amount of water, which immediately vaporizes. These nozzles cross the flame and the drops size must be as small as possible, in order to minimize the heat transfer and to obtain immediately the requested steam; moreover, to preserve the concrete in good

health and preserve it from rifts, it is important to avoid thermal shocks by putting it in touch with liquid.
The maximum flow rate given by these nozzles is strictly linked to the upstream pressure, which should be maintained above 5 barg. Two pressurized tanks were placed close the burner chamber to have pressurized water and to grant continuous operations: the vessels are connected to the compressed air provided by the factory at 7 barg, a regulating pressure valve placed in between, maintain the right value of pressure inside the tanks avoiding fluctuations.
The same type of atomizer is placed at the entrance of the cyclone and the small quantity of water is used, if it is necessary, to cool the syngas coming out the reactor.
In the water scrubber, the exhaust gas passes in counter-flow respect the water nebulised by four sprinklers; the shape of empty cone allows entrapping fines eventually not stopped in the cyclone. At the upper cover of the scrubber, other four sprayers spill water homogeneously over the underlying demister.

Figure 5.17 – From right to left: nozzle for the burner, for the scrubber and for the demister.

- Flow-meters

A flow-meters panel was realized in order to regulate and visualize the volumetric flows of all the streams. Figure 5.18 shows the sequence of instruments placed.
The flow-meters, from left to right regulate: LPG, air, water for the burner nebuliser, water for the scrubber, water for the demister and water for the cyclone nebuliser.

Figure 5.18 – Flow-meters panel control.

- Temperature control

The temperature in the experimental unit is monitored by several thermocouples, as depicted in the scheme presented in Figure 5.19. The rig makes use of probes K-type, 3 mm diameter, 300 length.
A data logger connected to all the thermocouples, is able to visualize easily all the data acquired and to record the temperature evolution.

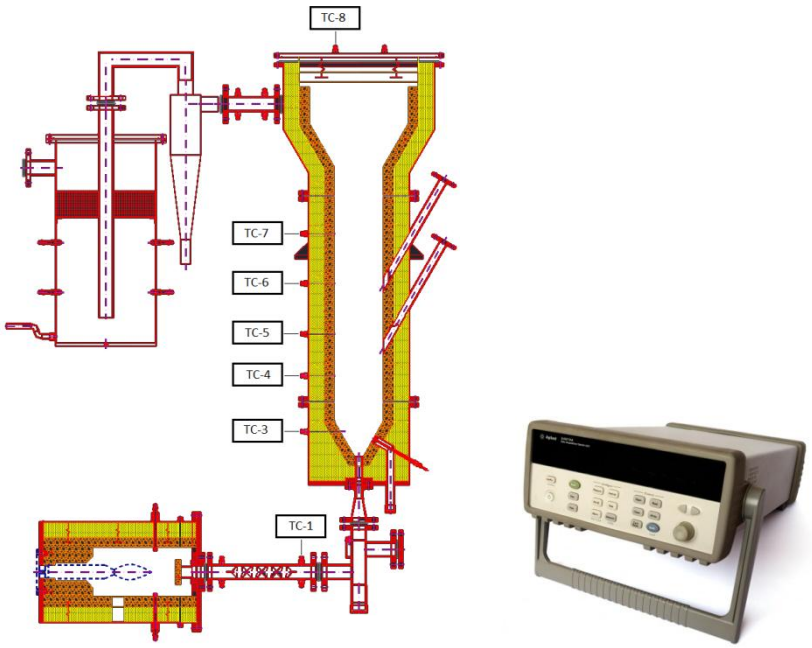

Figure 5.19 – Thermocouple in the experimental unit.

The above Figure 5.19 shows the codes and visualizes the position of them in the rig. More detail are presented in Table 5.5

Table 5.5 – Additional information on the thermocouples.

Name	Equipment	Note
TC-1	Static mixer	/
TC-3	Base of the reactor	65 mm from the base
TC-4	Base of the rector	155 mm from the base
TC-5	Middle section of the reactor	285 mm from the base
TC-6	Middle section of the reactor	455 mm from the base
TC-7	Middle section of the reactor	855 mm from the base
TC-8	Top of the reactor	/
TC-9	Cyclone	/
TC-10	/	/

5.3 Pre-commissioning

Before performing operations at high temperature, the refractory should be conditioned in order to avoid thermal shocks and fractures. The temperature has to be increased gradually in order to remove the excess of water and humidity still present in the concrete matrix. This operation requests several hours and should be repeated for different cycles.
The rig, at first, was gradually heated at low thermal power for several hours; as an example, the Figure 5.20, shows the increment of the temperature in the different areas of the experimental unit. The burner was set at 11 kW thermal power, with a slightly excess of air (λ=1.2); in this preliminary test the water was not added in the combustion chamber, only a small amount of air passes through the nozzles to maintain them cooled. The reactor was kept empty to help the water removal.
The thermocouples inside the gasifier stick out from the wall of 10 mm; the sudden increment that can be seen for thermocouple TC-3 at 4000 s, is due to the repositioning of this probe perpendicular to the gas inlet, in the middle section of the reactor.
The first observation that can be done is the wide spread between TC-1 and the others thermocouples; this is linked to the slowness of the concrete to reach the equilibrium temperature. Another important aspect is linked to the difference in temperature between TC-1 and TC-3, after its repositioning. Since TC-1 is downstream the static mixer and TC-3 is above the gas inlet, this gap represents the heat lost in the vertical pipe; a proper insulation can reduce this gap (Figure 5.14 shows the final insulation), while nothing can be done for the last 150 mm where the inlet cross the concrete and part of the heat is lost.

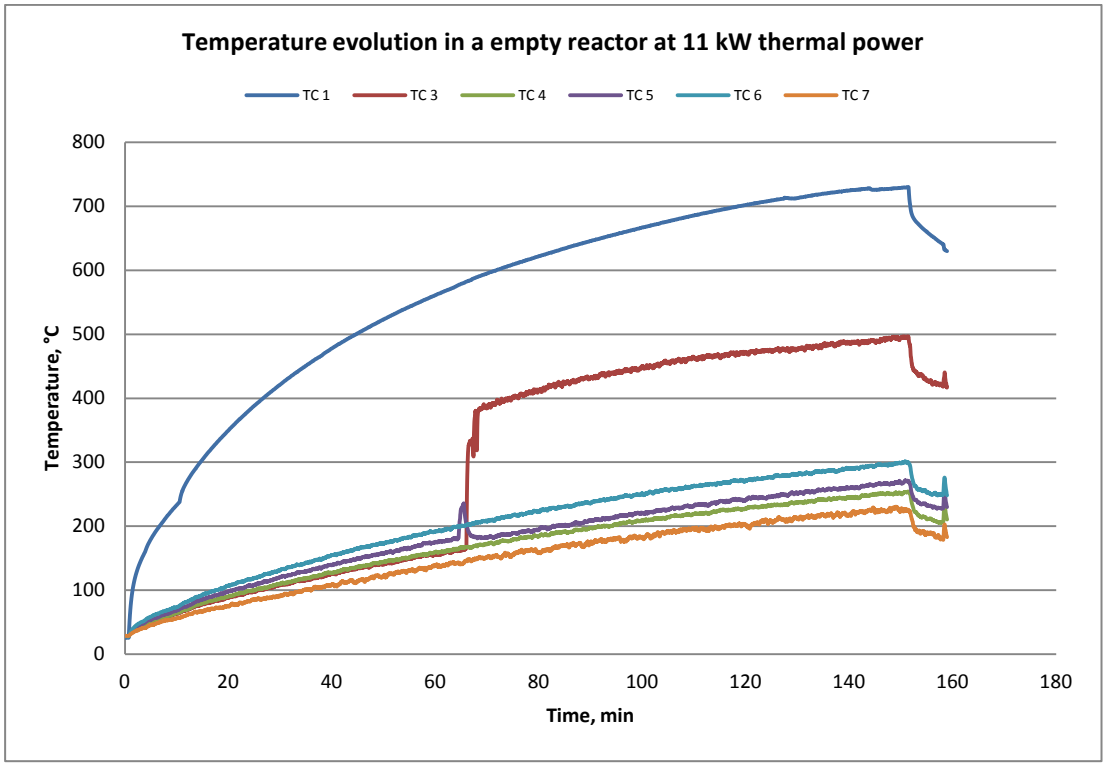

Figure 5.20 – Temperature evolution in the rig, 11 kW thermal power, empty reactor.

The concrete conditioning was performed several times; the last operation was carried out at 22 kW thermal power. Again, the water was not added in the reactor and it was maintained empty.

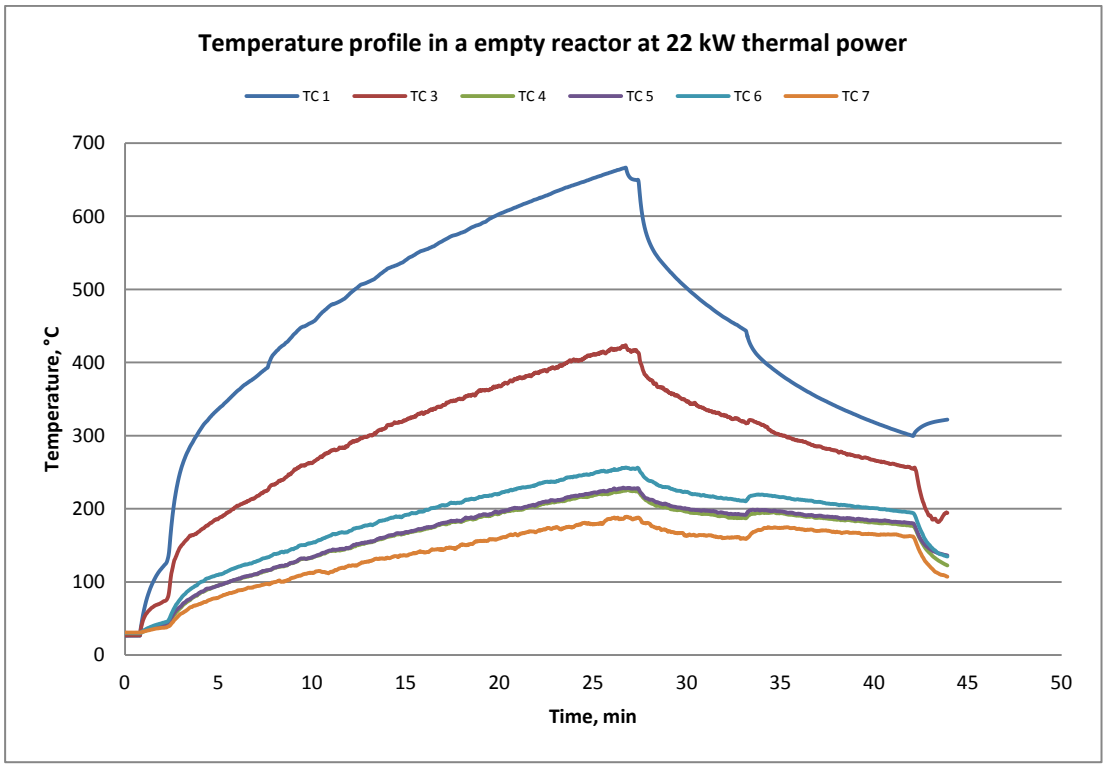

Figure 5.21 – Temperature profile for 22 kW thermal power in an empty reactor.

Figure 5.21 shows the last thermal profile obtained in an empty reactor; the insulation is now optimised as much as possible and this can be verified by the reduction of the gap between TC-1 and the other probes. Doubling the power and with the proper insulation, the time needed to reach the same temperature, is reduced more than a half.
As soon as the concrete is conditioned in the proper way, it is possible to introduce the inert and to see how the spouted bed works at high temperature. A small amount of sand was then introduced in the reactor, just a couple of litres in order to fill completely the base.
The first test was performed at 11 kW, while all the thermocouples (TC-3 included) protrude 10 mm from the wall.
The results are shown in Figure 5.22. In this case, the presence of the inert improves the thermal transfer since it holds the heat, denying its loss through the exhaust gas. It can be verified, as the thermocouple TC-3, immerged in the sand, shows a clear increment in the temperature. A thermal power of 11 kW for the start-up phase, seems to be appropriate as the sands temperature reaches 400 °C in about one hour.

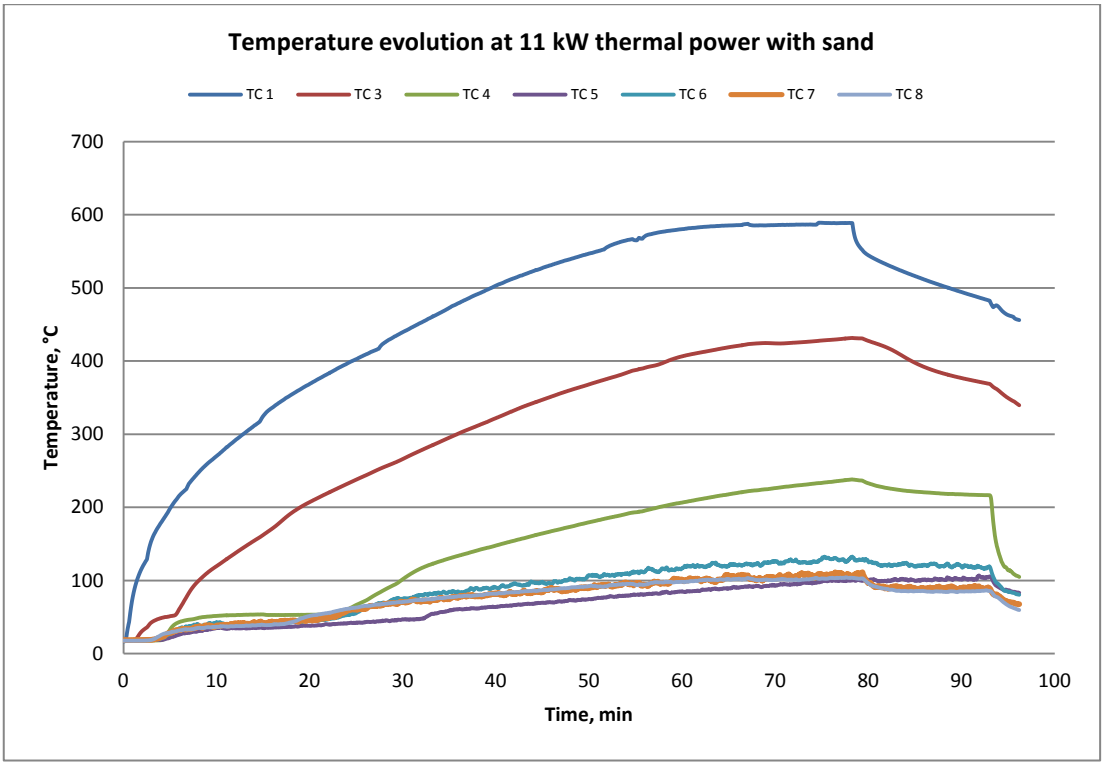

Figure 5.22 – Temperature profile for 11 kW thermal power; 2 L of sand as hold-up

The last step on the pre-commissioning at high temperature is to consider the apparatus behaviour in terms of temperature profile, in presence of water nebulised in the combustion chamber.
Figure 5.23 depicts the temperature profile, while additional information on the streams of Air, LPG and water are given below in the same figure. The O_2 index (λ), represents the ratio between air and the stoichiometry propane at the burner, always maintained above 1.05 for safety reasons.

The start-up was performed as before at 11 kW, with a slightly excess of air, for 30 minutes. The following sudden increment in the air flow mixes the solids; this initially brings to a temperature drop, then the sand temperature rises again.
At the 45th minute, water was injected in the combustion chamber and immediately vaporized; this phenomenon does not affect heavily the temperature inside the reactor, since the temperature gradient was not modified particularly, save the temperature in the static mixer, which decreases at the operative value of about 500°C.
In the last 30 minutes the flows of air, LPG and water were kept at the operative condition depicted in Chapter 5.1.

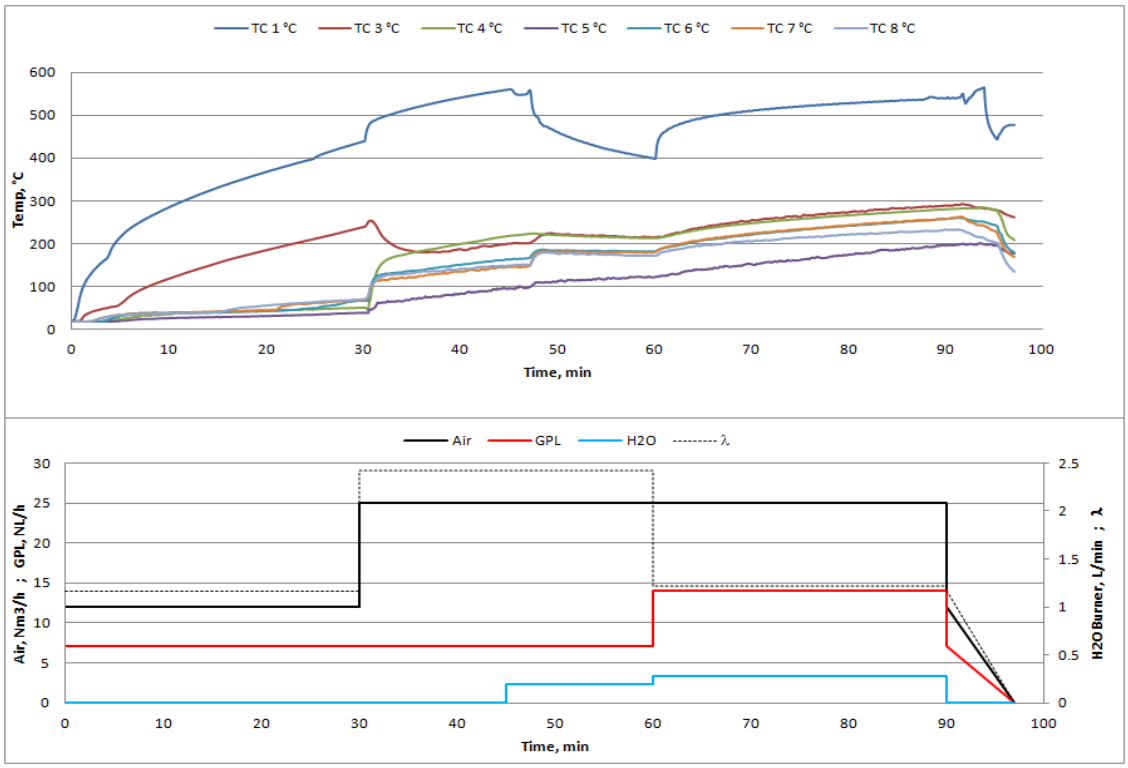

Figure 5.23 – Temperature and flow profiles in the rig, in absence of chemical reactions

The pre-commissioning without thermal reaction can be considered concluded with this last experiment. In the following phase, some reacting materials were introduced inside the reactor to analyze its behaviour.

5.4 Achievement of the steady-state

Up to now, no thermal reactions were performed inside the reactor, nevertheless to reduce the start-up phase and reach the operative field for the gasification, a temperature above 800°C inside the reactor must be grant. The achievement of the reacting condition is shown in Figure 5.24.
The initial step was given by preheating the spouted bed to about 400°C (by reading the thermocouple output in the sand bed), this temperature guaranteeing the ignition point of a fibrous waste having a standard composition. This step was carried out by regulating the furnace thermal power at 11 kW with a suitable LPG flow rate and minimal extra-stoichiometric air. The desired temperature was reached in about 60 min, as shown in Figure 5.24A). A solid particulate combustion mode in the spouted bed was then chosen to speed up the whole reactor heating and reach the actual gasification temperature. The following step was given by switching to combustion regime by minimizing the LPG flow; at these conditions the stoichiometry ratio λ between oxygen and gaseous fuel was increased to about 10. The prompt peak of temperature at 90 min was given by the oxidative regime. Subsequently the air flow was decreased to have a reducing reaction mode (endothermic pyrolysis) in the 90 to 110 minute interval. A partially oxidative regime to gasify the pyrolytic solid residue previously generated followed by regulating the LPG flow and water spraying in the pre-burner to maintain an adequate in-line steam generation. The sequence of different LPG/air ratios was conceived to demonstrate the feasibility of easy reaction control in the whole range of possible operations. Figure 5.24B) gives an account of flow rates in the various conditions tested.

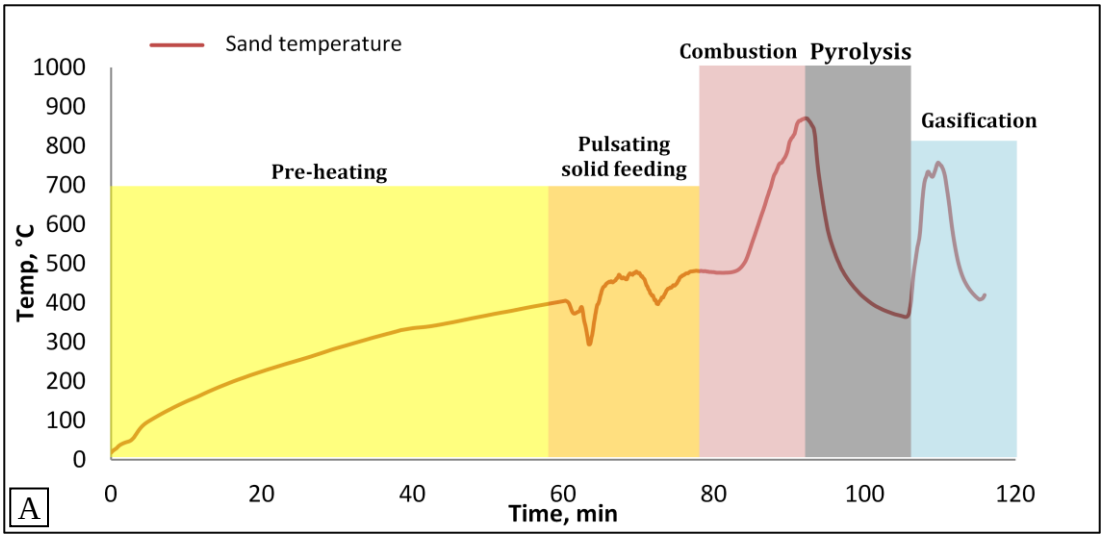

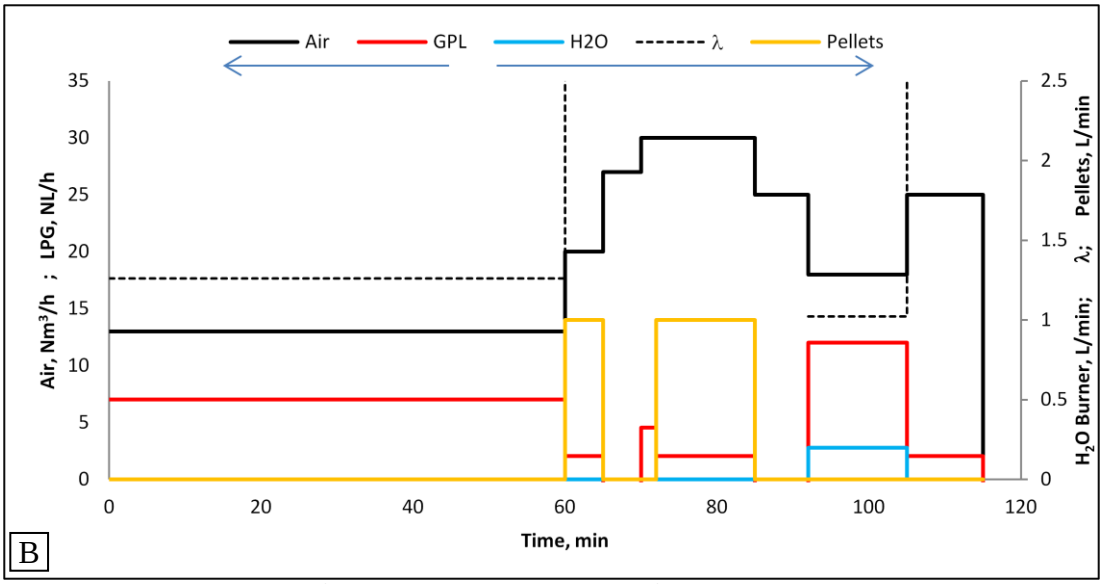

Figure 5.24 – Thermal transitory and flow regulation in the spouted bed gasifier

The solution adopted makes use of a pre-heating of the bed at about 400°C (TC-3), which needs about 60 min at 11 kW. At this point some wood pellets were added inside the reactor; the reduction of LPG flow and the increase of the air flow, grants a high oxidizing atmosphere ($\lambda \approx 10$). The total combustion of this material provides an addition boost of energy and the enthalpy of reaction transferred to the inert and to the rig causes a sudden increment of the temperature.

5.5 Syngas analyzer

The composition of the syngas, continuously generated during the thermal process, may vary since the reaction kinetics is influenced by the many factors, as the reactor temperature, the inlet gas composition and the quality of the waste. A medium chemical composition can be used to determine the goodness of the process, however it can be tricky to determine, since it has not been possible to arrange a gas-chromatography apparatus near the prototype unit.
The possibility to stock the gas in bags to analyze later was not followed, since some heavy hydrocarbons may condensate or adsorb during carriage, compromising the final result. Portable gas-chromatographers are not sufficiently accurate to determine all the compounds in the syngas. In any case the gas-chromatography technique gives a response after a long time of sampling, due to the retention time of each component in the capillary columns.
A TFS spectroscopy has been chosen to analyze continuously the produced syngas.
The TFS Analyzer (Tunable Filter Spectroscopy) is a non-contact, light absorption based gas analyzer capable of ppm to percent level concentration monitoring of multiple gas compounds. The analyzer consists of a light spectrometer, a flow-through sample cell, a single-element photo-detector, and the supporting electronics. The spectrometer

provides wavelength scanning with high optical throughput. An advanced spectral processing algorithm computed in the embedded electronics provides highly accurate and robust quantitative measurements.
The TFS gas analyzer is configured and calibrated for a specific wavelength analysis region depending on the application for which it is intended. It is designed to be a dedicated on-line monitoring system.
The syngas analyzer was provided by "ETG Risorse e Tecnologia", named ETG-6700, a tunable unit that, besides the standard configurations, can be equipped with other additional devices ad hoc.

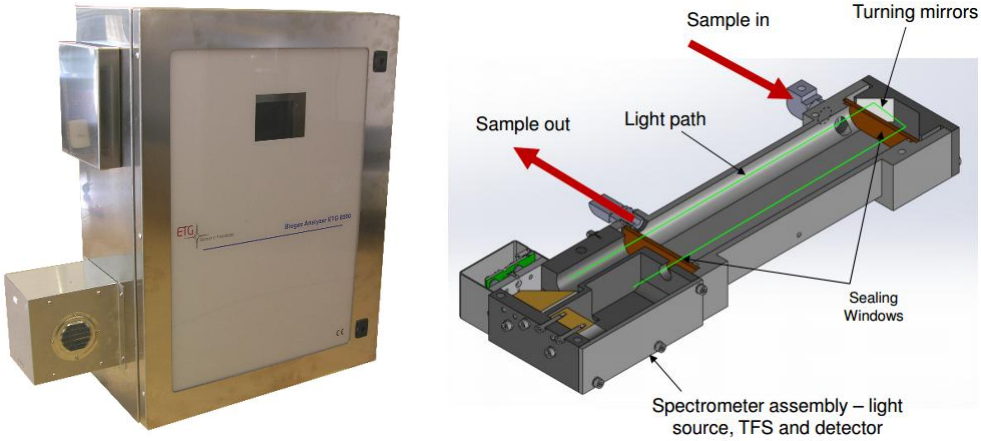

Figure 5.25 – On-line syngas analyzer and scheme of the principle of operation.

The principle of operation in based on light absorption: when a gas sample is introduced into the gas cell, the light radiation provided by a broadband light source is partially absorbed by the gas species present. The light absorption occurs at specific frequencies and magnitudes depending on the gas compound and the concentration of that compound.
The TFS gas analyzer spectrometer module scans the wavelength and measures the true absorption spectra and compares them with the pre-loaded calibration spectra. The on-board analysis algorithm computes the predicted gas concentrations in real-time, which can then be outputted through the MODBUS TCP/IP protocol.
In principal, the absorption spectrum of each compound is unique which acts as a "fingerprint" for identification or speciation analysis. In addition, the magnitude of the absorption is a function of the number of molecules of the gas. With a known path length, pressure, and temperature, the magnitudes of the absorption spectra are then used to compute volumetric concentrations.

Table 5.6 – Performance of the syngas analyzer.

	Field	Accuracy
Methane	0 - 100%	± 0.5%
Ethane	0 - 25%	± 0.2%
Propane	0 - 25%	± 0.2%
Iso-butane	0 - 10%	± 0.1%
n-butane, n-pentane	0 - 10%	± 0.1%
C-5 lumped	0 - 10%	± 0.2%
CO_2	0 - 100%	± 0.2%

This first principle based technique provides accurate and robust measurements with minimal span and baseline drifts.

The TFS Gas Analyzer employs an internal pressure transducer to measure the sample pressure in real-time enabling pressure variation corrections. The flow cell is heated to a constant temperature (default value is 60°C) with a sample preheat module to maintain both sample and optical sensor temperature at a constant calibrated temperature, thereby ensuring measurement accuracy and stability despite sample and environmental variations.

This technology allows real time analysis, since it is possible to obtain the gas composition each 5 seconds. The non contact between the gas and the detector, avoids sensor poisoning and long-term stability.

Some additional boards installed on the analyzer, allow determining the quantity of H_2 and O_2 in the outlet gas. The latter is particular important for all the operative phases, since the presence of oxygen in the fluid is a key point on the performances of the thermal reaction.

6 Conclusions

This PhD work aims at generating a comprehensive work on square based spouted bed reactors, as an alternative system to carry out thermal treatments on solid wastes. Instead of a standard cylindrical section, the squared one was adopted since it allows further developments in terms of scale up.
The scale up of a spouted bed presents several uncertainties and it cannot be achieved only by the linear increment of size. The concept of a multiple unit overcomes this problem, as the total hold-up is given by the number of the modules; furthermore, if a sequence of units is set, the total residence time of solids approaches a plug flow. Only through a careful hydrodynamical evolution, it is possible to conceive non-interacting units.

The entire work can be divided in four sections:

- experimental comparison between cylindrical and square-based sections;
- optimization of the feature of a multiple unit;
- hydrodynamical modelling of multiple spouted bed;
- design and construction on o a pilot unit for gasification;
- thermal treatment of textile waste material.

Comparison between circular and square-based sections

Several square-based spouted bed vessels were built for a sequence of operations at room temperature.
The square-based section has demonstrated a fluid mechanics that does not differ from the cylindrical one. The experiments performed over a several types of solid particles, shown the absence of dead zones, together with a regular circulation of the particles. The use of several pressure probes in the annular section has demonstrated that the gas distribution is homogeneous and increases from the base to the surface, due to the axial-distribution of cross flow of gas from the spout to the annulus, according to the findings existing for cylindrical units.

The fundamental operating parameters as the maximum spoutable bed depth or the gas velocity to maintain stable spouting, do not different substantially on the two geometries. Empirical correlations, devised for the cylindrical unit, work properly in the parallelepiped one, even thought the physical properties of the solids may have some influence on the results.
Some additional devices such as draft tube or auxiliary fluidization were adopted to modify the solids recirculation time and the gas distribution in the annulus. A non-porous draft tube hinder the air cross flow from spout to annulus, therefore the gas flow rate crossing the annulus is strictly linked to the gap left between the draft tube and the reactor base. Since the maximum spoutable bed depth related the flow of gas passing through the annulus, the draft tube allows to overcome the limitation, predicted by the existing correlations.
The auxiliary fluidization is generally employed in larger units to improve the solids circulation at the base. The secondary fluidization used together with a draft tube allows a fine regulation of the gas flowing in the annulus.

Hydrodynamic study on multiple spouted bed units

Since the scale-up can be performed by the repetition of several adjacent units, a multiple spouted bed rig have been used to define which are the main geometrical features that have to be taken into account to optimize the fluid mechanics inside the vessels, ensure stability at the operative conditions and to simplify the start-up as well.
The conclusions drawn are derived both from the numerical results, both from direct observation and from personal experience.
Some geometrical features adopted to improve the global behaviour in the multiple units are the following:

- Solids feeding point: feeding the solid directly on the lateral surface of the ring is preferable to eliminate, or at least minimize, the effect of by-pass that would occur if the feed drop directly over the fountain. The clearance between the vertical baffle and the annulus top must ensure an adequate passage to prevent any head in the solids downcomer.
  It is also suggested to set a distributor in the solids duct to dose it homogeneously along the entire side.

- Fountain separators: fountain separators have the purpose of minimizing the interaction between modules, preventing a by-pass of solids between adjacent units in the freeboard. To relegate the fountain in its own module, two geometric configurations were adopted. The first makes use of some sheets vertical separator between two modules, protruding down to few centimetres of the bed free surface. The second solution adopts some fountain regulators (the so-colled "Chinese

hats"), made of a metal mesh, able to control the height of the fountain and drive back the solids to the spouted bed.
The vertical baffles have shown to facilitate the start-up of the equipment; while the fountain regulator alone cannot control the fountains characteristics at the spouting onset. Additionally the regulator acts as a target against particles, given origin to a relevant comminution.

- Relative elevation between vessels: the employment of several modules in series makes necessary to define the relative position optimal for operating the equipment. At low flow rates and in batch conditions, the hydrodynamic of the overall system does not show any particular changes between a configuration with beds placed at the same level or staggered. However, the start-up phase is extremely simplify by operating staggered unit beds. This configuration was successful also at high flow rates of solids, which overflow to maintain the hold-up in each unit constant.
  On the contrary, reducing the relative elevation of the spouted bed units brought to a progressive accumulation of solid, which eventually led to instability due to different spouting pressure drop.

Mathematical modelling of multiple spouted bed

The hydrodynamics proper of a continuously operating spouted bed reactor was described by means of a stimulus-response analysis and calculated by Simulink.
Considering the annulus given by a limited number of parallel plug-flow systems, the spout a low solids holdup transported pneumatically and the fountain a well-mixed region, this mathematical model is able to properly describe the fluid mechanics of a spouted bed apparatus. The mathematical modelling considers the interaction between simple units; mass flows, residence times and degree of recycling were drawn from experimental and direct observation of the units.
It was quite confirmed the consolidated description of a spouted bed as a well-mixed system with a minor plug-flow contribution, as the solids recirculation prevails over the clearly vision of piston movement of particles in the annulus.

Construction of a pilot unit for gasification

As spouted bed equipments have demonstrated advantages over the standard fluidization, a significant reduction of the segregation phenomena.
This is the case of thermal reaction s where a light reacting phase is mixed with an inert and dense phase.
The construction of a pilot prototype was necessary to validate hydrodynamical findings obtain from experimental data for the gasification reaction of various materials.

A relevant work of designing, planning the construction of various components, followed by the assembly of all the elements was necessary.
The geometrical features to realize a unit characterized by 20 kW thermal power were chosen. The design was carried out by a process calculation sheets to define all the streams.
The main body of the prototype is composed of three joinable pieces. As the construction of a high temperature reaction, requires an internal refractory lining and an external steel shell, with an intermediate insulation. Casting the system requires great alignment care, both to run the gasification and to assess the hydrodynamics of a spouted bed unit operating at high temperature.
This unit was conceived to operate in batch and in continuous modes, both for feeding and overflow discharging of solids.
The thermal start-up of the unit, carried out with an upstream LPG combustion unit, allows feeding a low oxidizing, neutral or reducing gas steam to cover the broadest range of gasification conditions.

Thermal treatments of fibrous scraps

Textile waste represents an important issue for this industrial sector.
The most common solution adopted up to now has been provided by landfilling, according the classification of "special waste".
This type of waste has a high chemical potential, as it can be transformed into medium heating value syngas. This gas, essentially a mixture of hydrogen, methane and carbon monoxide can be considered a valuable fuel or a chemical intermediate.
The spouted bed reactor, built for this project was used to gasify woody biomass and textile waste upon pelletization.
The reactor need a pre-heating step in which the inert bed constituent is heated up to 400°C.
As a preliminary strategy to reach thermal steady state, wood biomass was used to reach the desired temperature. Then, pelletized waste material replaced wood chips, being both feedstock compatible with the feeding system and he spouted bed hydrodynamics.
A detailed characterization of the syngas produced by means of an on-line analyzer is planned as a second project step.

7 Bibliography

Arnold, M.St.J., Gale, J.J. and Laughlin, M.K. "The British Coal spouted fluidized bed gasification process". *Can. J. Chem. Eng.*, 70 (1992), 991–997.

Aumann, F., Donnerbrink, H., Altenhovel, O. "Data base on the rise of textile waste from different textile branches in Germany". University of Munster, Germany. pp. 2-44, JOF3-CT95-0010.

Beltramo, C., Rovero, G. and Cavaglià, G. "Hydrodynamics and thermal experimentation on square-based spouted beds for polymer upgrading and unit scale-up". *The Can. J. Chem. Eng.*, 87 (2009), 394-402.

Bernocco, D., "Innovative application of spouted bed technology to the high temperature conversion of biomass into energy". PhD Thesis, University of Genova (2013).

Bjerle, I., Padban, N., Wang, W., Ye, Z. "PFB Co-gasification of fuel blends coal/textile"; biomass/textile wastes Lund University, Sweden. pp. 147-166, JOF3-CT95-0010.

Cavaglià, G., "Reactor and process for solid state continuous polymerisation of poly-ethylene terephthalate (PET)" Patent EP 1576028 B1, (2003).

Cui H. and Grace J.R. "Spouting of biomass particles: a review". *Bioresource Technol.*, 99 (2008), 4008-4020.

Chandnani, P.P., Epstein, N., Ostergaard, K. and Sorensen, K. "Spoutability and spout destabilization of fine particles with a gas". *Fluidization V: Engineering Foundation*, NewYork (1986), pp. 233–240.

Chatterjee, A. "Spout-fluid bed technique". *Ind. Eng. Chem. Process Des. Develop*, 9 (1970), 340-341.

Chen, Z.W. "Hydrodynamics, stability and scale-up of slot-rectangular spouted beds". PhD thesis, University of British Columbia (2007).

Crudo, D. “Criteri di scale-up per letti a getto multistadio per il riscaldamento di chips di PET”. Master degree thesis, Politecnico di Torino (2008).

Epstein, N. and Grace, J. “Spouted and spout-fluid beds”. *Cambridge Univ. Press*, ISBN 978-0-521-51797-3, New York (2011).

Freitas, L.A.P.O., Dogan, M.C., Lim, J., Grace, J.R. and Luo, B. “Hydrodynamics and stability of slot-rectangular spouted beds increasing bed thickness”. *Chem. Eng. Comm*., 181 (2000), 243–258.

Geldart, D. “Type of fluidization”. *Powder Technology*, 7 (1973), 285-292.

Gale, J. and Bower, C. J. “Development of the British Coal gasification process for themanufacture of low calorific value gas”. Presented at Applied Energy Conference, Swansea (1989).

Gishler, P.E. and Mathur, K.B. “Method of contacting solid particles with fluids”. U.S. Patent No.2,786,280 (1957) to National Research Council of Canada.

Grbavčić, Ž.B., Vuković, D.V., Hadžismajlovic, D.E., Garić, R.V. and Littman, H. “Fluid mechanical behaviour of a spouted bed with draft tube and external annular flow”. *2nd Int. Symp. on Spouted Beds, 32nd Can. Chem. Eng. Conf.*, Vancouver (1982), Canada.

Hayakawaa, Y. and Oguchib, T. “Evaluation of gravel sphericity and roundness based on surface-area measurement with a laser scanner”. *Computers and Geosciences*, 31 (2005), 735-741.

Khoe, G.K., Ruda, M.M. and Epstein, N. “Batch comminution of coal in a spouted bed”. *Powder Technology*, 39 (1984), 249-262.

Kunii, D., Levenspiel, O. “Fluidization Engineering”. *Butterworth-Heinemann* USA (1991)..

Lim, C.J. and Grace, J.R. “Spouted bed hydrodynamics in a 0.91 m diameter vessel”. *Can. J.Chem. Eng*., 65 (1987), 366–372.

Mamuro T., Hattori H., “Flow pattern of fluid in spouted beds”, *J. Chem. Eng. Jap*., 1 (1968), 1.

Mathur, K.B., Epstein, N. *“*Spouted Beds*”*. *Academic Press*, New York (1974).

Rovero, G., Piccinini, N. and Lupo, A. “Vitesses des particules dans les lits à jet tridimensional et semi-cylindriques”. *Entropie*, 124, (1985) 43-49.

Metcalf, J.R. “The mechanics of the screw feeder”. *Proc. Inst Mech. Eng*. 180 (1965-66), 131-146.

Mujumdar, A.S. “Spouted bed technology – a brief review”. *Drying*, New York: Hemisphere (1984), pp. 151–157.

Nemeth, J. and Pallai, I. “Spouted bed technique and its application”. *Magy. Kem. Lapja*, 25 (1970), 74–82.

Nemeth, J., Pallai, E. and Arabi, E. “Scale-up examination of spouted bed dryers”. *Can. J. Chem.Eng*., 61 (1983), 419–425.

Olazar, M.M., San Jos´e, J., Aguayo, A.T., Arandes, J.M. and Bilbao, J. “Stable operation conditions for gas-solid contact regimes in conical spouted beds”. *Ind. Eng. Chem. Res*., 31 (1992), 1784–1791.

Piccinini, N. “Particle segregation in continuously operating spouted beds”. In: *Fluidization III*, J.R Grace and J.M. Matsen, 279-285, Plenum Press, ISBN 0-306-40458-3, New York USA, (1980).

Rovero G., Curti M., Cavaglià G. “Optimization of Spouted Bed Scale-Up by Squared-Based Multiple Unit Design” in “*Advances in Chemical Engineering*”. Edited by Zeeshan Nawz and Shahid Naveeds, Chapter16, 405-434. ISBN 978-953-51-0392-9. (2012).

Rovero, G. and Watkinson, A.P. “A two-stage spouted bed process for auto-thermal pyrolysis or retorting”. *Fuel Proc. Technol*., 26 **(**1990), 221–238.

Schilde W. “PFB Upgrading and preparation of textiles”; Sachsisches textilforschungsinstitut E.V.. pp. 59-86, JOF3-CT95-0010.

Sue-A-Quan, T., Cheng, G., and Watkinson, A. P. “Coal gasification in a pressurized spouted bed”. *Fuel*, 74 (1995), 159–164.

Sue-A-Quan, T., Watkinson, A.P., Gaikwad, R.P., Lim, C.J., and Ferris, B.R. “Steam gasification in a pressurized spouted bed reactor”. *Fuel Proc. Technol*., 27 (1991), 67–81.

Tanger, P., Field, J.L., Jahn, C.E., DeFoort, M.W. and Leach J.E. “Biomass for thermochemical conversion: targets and challenges”. *Front Plant Sci* (2013), pp 4-218.

Tsuji, T. and Uemaki, O. Coal gasification in a jet-spouted bed. *Can. J. Chem. Eng*., 72 (1994), 504–510.

Zenz, F.A. and Othmer, D.F. “Fluidization and Fluid-Particle Systems”. *Princeton*, New York, Reinhold (1960).

Appendix

Symbols:

Greek letters

α	solids repose angle, deg
ΔP	pressure drop, cmH_2O
ΔP_M	maximum bed pressure drop, cmH_2O
ε_{spout}	spout void fraction
ε_{mf}	annulus void fraction at minimum fluidization
γ	included angle, deg
λ	shape factor
Φ	sphericity
ρ_b	bulk density, kg/m^3
ρ_s	solid density, kg/m^3

Nomenclature

A_c	column section, m^2
A_r	Archimedes number
D_c	column diameter, m
D_s	spout diameter, mm
d_i	inlet diameter, mm
d_p	particle diameter, mm
D_{dt}	draft tube diameter, mm
g	gravity force 9.81 m/s^2
H	bed depth, m
H_d	draft tube distance from the base, mm
H_m	maximum bed depth, m
L_d	draft tube length, mm
U	gas velocity, m/s
U_{mf}	minimum fluidization velocity, m/s
U_{ms}	minimum spouting velocity, m/s
U_{os}	on-set spouting velocity, m/s